

Studies on Synthesis of Narrow Bandgap Polymers Aiming at Application to Polymer Solar Cells

メタデータ	言語: eng 出版者: 公開日: 2017-10-05 キーワード (Ja): キーワード (En): 作成者: メールアドレス: 所属:
URL	http://hdl.handle.net/2297/42359

This work is licensed under a Creative Commons Attribution-NonCommercial-ShareAlike 3.0 International License.



博 士 論 文

Studies on Synthesis of Narrow Bandgap Polymers

Aiming at Application to Polymer Solar Cells

有機薄膜太陽電池への応用を指向した

ナローバンドギャップポリマーの合成に関する研究

金沢大学大学院自然科学研究科

物質科学専攻

学籍番号: 1223132006

氏名: 山本 倫行

主任指導教員名: 前田 勝浩

提出年月: 2015 年 3 月

**Studies on Synthesis of Narrow Bandgap Polymers
Aiming at Application to Polymer Solar Cells**

Table of Contents

General Introduction	1
Chapter 1	25
Synthesis and Characterization of Thieno[3,4- <i>b</i>]thiophene-Based Copolymers Bearing 4-Substituted Phenyl Ester Pendants: Facile Fine-Tuning of HOMO Energy Levels	
Chapter 2	53
Fine Tuning of Frontier Orbital Energy Levels in Dithieno[3,2- <i>b</i> :2',3'- <i>d</i>]silole-Based Copolymers Based on the Substituent Effect of Phenyl Pendants	
Chapter 3	79
Influence of 4-Fluorophenyl Pendants in Thieno[3,4- <i>b</i>]thiophene–Benzo[1,2- <i>b</i> :4,5- <i>b'</i>]dithiophene-Based Polymers on the Performance of Photovoltaics	
Chapter 4	109
Thieno[3,4- <i>b</i>]thiophene–benzo[1,2- <i>b</i> :4,5- <i>b'</i>]dithiophene-Based Polymers Bearing Optically Pure 2-Ethylhexyl Pendants: Synthesis and Application in Polymer Solar Cells	
List of Publications	139
Acknowledgment	141

General Introduction

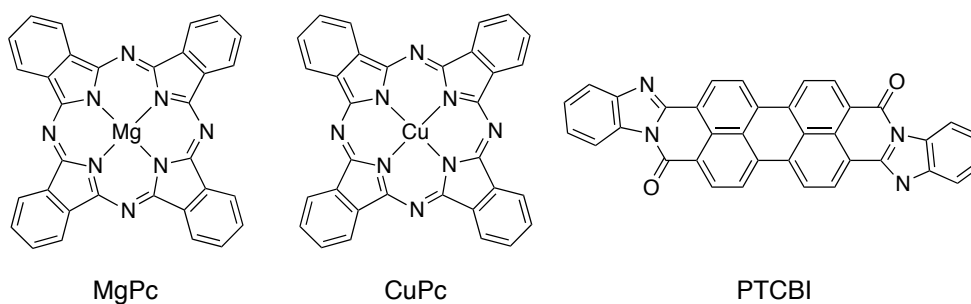
Today, the thermal power generation is a flagship of world energy productions, which is mainly based on the combustion of exhaustible fossil fuel accompanying the global warming by carbon-dioxide (CO₂) emissions. Although the nuclear power generation has also given us the benefit of a great amount of energy at low cost, it has a potential risk of a nuclear accident and the extraordinary disasters have actually happened at nuclear power plants in Three Mile Island (USA, 1979), Chernobyl (Ukrayina, 1986), Tokaimura (Japan, 1999), Fukushima (Japan, 2011), and so on. On the other hand, the solar power generation can directly convert the light energy into electrical energy without any hazardous emissions, such as CO₂ and radioactive materials. Because the sun eternally irradiates a huge amount of light energy to the Earth, the solar power generation is considered as one of the most promising candidates for sustainable, clean, and safety energy productions. However, as it is now, the energy derived from the solar power generation account for only a small percentage of the total energy production. In order to realize a perfect sustainable world, a further development of the solar power generation is absolutely necessary and “highly-efficient and low-cost solar cell devices” have been strongly demanded.

Solar cells are roughly categorized into inorganic- or organic-type devices on the basis of the difference in photoelectric conversion materials. Since Chapin, Fuller, and

Pearson have reported the first silicon solar cell with a power-conversion efficiency (PCE) of 6% in 1954,¹ the inorganic-type cells have been extensively studied to improve their efficiency and practicality. Various types of silicon-based cells, including single-crystalline, polycrystalline, and amorphous thin-film cells, have been developed over the past years and some of them are now commercially available. Silicon-free compound-semiconductor cells have been also developed and the highest PCE of 46% has been achieved using four-junction cells based on a selection of the III-V compound semiconductors by Soitec, inc. Although these inorganic-type solar cells exhibit much higher efficiencies than organic-type cells as described later, inorganic-type cells have drawbacks of not only heavy, uncolorful, and non-flexible characters but also a high manufacturing cost due to a necessity for highly-pure photoelectric materials.

Organic-type solar cells using organic semiconductors as the photoelectric materials are further classified into dye-sensitized solar cell (DSSC) and organic photovoltaic cell (OPV). In 1991, Grätzel et al. reported the first DSSC with a PCE of 7.12%.² A typical DSSC consists of a redox-active electrolytic solution, which is sandwiched between a counter electrode and a dye-coated titanium oxide (TiO₂). Although a PCE of DSSC has already been increased to a practical level (~13%),³ DSSC has fatal safety problems of leakage and volatilization of liquid electrolyte. In contrast to DSSCs, OPVs are electrolyte-free devices and have attracted much interest because of their potential advantages of the lightweight and flexible characteristics and the low manufacturing cost of large-scale devices using printing processes.⁴

The innovation history in OPVs is shortly summarized as following. In 1958, Calvin et al. have developed the first OPVs, in which magnesium phthalocyanine (MgPc) was used as an organic semiconductor for a single-component active layer.⁵ This device showed a very poor PCE less than 0.1%. The main reason for this low efficiency is probably due to a frequent recombination of the holes and electrons produced in the active layer. In 1986, Tang et al. have implemented a p-n bilayer device with a simple planar heterojunction configuration containing copper phthalocyanine (CuPc) as a hole-transport material (p-layer) and 3,4,9,10-perylene tetracarboxylic bis-benzimidazole (PTCBI) as an electron-transport material (n-layer).⁶ Although the PCE was reached to about 1%, the p-n bilayer devices suffered from an inefficient charge separation and charge transporting because of a small donor/acceptor interface area and a long charge transport pathway to electrodes, respectively.



In 1991, Hiramoto et al. proposed an epoch-making concept of bulk heterojunction (BHJ) active layer, in which electron donor and acceptor materials formed a bicontinuous network structure with nanometer-size domains (Figure 1).⁷ They fabricated the OPV device consisting of a BHJ interlayer (i-layer) sandwiched between a p-layer of metal-free phthalocyanine (H₂Pc) and an n-layer of perylene tetracarboxylic derivative (Me-PTC), which could be prepared through co-deposition of H₂Pc and Me-PTC under high-vacuum conditions. This kind of p-i-n trilayered cell with the BHJ structure exhibited a considerable photocurrent enhancement compared to the above-mentioned p-n bilayer device.

(a) Bulk-heterojunction structure



(b) Interdigitated structure

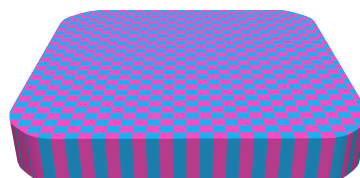
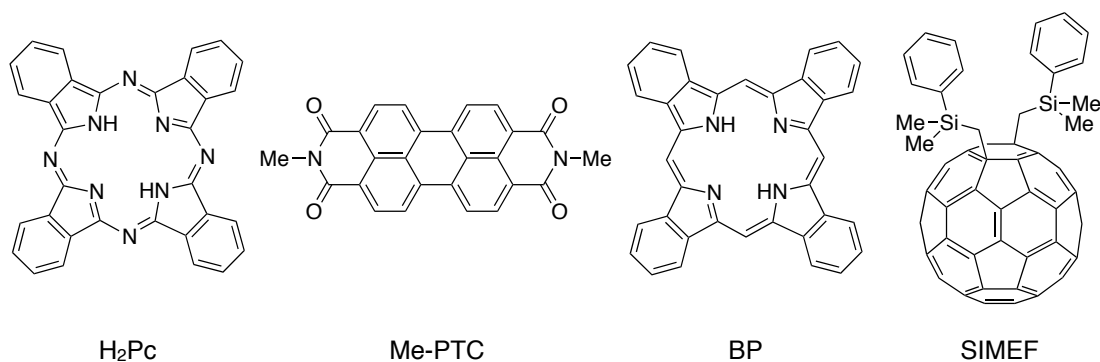


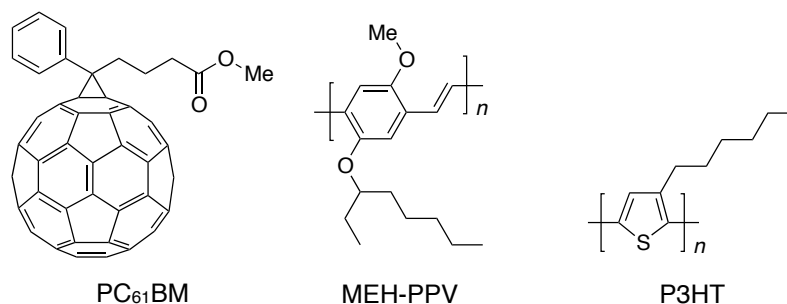
Figure 1. Architectures of activelayer : (a) bulk-heterojunction structure; (b) interdigitated structure.



As an alternative morphology to the BHJ structure, Matsuo et al. realized a construction of a highly-ordered and interdigitated active layer using tetrabenzoporphyrin (BP) and bis(dimethylphenylsilylmethyl)[60]fullerene (SIMEF) in 2009.⁸ BP and SIMEF could form a clear interdigitated structure through co-crystallization by thermal processing. The device with the defined interdigitated structures showed a higher PCE of 5.2% than the devices without interdigitated structures. However, there are no examples to construct this type of morphology using other organic semiconductors.

π -Conjugated polymers have also been used as photoelectric materials for OPV and those cells are called polymer solar cells (PSCs). In 1995, Heeger et al. prepared BHJ PSCs consisting of MEH-PPV and [6,6]-phenyl-C₆₁-butyric acid methyl ester (PC₆₁BM) as an electron donor and acceptor, respectively, by a facile coating manner.^{4a} Compared with a vapor-deposition technique for small molecule-based organic semiconductors, the coating method specifically for polymer-based semiconductors could simplify a device fabrication process and have been used for preparing most of the recently-reported PSCs. In 2002, Brabec et al. achieved a PCE of 2.8% in a BHJ PSC using P3HT as an electron donor.⁹ Since then, an optimization of fabrication conditions of P3HT-based devices, including dissolution, coating, and annealing conditions, has been extensively investigated all over the world and their PCE have been increased to ca. 5%.¹⁰ However, the further performance improvement of the P3HT-based devices cannot be expected due to an absorption property and a frontier orbital energy level of

P3HT as discussed later. To increase a PCE of OPVs to a practical level, a huge number of donor materials have been developed according to the following molecular design strategies.



Narrowing Bandgap

There are several steps in the photoelectric conversion process of the OPV devices. The first and most important step is the light absorption process by donor polymers and an efficient harvesting of solar photons is necessary to increase a short-circuit current density (J_{sc}) of the devices.¹¹ As shown in Figure 2, the photons in the sunlight are densely distributed in the region from 500 to 900 nm, while the absorption band of P3HT is located at wavelengths of less than 650 nm ($E_g = 1.9$ eV). In other words, P3HT can only harvest at most ca. 23% of the available solar photons. To efficiently absorb the solar photons and improve the performance of OPV devices, the donors should have bandgap energies (E_g) less than 1.5 eV. The following three approaches have been usually used to narrow the bandgap of π -conjugated polymers.

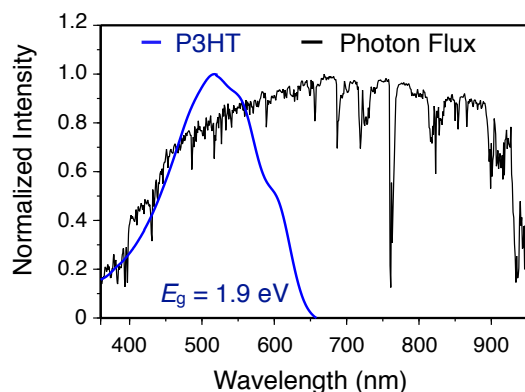


Figure 2. Absorption spectrum of P3HT (blue) and solar photon flux (black) spectra (AM1.5).

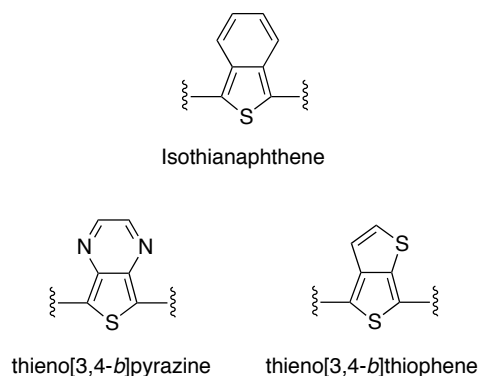


Figure 3. Representative units to stabilize their quinoidal resonance structures.

The first approach is to use a stabilization of quinoidal resonance structures in the polymer main-chains. π -Conjugated polymers have two possible resonance structures in their ground state, such as benzenoid and quinoid structures. The quinoid structures possess a narrower bandgap than the corresponding benzenoid structures because a quinoidal polymer backbone is more planar and their π -electrons can be highly-delocalized along a backbone. However, the quinoid structures usually contribute less to the resonance due to a lack of aromatic resonance energy. If the quinoid structure can be stabilized and its resonance contribution can be increased, the bandgaps of the polymers are expected to become narrow. Isothianaphthene, thieno[3,4-*b*]pyrazine, and thieno[3,4-*b*]thiophene (TT) are representative units to stabilize their quinoidal resonance structure (Figure 3). For example, when polythieno[3,4-*b*]thiophene (PTT) adapts the quinoid structure, one of the thiophene rings maintains the aromatic character, whose aromatic resonance energy contributes to

the stabilization of the quinoidal polymer backbone (Figure 4). In contrast, the quinoidal structure of polythiophene (PT) thoroughly loses the aromaticity. Examples of the donor polymers with a stabilization effect on quinoidal resonance structures are shown in Figure 5.¹² A bandgap of PTT derivative (PDTT) is 0.92 eV ($\lambda_{\text{onset}} = 1350$ nm) and greatly becomes narrower than that of P3HT ($E_g = 1.9$ eV).^{12a}

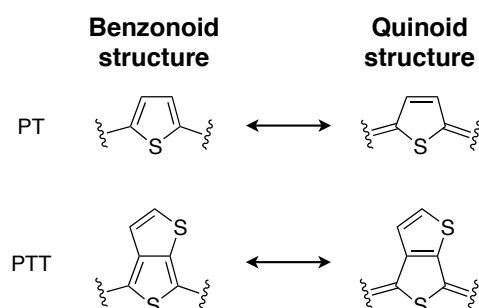


Figure 4. Benzoid and quinoid resonance forms of polythiophene, and polythienothiophene.

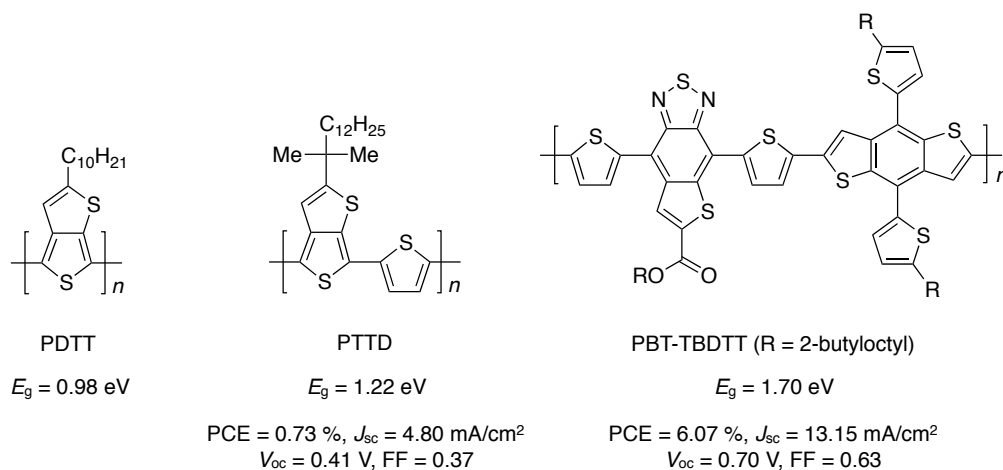


Figure 5. Examples of the polymers to stabilize their quinoidal resonance structures.

The second is to incorporate alternating electron-rich (D) and electron-deficient (A) units in the polymer main-chains, which can induce an intramolecular charge-transfer interaction to narrow the bandgaps effectively. Representative examples of D units are thiophene, benzo[1,2-*b*:4,5-*b'*]dithiophene (BDT), and dithieno[3,2-*b*:2',3'-*d*]silole (DTS), while thieno[3,4-*c*]pyrrole-4,6-dione (TPD), 2,1,3-benzothiadiazole, and diketopyrrolopyrrole are known as typical A units. In these systems, precise tuning of the energy levels of the highest occupied molecular orbital (HOMO) and lowest unoccupied molecular orbital (LUMO) energy levels in the polymer is possible by combination of D and A units. Figure 6 shows the recent examples of high-performance narrow bandgap polymers containing D and A units.¹³

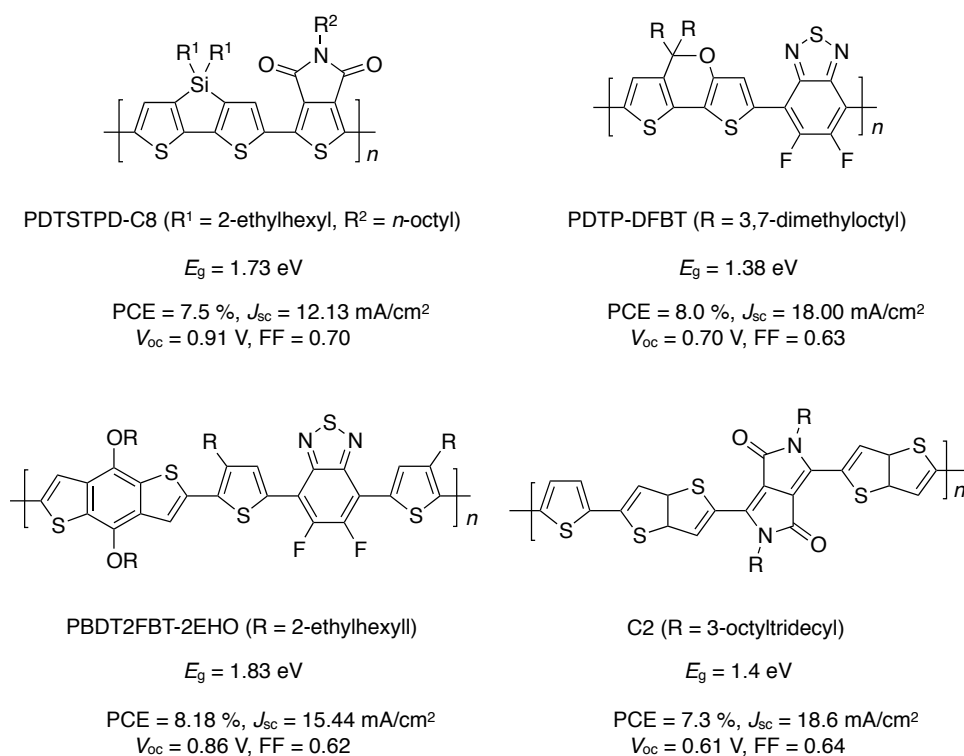


Figure 6. Examples of the polymers containing D and A units.

The third is to adopt polycyclic aromatic units as the polymer main-chains, which force to extend π -conjugation, facilitate electron delocalization, and reduce their bandgaps. Examples of the polymers bearing polycyclic aromatic units in the polymer main-chains are shown in Figure 7.¹⁴

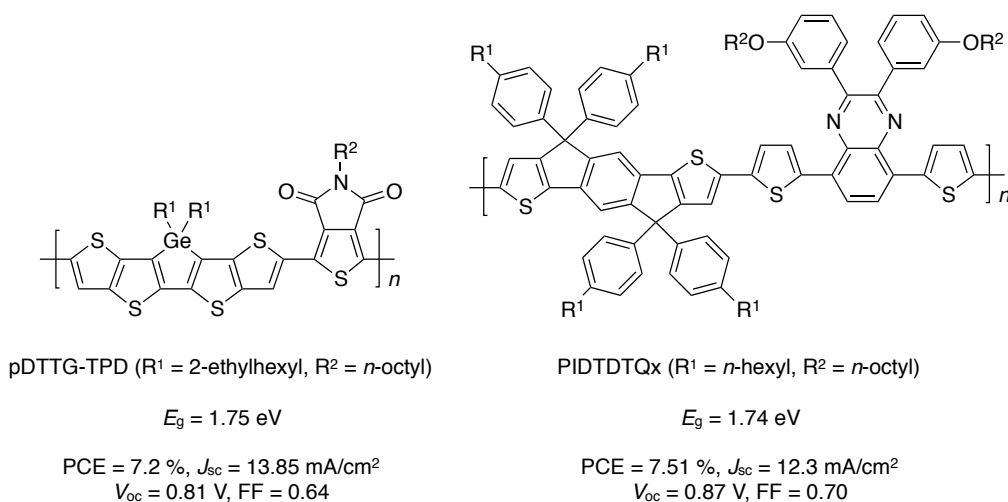
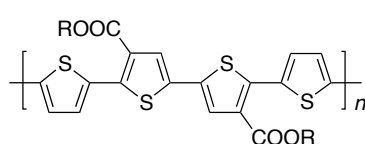


Figure 7. Examples of the polymers bearing polycyclic aromatic units.

Tuning HOMO Energy Levels

It has been reported that open-circuit voltage (V_{oc}) of OPVs devices is closely related to the difference between HOMO of electron donors and LUMO of electron acceptors.¹⁵ This means that deepening HOMO energy levels of narrow bandgap polymers is a useful strategy to develop efficient OPVs with high V_{oc} and J_{sc} values. Introduction of electron-withdrawing groups, such as fluorine and ester groups, into polymer backbones has been widely used to deepen the HOMOs of donor polymer and to enhance the V_{oc} values of the devices (Figure 8).¹⁶ For example, a polythiophene

derivative PDCBT bearing electron-withdrawing alkyl ester pendants showed a 0.36 eV deeper HOMO level and 0.3 V higher V_{oc} than P3HT bearing alkyl pendants.^{16b}

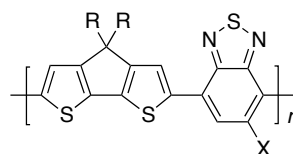


PDCBT (R = 2-butyloctyl)

HOMO = -5.26 eV

PCE = 7.2 %, J_{sc} = 11.00 mA/cm²

V_{oc} = 0.91 V, FF = 0.72



X = F, R = 2-ethylhexyl

HOMO = -5.35 eV

PCE = 6.16 %, J_{sc} = 14.08 mA/cm²

V_{oc} = 0.74 V, FF = 0.58

X = H, R = 2-ethylhexyl

HOMO = -5.25 eV

PCE = 3.59 %, J_{sc} = 11.46 mA/cm²

V_{oc} = 0.61 V, FF = 0.50

Figure 8. Examples of the polymers with (upper) or without (lower) electron-withdrawing groups.

Effective Intermolecular π - π stacking Interaction

The holes generated by light irradiation need to be efficiently transported to a positive electrode.¹⁷ An intermolecular charge transporting between adjacent polymers is usually a more limiting step compared with an intramolecular transporting within a single polymer. Polycyclic structures are often introduced into the polymer backbones as shown in Figure 9 in order to induce a strong overlapping of π -electrons through an effective intermolecular π - π -stacking interaction.¹⁸

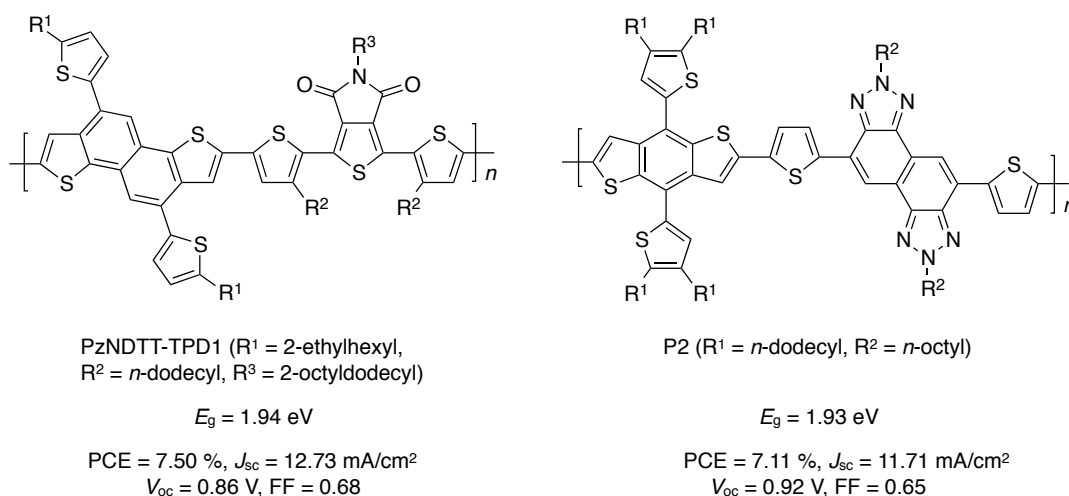


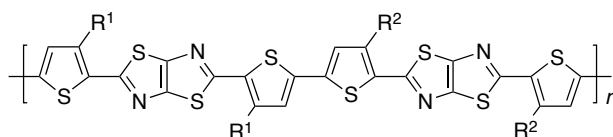
Figure 9. Examples of the polymers with a high hole-mobility.

Alkyl side-chains introduced onto the polymer backbones are also an important factor for an effective intermolecular stacking. Too long or bulky alkyl chains inhibit the efficient π - π stacking interactions between donor polymers, and consequently these chains decrease a hole transport property of the polymers.¹⁹ Too shorter alkyl pendants reduce the solubility of donor polymers, which is necessary to fabricate PSCs by solution processing. Therefore, the alkyl chains on the polymer backbones need to be appropriate.

Control of Molecular Orientation

The molecular orientations of conjugated polymers lead to anisotropic charge transport properties. The face-on orientations enhance the orthogonal hole transporting because π -orbitals in polymers are perpendicularly ordered against the substrate surface. On the other hand, the edge-on oriented structures facilitate the lateral hole transporting.

In the case of OPV devices, the face-on orientation is more favorable for efficient hole transport due to their device configurations. Osaka et al. have reported that PTzBT-14HD and PTzBT-BOHD mostly had the edge-on and face-on orientations in their film states, respectively. The latter blend film showed a 4.3 times higher hole mobility compared with the corresponding PTzBT-14HD-based film (Figure 10).²⁰



PTzBT-14HD (R¹ = *n*-tetradecyl, R² = 2-hexyldecyl)

PTzBT-BOHD (R¹ = 2-butylloctyl, R² = 2-hexyldecyl)

edge-on

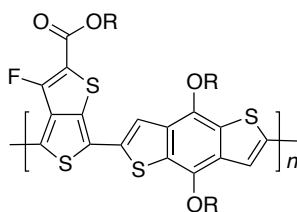
face-on

PCE = 5.4 %, J_{sc} = 9.9 mA/cm²
 V_{oc} = 0.82 V, FF = 0.66

PCE = 6.7 %, J_{sc} = 11.4 mA/cm²
 V_{oc} = 0.89 V, FF = 0.65

Figure 10. Examples of the polymers mostly having the edge-on and face-on orientations in their film states.

Among a tremendous amount of π -conjugated polymers developed so far, π -conjugated polymers consisting of alternating TT and BDT units (PTB-based polymers) have been recognized one of the most promising donor materials. Since Yu et al. have reported the first PTB-based polymer in 2009,²¹ various structural modifications have been investigated to improve the PCE of their PSCs. For example, replacements of the alkyl esters with alkylketones²² and direct introduction of fluoro groups²³ or thienyl units²⁴ onto the polymer backbone successfully increased the PCE of the resulting PSCs. At present, an excellent PCE over 9% was achieved using the polymer called PTB7.^{23b,25} To realize a truly practical OPV device, the further improvement of electron donor materials has been required.



PTB7 (R = 2-ethylhexyl)

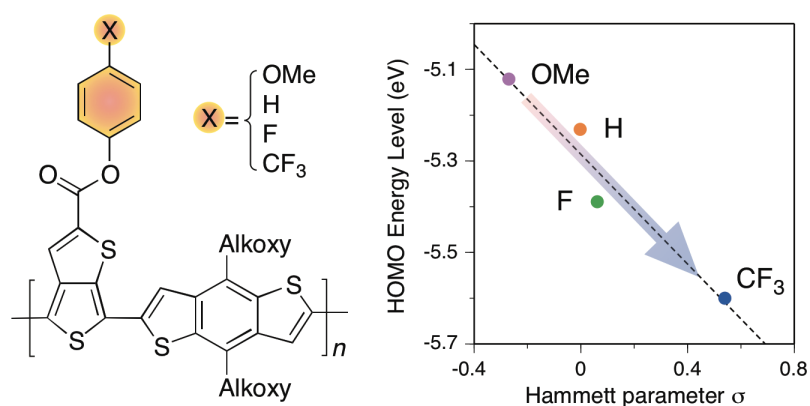
PCE = 9.21 %, J_{sc} = 17.46 mA/cm²
 V_{oc} = 0.75 V, FF = 0.70

On the basis of the above information, the author studied the following four themes concerning the development of novel π -conjugated polymers as electron donor materials for efficient polymer solar cells.

- (1) Synthesis and Characterization of Thieno[3,4-*b*]thiophene-Based Copolymers Bearing 4-Substituted Phenyl Ester Pendants: Facile Fine-Tuning of HOMO Energy Levels
- (2) Fine Tuning of Frontier Orbital Energy Levels in Dithieno[3,2-*b*:2',3'-*d*]silole-based Copolymers Based on the Substituent Effect of Phenyl Pendants
- (3) Influence of 4-Fluorophenyl Pendants in Thieno[3,4-*b*]thiophene–Benzo[1,2-*b*:4,5-*b'*]dithiophene-Based Polymers on the Performance of Photovoltaics
- (4) Thieno[3,4-*b*]thiophene–benzo[1,2-*b*:4,5-*b'*]dithiophene-based Polymers Bearing Optically Pure 2-Ethylhexyl Pendants: Synthesis and Application in Polymer Solar Cells

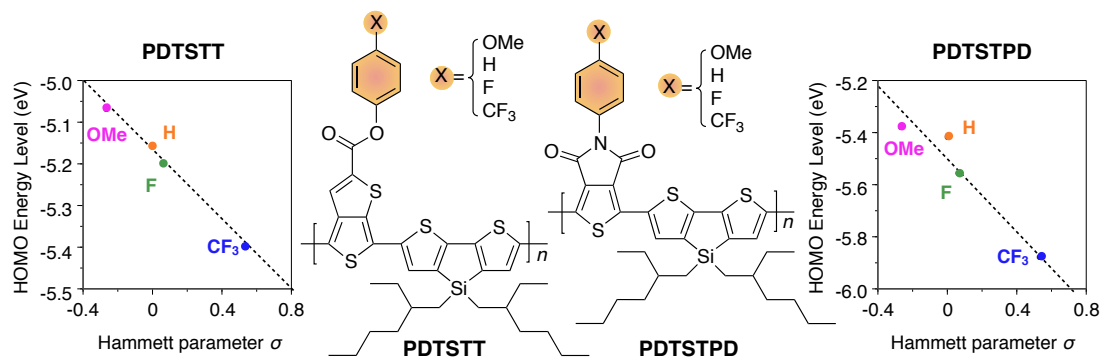
These studies will be described in the following four chapters.

In Chapter 1, the author synthesized novel π -conjugated polymers consisting of alternating TT units bearing 4-substituted phenyl ester pendants and BDT units and their thermal, optical, and electrochemical properties were investigated. The author found that the introduction of electron-withdrawing substituents on the phenyl rings connected to the TT units effectively lowered the HOMO energy level. By changing the substituent on the phenyl rings from a methoxy group to a trifluoromethyl group, the HOMO energy levels of the polymers decreased from -5.12 to -5.60 eV. A good linear relationship was observed between the HOMO energy levels and the Hammett substituent constants.

Chart 1

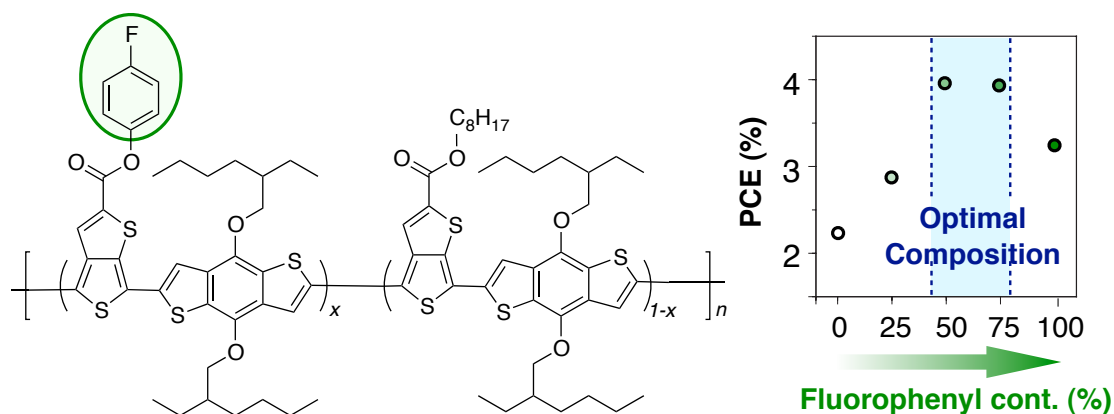
In Chapter 2, the author synthesized a series of DTS-based π -conjugated copolymers containing TPD or TT units bearing 4-substituted phenyl pendants and systematically investigated their thermal stability, optical properties and frontier orbital energy levels. The introduction of electron-withdrawing substituents on the phenyl rings lowered their frontier orbital energy levels without deteriorating their thermal and optical properties. By replacing an electron-donating methoxy group with an electron-withdrawing trifluoromethyl group, both the HOMO and LUMO energy levels of the polymers were deepened by more than 0.3 eV. A relatively linear relationship was observed between the HOMO energy levels and the Hammett substituent constants.

Chart 2

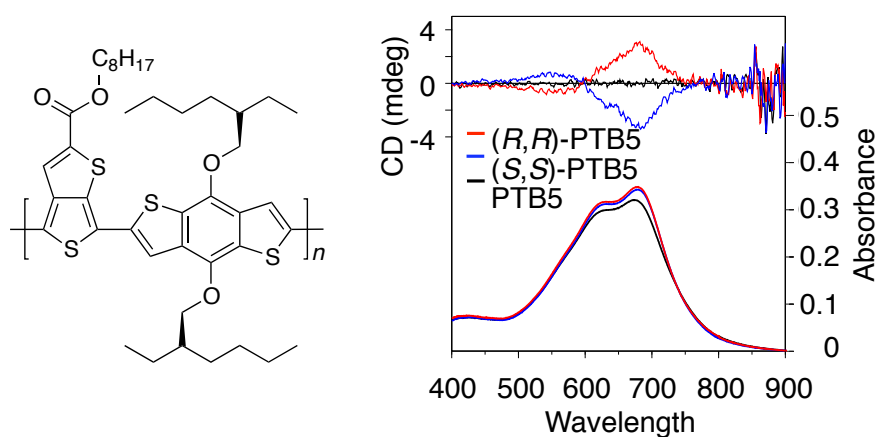


In Chapter 3, the author synthesized novel PTB-based polymers either fully or partially containing 4-fluorophenyl pendants, as electron donor materials for inverted-type PSCs. The influence of the 4-fluorophenyl pendant content on their optical properties, HOMOs and LUMOs, and photovoltaic performances are carefully investigated. The author found that the HOMOs and LUMOs of the polymers were deepened proportionally and the open-circuit voltages of the PSCs improved with increasing 4-fluorophenyl pendant content. Incorporation of 4-fluorophenyl pendants into the polymers also affected the crystallinity, orientation, and compatibility with PC₆₁BM in the active layers. As a result, the PTB-based polymers bearing a moderate content of 4-fluorophenyl pendants (50–75%) provided best PSC performances.

Chart 3



In Chapter 4, the author synthesized optically active narrow-bandgap polymers ((*R,R*)- and (*S,S*)-PTB5) consisting of alternating *n*-octyl thieno[3,4-*b*]thiophene-2-carboxylate and BDT units bearing optically pure (*R*)- and (*S*)-2-ethylhexyl pendants, respectively, for the first time. (*R,R*)- and (*S,S*)-PTB5 films showed apparent circular dichroism in their absorption regions of the polymer backbone due to the formation of a chirally ordered superstructure induced by the chirality of the branched alkyl pendants. Inverted-type BHJ PSCs were fabricated using (*R,R*)- or (*S,S*)-PTB5 as electron donors and PC₆₁BM as an electron acceptor. The photovoltaic properties of the PSCs were compared with those of the corresponding PSC containing optically inactive PTB5 bearing racemic 2-ethylhexyl pendants.

Chart 4

References

- (1) Chapin, D. M.; Fuller, C. S.; Pearson, G. L. *J. Appl. Phys.* **1954**, *25*, 676.
- (2) O'Regan, B.; Gratzel, M. *Nature* **1991**, *353*, 737.
- (3) Mathew, S.; Yella, A.; Gao, P.; Humphry-Baker, R.; CurchodBasile, F. E.; Ashari-Astani, N.; Tavernelli, I.; Rothlisberger, U.; NazeeruddinMd, K.; Grätzel, M. *Nat. Chem.* **2014**, *6*, 242.
- (4) (a) Yu, G.; Gao, J.; Hummelen, J. C.; Wudl, F.; Heeger, A. J. *Science* **1995**, *270*, 1789. (b) Cheng, Y.-J.; Yang, S.-H.; Hsu, C.-S. *Chem. Rev.* **2009**, *109*, 5868. (c) Brabec, C. J.; Gowrisanker, S.; Halls, J. J. M.; Laird, D.; Jia, S.; Williams, S. P. *Adv. Mater.* **2010**, *22*, 3839. (d) Beaujuge, P. M.; Fréchet, J. M. J. *J. Am. Chem. Soc.* **2011**, *133*, 20009. (e) Facchetti, A. *Chem. Mater.* **2011**, *23*, 733. (f) Li, G.; Zhu, R.; Yang, Y. *Nat. Photon.* **2012**, *6*, 153. (g) Søndergaard, R.; Hösel, M.; Angmo, D.; Larsen-Olsen, T. T.; Krebs, F. C. *Mater. Today* **2012**, *15*, 36. (h) Kim, J.-H.; Song, C. E.; Kim, B.; Kang, I.-N.; Shin, W. S.; Hwang, D.-H. *Chem. Mater.* **2013**, *26*, 1234. (i) Heeger, A. J. *Adv. Mater.* **2014**, *26*, 10.
- (5) Kearns, D.; Calvin, M. J. *J. Chem. Phys.* **1958**, *29*, 950.
- (6) Tang, C. W. *Appl. Phys. Lett.* **1986**, *48*, 183.
- (7) Hiramoto, M.; Fujiwara, H.; Yokoyama, M. *Appl. Phys. Lett.* **1991**, *58*, 1062.
- (8) Matsuo, Y.; Sato, Y.; Niinomi, T.; Soga, I.; Tanaka, H.; Nakamura, E. *J. Am. Chem. Soc.* **2009**, *131*, 16048.
- (9) Schilinsky, P.; Waldauf, C.; Brabec, C. J. *Appl. Phys. Lett.* **2002**, *81*, 3885.

- (10) Kim, Y.; Cook, S.; Tuladhar, S. M.; Choulis, S. A.; Nelson, J.; Durrant, J. R.; Bradley, D. D. C.; Giles, M.; McCulloch, I.; Ha, C.-S.; Ree, M. *Nat. Mater.* **2006**, *5*, 197.
- (11) (a) Bundgaard, E.; Krebs, F. C. *Sol. Energy Mater. Sol. Cells* **2007**, *91*, 954. (b) Chen, J.; Cao, Y. *Acc. Chem. Res.* **2009**, *42*, 1709. (c) Boudreault, P.-L. T.; Najari, A.; Leclerc, M. *Chem. Mater.* **2011**, *23*, 456. (d) Zhou, H.; Yang, L.; You, W. *Macromolecules* **2012**, *45*, 607.
- (12) (a) Pomerantz, M.; Gu, X.; Zhang, S. X. *Macromolecules* **2001**, *34*, 1817. (b) Liang, Y.; Xiao, S.; Feng, D.; Yu, L. *J. Phys. Chem. C* **2008**, *112*, 7866. (c) Zhou, P.; Zhang, Z.-G.; Li, Y.; Chen, X.; Qin, J. *Chem. Mater.* **2014**, *26*, 3495.
- (13) (a) Chu, T.-Y.; Lu, J.; Beaupré, S.; Zhang, Y.; Pouliot, J.-R.; Zhou, J.; Najari, A.; Leclerc, M.; Tao, Y. *Adv. Funct. Mater.* **2012**, *22*, 2345. (b) Dou, L.; Chen, C.-C.; Yoshimura, K.; Ohya, K.; Chang, W.-H.; Gao, J.; Liu, Y.; Richard, E.; Yang, Y. *Macromolecules* **2013**, *46*, 3384. (c) Meager, I.; Ashraf, R. S.; Mollinger, S.; Schroeder, B. C.; Bronstein, H.; Beatrup, D.; Vezie, M. S.; Kirchartz, T.; Salleo, A.; Nelson, J.; McCulloch, I. *J. Am. Chem. Soc.* **2013**, *135*, 11537. (d) Lee, J.; Jo, S. B.; Kim, M.; Kim, H. G.; Shin, J.; Kim, H.; Cho, K. *Adv. Mater.* **2014**, *26*, 6706.
- (14) (a) Guo, X.; Zhang, M.; Tan, J.; Zhang, S.; Huo, L.; Hu, W.; Li, Y.; Hou, J. *Adv. Mater.* **2012**, *24*, 6536. (b) Zhong, H.; Li, Z.; Deledalle, F.; Fregoso, E. C.; Shahid, M.; Fei, Z.; Nielsen, C. B.; Yaacobi-Gross, N.; Rossbauer, S.; Anthopoulos, T. D.; Durrant, J. R.; Heeney, M. *J. Am. Chem. Soc.* **2013**, *135*, 2040.

- (15) (a) Brabec, C. J.; Cravino, A.; Meissner, D.; Sariciftci, N. S.; Fromherz, T.; Rispens, M. T.; Sanchez, L.; Hummelen, J. C. *Adv. Funct. Mater.* **2001**, *11*, 374. (b) Scharber, M. C.; Mühlbacher, D.; Koppe, M.; Denk, P.; Waldauf, C.; Heeger, A. J.; Brabec, C. J. *Adv. Mater.* **2006**, *18*, 789. (c) Li, Y. *Acc. Chem. Res.* **2012**, *45*, 723.
- (16) (a) Albrecht, S.; Janietz, S.; Schindler, W.; Frisch, J.; Kurpiers, J.; Kniepert, J.; Inal, S.; Pingel, P.; Fostiropoulos, K.; Koch, N.; Neher, D. *J. Am. Chem. Soc.* **2012**, *134*, 14932. (b) Zhang, M.; Guo, X.; Ma, W.; Ade, H.; Hou, J. *Adv. Mater.* **2014**, *26*, 5880.
- (17) (a) McCulloch, I.; Heeney, M.; Chabinyc, M. L.; DeLongchamp, D.; Kline, R. J.; Cölle, M.; Duffy, W.; Fischer, D.; Gundlach, D.; Hamadani, B.; Hamilton, R.; Richter, L.; Salleo, A.; Shkunov, M.; Sparrowe, D.; Tierney, S.; Zhang, W. *Adv. Mater.* **2009**, *21*, 1091. (b) Osaka, I.; Kakara, T.; Takemura, N.; Koganezawa, T.; Takimiya, K. *J. Am. Chem. Soc.* **2013**, *135*, 8834.
- (18) (a) Dong, Y.; Hu, X.; Duan, C.; Liu, P.; Liu, S.; Lan, L.; Chen, D.; Ying, L.; Su, S.; Gong, X.; Huang, F.; Cao, Y. *Adv. Mater.* **2013**, *25*, 3683. (b) Zhu, X.; Fang, J.; Lu, K.; Zhang, J.; Zhu, L.; Zhao, Y.; Shuai, Z.; Wei, Z. *Chem. Mater.* **2014**, *26*, 6947.
- (19) Mei, J.; Bao, Z. *Chem. Mater.* **2014**, *26*, 604.
- (20) Osaka, I.; Saito, M.; Koganezawa, T.; Takimiya, K. *Adv. Mater.* **2014**, *26*, 331.
- (21) Liang, Y.; Wu, Y.; Feng, D.; Tsai, S.-T.; Son, H.-J.; Li, G.; Yu, L. *J. Am. Chem. Soc.* **2009**, *131*, 56.
- (22) (a) Chen, H.-Y.; Hou, J.; Zhang, S.; Liang, Y.; Yang, G.; Yang, Y.; Yu, L.; Wu,

Y.; Li, G. *Nat. Photon.* **2009**, *3*, 649. (b) Hou, J.; Chen, H.-Y.; Zhang, S.; Chen, R. I.;

Yang, Y.; Wu, Y.; Li, G. *J. Am. Chem. Soc.* **2009**, *131*, 15586.

(23) (a) Liang, Y.; Feng, D.; Wu, Y.; Tsai, S. T.; Li, G.; Ray, C.; Yu, L. *J. Am. Chem.*

Soc. **2009**, *131*, 7792. (b) Liang, Y.; Xu, Z.; Xia, J.; Tsai, S.-T.; Wu, Y.; Li, G.; Ray,

C.; Yu, L. *Adv. Mater.* **2010**, *22*, E135. (c) Son, H. J.; Wang, W.; Xu, T.; Liang, Y.;

Wu, Y.; Li, G.; Yu, L. *J. Am. Chem. Soc.* **2011**, *133*, 1885.

(24) Huo, L.; Zhang, S.; Guo, X.; Xu, F.; Li, Y.; Hou, J. *Angew. Chem. Int. Ed.* **2011**,

50, 9697.

(25) He, Z.; Zhong, C.; Su, S.; Xu, M.; Wu, H.; Cao, Y. *Nat. Photon.* **2012**, *6*, 591.

Chapter 1

Synthesis and Characterization of Thieno[3,4-*b*]thiophene-Based Copolymers Bearing 4-Substituted Phenyl Ester Pendants: Facile Fine-Tuning of HOMO Energy Levels

Abstract: The author synthesized novel π -conjugated polymers consisting of alternating thieno[3,4-*b*]thiophene units bearing 4-substituted phenyl ester pendants and benzo[1,2-*b*:4,5-*b'*]dithiophene units and their thermal, optical, and electrochemical properties were investigated. The author found that the introduction of electron-withdrawing substituents on the phenyl rings connected to the thieno[3,4-*b*]thiophene units effectively lowered the highest occupied molecular orbital (HOMO) energy level. By changing the substituent on the phenyl rings from a methoxy group to a trifluoromethyl group, the HOMO energy levels of the polymers decreased from -5.12 to -5.60 eV. A good linear relationship was observed between the HOMO energy levels and the Hammett substituent constants.

Introduction

Polymer solar cells (PSCs) have been attracting much interest because of their advantages; they are low cost, lightweight, and flexible and have the potential for the production of large-area devices.¹ Bulk heterojunction (BHJ) PSCs have become the most successful device configurations. In such devices, conjugated polymers, as an electron donor, and fullerene derivatives, as an electron acceptor, form an interpenetrating network on the nanometer scale.² For BHJ PSCs, regioregular poly(3-hexylthiophene) (P3HT) has been extensively used as the electron-donor material because of its solubility, stability, and compatibility with the typical electron acceptor [6,6]-phenyl-C₆₁-butyric acid methyl ester (PC₆₁BM).^{1,3} However, P3HT can only harvest less than ca. 23% of the available solar photons because its absorption band is located at wavelengths of less than 650 nm.⁴ Extensive research efforts have therefore been devoted to developing novel conjugated polymers with low bandgaps to better harvest the solar energy and improve the power-conversion efficiencies (PCEs) of PSCs.^{4,5}

In 2009, Yu et al. reported π -conjugated polymers consisting of alternating thieno[3,4-*b*]thiophene (TT) and benzo[1,2-*b*:4,5-*b'*]dithiophene (BDT) units (PTB-based polymers), promising donor materials for PSCs, whose absorption region reached ca. 800 nm as a result of the stabilization of the quinoidal resonance structure in the polymer main chain by the thieno[3,4-*b*]thiophene unit.⁶ The extended absorption of sunlight directly contributed to increasing the short-circuit current density (J_{sc}), and

these PSCs exhibited high PCEs of over 5%, while the open-circuit voltages (V_{oc}) of the PSCs were relatively low, at ~ 0.6 V. It is known that the V_{oc} of a PSC is closely related to the difference between the highest occupied molecular orbital (HOMO) of the donor component and the lowest unoccupied molecular orbital (LUMO) of the acceptor, and deepening the HOMO energy level of the donor polymer is a potential way of developing highly efficient PSCs with a high V_{oc} .⁷ The following two strategies have been used to deepen the HOMO energy level of PTB-based polymers: the introduction of a fluorine atom, which is the atom with the highest electronegativity, in the TT ring^{6b} and the replacement of the alkyl ester pendants of the TT unit with alkyl ketone pendants.⁸ These modifications reduced the HOMO energy levels of the polymers from -5.01 to -5.12 eV, and the PCEs were effectively improved from 5.15 to 6.10 and 6.58, respectively. A remarkable PCE of 7.73% was achieved by combining the two strategies.⁹ However, the synthesis of PTB-based polymers bearing a fluorine atom on the polymer main-chains is very time-consuming, and further structural modifications are quite limited.

In this chapter, the author designed and synthesized PTB-based polymers bearing 4-substituted phenyl esters instead of the previously reported alkyl esters as the pendants of the TT unit and found that their HOMO energy levels could be readily fine-tuned by changing the substituents on the phenyl groups.

Experimental Section

Materials

Anhydrous solvents (toluene, DMF, THF), common organic solvents, and phenol were purchased from Kanto (Tokyo, Japan). Trimethyltin chloride was available from Tokyo Kasei (Tokyo, Japan). Oxalyl chloride, *n*-octanol, 4-trifluoromethylphenol, zinc, tetrabutylammonium bromide, and *n*-butyllithium (1.6 M in hexane) were purchased from Wako (Osaka, Japan). 4-Methoxyphenol and chlorobenzene were obtained from Kishida (Osaka, Japan). Tetrakis(triphenylphosphine)palladium(0) and sodium hydroxide were purchased from Nacalai (Kyoto, Japan). Poly(3,4-ethylenedioxythiophene):poly(4-styrenesulfonic acid) (PEDOT:PSS) 1.3 wt% dispersion in water, polyoxyethylene tridecyl ether (PTE), 4-fluorophenol, anhydrous pyridine, and chlorobenzene were purchased from Sigma-Aldrich. Indium tin oxide (ITO) glass substrates (sheet resistance = 10 Ω /sq.) and Au wire were obtained from Furuuchi Chemical Co. (Tokyo, Japan). 4,6-Dibromothieno[3,4-*b*]thiophene-2-carboxylic acid (**1**),¹⁰ 4,8-dihydrobenzo[1,2-*b*:4,5-*b'*]dithiophen-4,8-dione,¹¹ 1-iodo-2-octyldodecane,¹² and 2,6-bis(trimethyltin)-4,8-bis(2-ethylhexyloxy)benzo[1,2-*b*:3,4-*b'*]dithiophene (**BDTa**)^{6b} were prepared according to literature procedures.

Instruments

The ¹H and ¹³C NMR spectra were measured in CDCl₃ at room temperature or 50 °C

with a JEOL ECA-500 spectrometer (JEOL, Tokyo, Japan). IR spectra were obtained using a JASCO FT/IR-460Plus spectrometer (JASCO, Tokyo, Japan) as a KBr pellet. Molecular weights and distributions of polymers were estimated by size exclusion chromatography equipped with a Shodex KF-805L column (Showa Denko, Tokyo, Japan), JASCO PU-2080Plus HPLC pump, JASCO UV-970 UV/VIS detector at 650 nm, and JASCO CO-1560 column oven. THF was used as eluent and polystyrene as standards. Thermogravimetric analysis (TGA) was conducted with a TG/DTA6200 (SII NanoTechnology Inc., Chiba, Japan) at a heating rate of 10 °C/min under a nitrogen flow. UV-vis-NIR spectra were measured in chlorobenzene with 10 mm quartz cell using a JASCO V-570 spectrometer. Spin-coated films on glass plate substrates from chlorobenzene solution (5 mg/mL) were used for solid state UV-vis-NIR spectra measurements. HOMO levels of polymers were measured using a photoelectron spectrometer AC-2 (Riken Keiki, Tokyo, Japan) by measuring the ionization potential of polymer film in air. The ionization potential of the polymers was estimated by the plots of the photoelectron quantum yield from the polymer solid surface against the incident photon energy. That is, the threshold of the photoelectron quantum yield was correlated with the ionization potential. Space charge limited current (SCLC) measurements were carried out using an HZ-5000 electrochemical analyzer (Hokuto Denko, Japan). Atomic force microscopy (AFM) was performed using a SII SPI3800N AFM (Seiko, Japan).

Synthesis

4-Trifluoromethylphenyl 4,6-dibromothieno[3,4-*b*]thiophene -2-carboxylate (TT1). To 4,6-dibromo-thieno[3,4-*b*]thiophene-2-carboxylic acid (1) (500 mg, 1.46 mmol) in anhydrous toluene (5 mL) were added oxalyl chloride (371 mg, 2.92 mmol) and two drops of DMF at 0 °C under nitrogen atmosphere. The mixture was stirred at room temperature for 2 h and then volatile species were removed by evaporation in vacuo. To the residue were added 4-trifluoromethylphenol (355 mg, 2.19 mmol) and anhydrous pyridine (5 mL) at room temperature. After the reaction mixture was stirred at room temperature for 12 h, the solvent was removed in vacuo and the residue was extracted with dichloromethane. The organic layer was washed with brine, dried over anhydrous Na₂SO₄, and concentrated by evaporation. The crude product was purified by silica gel chromatography using hexane–dichloromethane (4/1) to yield TT1 as a yellowish solid (483 mg, 1.08 mmol, 72%). Mp 152.6 – 152.9 °C. IR (KBr): 1720 cm⁻¹ ($\nu_{\text{C=O}}$). ¹H NMR (500 MHz, CDCl₃, rt): δ 7.77 (s, 1H), 7.72 (d, 2H, $J = 9.0$ Hz), 7.38 (d, 2H, $J = 8.5$ Hz). ¹³C NMR (125 MHz, CDCl₃, rt): δ 160.68, 153.13, 145.75, 140.79, 139.49, 129.46, 129.19, 128.93, 128.67, 127.39, 125.67, 125.23, 122.37, 103.93, 97.99. Anal. Calcd for C₁₄H₅Br₂F₃O₂S₂: C, 34.59; H, 1.04. Found: C, 34.61; H, 1.09.

4-Fluorophenyl 4,6-dibromothieno[3,4-*b*]thiophene-2-carboxylate (TT2). The title compound was prepared from 1 and 4-fluorophenol in the same way for TT1 and obtained in 80% yield. Mp 151.4 – 151.6 °C. IR (KBr): 1735 cm⁻¹ ($\nu_{\text{C=O}}$). ¹H NMR (500

MHz, CDCl₃, rt): δ 7.74 (s, 1H), 7.21-7.18 (m, 2H), 7.12 (t, 2H, $J = 8.3$ Hz). ¹³C NMR (125 MHz, CDCl₃, rt): δ 161.59, 160.93, 159.65, 146.25, 145.54, 140.55, 139.66, 125.02, 123.04, 122.97, 116.53, 116.34, 103.36, 97.61. Anal. Calcd for C₁₃H₅Br₂FO₂S₂: C, 35.80; H, 1.16. Found: C, 36.07; H, 1.22.

Phenyl 4,6-dibromothieno[3,4-*b*]thiophene-2-carboxylate (TT3). The title compound was prepared from 1 and phenol in the same way for TT1 and obtained in 79% yield. Mp 134.8 – 135.1 °C. IR (KBr): 1720 cm⁻¹ ($\nu_{C=O}$). ¹H NMR (500 MHz, CDCl₃, rt): δ 7.75 (s, 1H), 7.44 (t, 2H, $J = 7.8$ Hz), 7.30 (t, 1H, $J = 7.5$ Hz), 7.23 (d, 2H, $J = 8.0$ Hz). ¹³C NMR (125 MHz, CDCl₃, rt): δ 160.95, 150.47, 145.63, 140.63, 140.08, 129.76, 126.52, 124.86, 121.54, 103.20, 97.55. Anal. Calcd for C₁₃H₆Br₂O₂S₂: C, 37.34; H, 1.45. Found: C, 37.33; H, 1.45.

4-Methoxyphenyl 4,6-dibromothieno[3,4-*b*]thiophene-2-carboxylate (TT4). The title compound was prepared from 1 and 4-methoxyphenol in the same way for TT1 and obtained in 92% yield. Mp 134.8 – 135.1 °C. IR (KBr): 1720 cm⁻¹ ($\nu_{C=O}$). ¹H NMR (500 MHz, CDCl₃, rt): δ 7.73 (s, 1H), 7.14 (d, 2H, $J = 9.0$ Hz), 6.94 (d, 2H, $J = 9.0$ Hz), 3.83 (s, 3H). ¹³C NMR (125 MHz, CDCl₃, rt): δ 161.32, 157.75, 145.65, 143.96, 140.64, 140.17, 124.73, 122.33, 114.71, 103.10, 97.52, 55.78. Anal. Calcd for C₁₄H₈Br₂O₃S₂: C, 37.52; H, 1.80. Found: C, 37.56; H, 1.89.

Octyl 4,6-dibromothieno[3,4-*b*]thiophene-2-carboxylate (TT5). The title compound was prepared from 1 and *n*-octanol in the same way for TT1 and obtained in 92% yield. Mp 64.8 – 65.0 °C. IR (KBr): 1719 cm⁻¹ ($\nu_{C=O}$). ¹H NMR (500 MHz, CDCl₃, rt): δ 7.53 (s, 1H), 4.31 (t, 2H, *J* = 6.5 Hz), 1.75 (quint, 2H, *J* = 7.1 Hz), 1.47-1.25 (m, 10H), 0.89 (t, 3H, *J* = 7.0 Hz), ¹³C NMR (125 MHz, CDCl₃, rt): δ 162.55, 145.73, 141.27, 140.57, 123.32, 102.38, 97.28, 66.35, 31.93, 29.34, 29.31, 28.71, 26.04, 22.79, 14.26. Anal. Calcd for C₁₅H₁₈Br₂O₂S₂: C, 39.66; H, 3.99. Found: C, 39.55; H, 3.99.

4,8-Bis(2-octyldodecyloxy)benzo[1,2-*b*:3,4-*b'*]dithiophene (2b). To a mixture of 4,8-dihydrobenzo[1,2-*b*:4,5-*b'*]dithiophen-4,8-dione (1.98 g, 9.00 mmol) and metallic zinc (sandy, 1.47 g, 22.5 mmol) was added 5 N NaOH aqueous solution (27 mL) and the mixture was stirred under reflux for 3 h. After 1-iodo-2-octyldodecane (14.7 g, 36.0 mmol) and tetrabutylammonium bromide (585 mg, 1.80 mmol) were added to the mixture, the reaction mixture was further refluxed for 12 h. The reaction mixture was then extracted with diethyl ether, and the organic layer was washed with brine and dried over anhydrous NaSO₄. After evaporating the solvent, the crude product was purified by silica gel chromatography using hexane–dichloromethane (10/1) to yield 2b as a colorless sticky oil (3.64 g, 4.64 mmol, 52%). ¹H NMR (500 MHz, CDCl₃, rt): δ 7.47 (d, 2H, *J* = 6.0 Hz), 7.36 (d, 2H, *J* = 5.5 Hz), 4.16 (d, 4H, *J* = 5.0 Hz), 1.88-1.83 (m, 2H), 1.66-1.60 (m, 4H), 1.53-1.21 (m, 60H), 0.90-0.87 (m, 12H).

2,6-Bis(trimethyltin)-4,8-bis(2-octyldodecyloxy)benzo[1,2-*b*:3,4-*b'*]dithiophene (BDTb). To a solution of 2b (4.40 g, 5.62 mmol) in anhydrous THF (67 mL) was added dropwise *n*-butyllithium (1.6 M in hexane, 8.78 mL, 14.1 mmol) via syringe at $-78\text{ }^{\circ}\text{C}$ under nitrogen atmosphere. The mixture was stirred at $-78\text{ }^{\circ}\text{C}$ for 30 min and then at room temperature for 30 min. After the mixture was cooled to $-78\text{ }^{\circ}\text{C}$ again, trimethyltin chloride (3.36 g, 16.9 mmol) in anhydrous THF (17 mL) was added. The mixture was warmed to room temperature and stirred for 12 h. After quenching the reaction with water, the volatile species were evaporated in vacuo. The residue was extracted with hexane, and the organic layer was washed with brine, dried over anhydrous NaSO_4 , and concentrated. The crude product was purified by recrystallization from 2-propanol to yield BDTb as a colorless crystals (4.78 g, 4.31 mmol, 77%). Mp $38.5 - 38.7\text{ }^{\circ}\text{C}$. ^1H NMR (500 MHz, CDCl_3 , rt): δ 7.51 (s, 2H), 4.17 (d, 4H, $J = 5.0\text{ Hz}$), 1.89-1.81 (m, 2H), 1.70-1.61 (m, 4H), 1.54-1.22 (m, 60H), 0.95-0.85 (m, 12H). ^{13}C NMR (125 MHz, CDCl_3 , rt): δ 143.40, 140.49, 134.01, 133.06, 128.13, 76.10, 39.37, 32.10, 31.59, 30.35, 29.95, 29.93, 29.89, 29.86, 29.57, 29.55, 27.25, 22.86, 14.28, -8.21. Anal. Calcd for $\text{C}_{56}\text{H}_{102}\text{O}_2\text{S}_2\text{Sn}_2$: C, 60.65; H, 9.27. Found: C, 60.69; H, 9.50.

Polymerization

Polymerization was carried out in a dry Schlenk flask under nitrogen atmosphere in a similar way previously reported.^{6b} Each monomer was purified by recrystallization

just before use. A typical polymerization procedure is described below.

TT1 (100 mg, 0.206 mmol), BDTb (228 mg, 0.206 mmol), and Pd(PPh₃)₄ (9.5 mg, 9.6 μmol) was placed in a Schlenk flask under nitrogen atmosphere. Anhydrous toluene (3.3 mL) and DMF (0.82 mL) were added with a syringe and the mixture was then heated at 120 °C. After 12 h, the reaction mixture was cooled to room temperature and poured into a large amount of methanol (MeOH). The resulting polymer was collected by centrifugation, and then purified by Soxhlet extraction for 12 h with MeOH and 12 h with hexane. After the polymer was collected with chlorobenzene, the chlorobenzene solution was passed through Celite to remove the metal catalyst and concentrated. The target polymer PTT1BDTb was obtained as dark red solid (142 mg, 62%) by precipitating in MeOH and drying in vacuo. IR (KBr): 1735 cm⁻¹ (ν_{C=O}). ¹H NMR (500 MHz, CDCl₃, 50 °C): δ 8.40-7.00 (7H, br), 4.40-3.80 (4H, br), 2.10-0.70 (78H, br). Anal. Calcd for (C₆₄H₈₉F₃O₄S₄)_n: C, 69.40; H, 8.10. Found: C, 69.56; H, 8.45.

In the same way, PTT2BDTb, PTT3BDTb, PTT4BDTb, PTT5BDTb, and PTT5BDTa were synthesized with the corresponding monomers. The polymerization results are summarized in Table 1-1.

Spectroscopic data of PTT2BDTb. IR (KBr): 1729 cm⁻¹ (ν_{C=O}). ¹H NMR (500 MHz, CDCl₃, 50 °C): δ 8.40-6.90 (7H, br), 4.40-3.80 (4H, br), 2.10-0.70 (78H, br). Anal. Calcd for (C₆₃H₈₉FO₄S₄)_n: C, 71.54; H, 8.48. Found: C, 71.31; H, 8.72.

Spectroscopic data of PTT3BDTb. IR (KBr): 1729 cm⁻¹ (ν_{C=O}). ¹H NMR (500 MHz, CDCl₃, 50 °C): δ 8.40-7.00 (8H, br), 4.40-4.00 (4H, br), 2.10-0.70 (78H, br). Anal.

Calcd for $(C_{63}H_{90}O_4S_4)_n$: C, 72.78; H, 8.73. Found: C, 72.63; H, 9.02.

Spectroscopic data of PTT4BDTb. IR (KBr): 1732 cm^{-1} ($\nu_{C=O}$). $^1\text{H NMR}$ (500 MHz, CDCl_3 , 50 °C): δ 8.40-6.70 (7H, br), 4.40-3.70 (7H, br), 2.10-0.70 (78H, br). Anal.

Calcd for $(C_{64}H_{92}O_5S_4)_n$: C, 71.86; H, 8.67. Found: C, 72.07; H, 9.07.

Spectroscopic data of PTT5BDTb. IR (KBr): 1717 cm^{-1} ($\nu_{C=O}$). $^1\text{H NMR}$ (500 MHz, CDCl_3 , 50 °C): δ 8.10-7.00 (3H, br), 4.70-4.00 (6H, br), 2.30-0.70 (93H, br). Anal.

Calcd for $(C_{65}H_{102}O_4S_4 \cdot 0.5\text{H}_2\text{O})_n$: C, 72.09; H, 9.57. Found: C, 72.10; H, 9.84.

Spectroscopic data of PTT5BDTa. IR (KBr): 1713 cm^{-1} ($\nu_{C=O}$). $^1\text{H NMR}$ (500 MHz, CDCl_3 , 50 °C): δ 8.30-6.40 (3H, br), 4.90-3.60 (6H, br), 2.60-0.70 (45H, br). Anal.

Calcd for $(C_{41}H_{54}O_4S_4 \cdot 0.6\text{H}_2\text{O})_n$: C, 65.66; H, 7.42. Found: C, 65.61; H, 7.41.

Computational study

All DFT calculations were performed at the B3LYP/6-31G (d,p) level¹³ using the Gaussian 03 package.¹⁴ The model compounds, which consist of one TT unit and two BDT units bearing methoxy groups instead of 2-octyldodecyloxy groups, were used for the computational study as simplified models.

Fabrication of hole-only devices

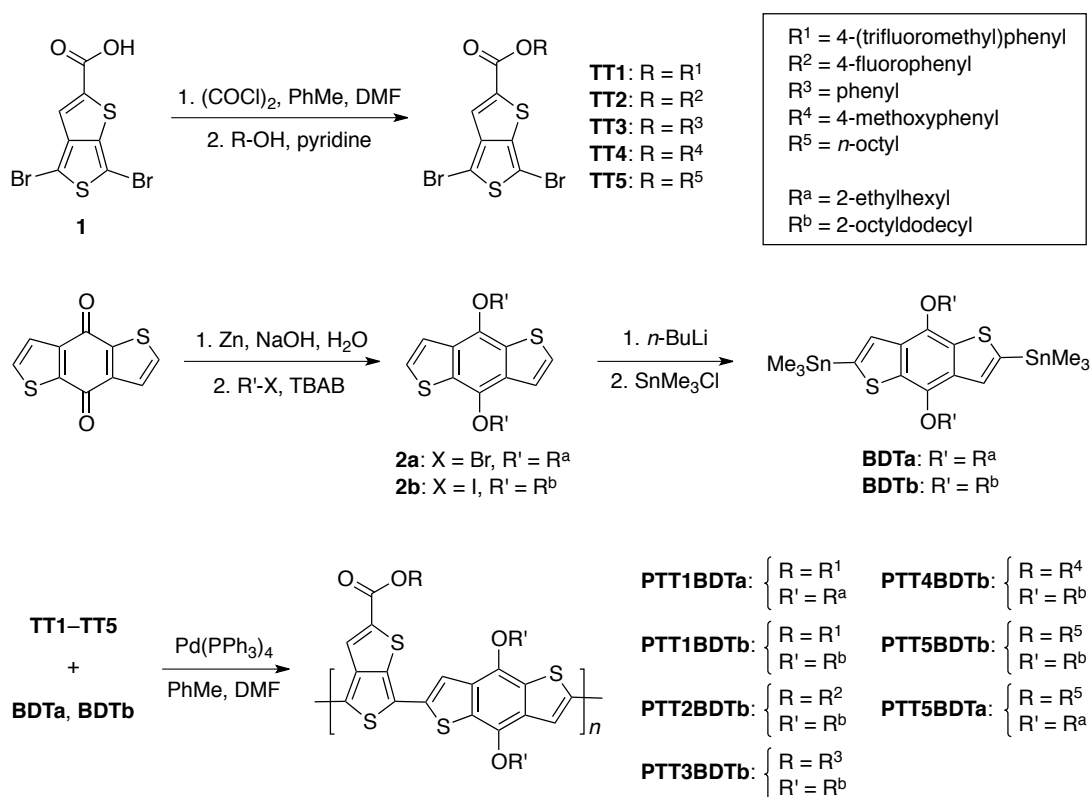
The ITO electrode was ultrasonicated in 2-propanol, cleaned in boiling 2-propanol, and then dried in air. A dispersion of PEDOT:PSS in water was spin-coated onto the clean ITO electrode at 6000 rpm, and then dried at 150 °C for 5 min. A solution of the

polymers in chlorobenzene (25 mg/mL) was spin-coated onto the ITO/PEDOT:PSS substrate at 700 rpm. A dispersion of PEDOT:PSS in water containing 0.01 wt.% PTE was heated to 85 °C, and then spin-coated onto the polymer layer at 6000 rpm. The Au electrode was vacuum deposited onto the PEDOT:PSS layer under a pressure of 2×10^{-5} Torr. The structure of the hole-only device is ITO/PEDOT:PSS/polymer/PEDOT:PSS/Au, whose effective area is 0.04 cm².

Hole mobility measurements

The hole mobilities of the polymers were estimated from the SCLC I - V characteristics of the hole-only devices.¹⁵ The SCLC behavior in the trap-free region can be characterized using the Mott-Gurney square law ($J = (9/8) \epsilon_0 \epsilon_r \mu_h (V^2/L^3)$), where J is the current density (A·cm⁻²), ϵ_0 is the vacuum permittivity (8.85×10^{-12} F·m⁻¹), ϵ_r is the dielectric constant of the organic material, μ_h is the hole mobility (cm²·V⁻¹·s⁻¹), L is the polymer thickness (m), and V is the applied voltage (V). The dielectric constant, ϵ_r , is assumed to be 3 in our analysis, which is a typical value for conjugated polymers. The thickness of the polymer films is measured by using AFM to be from 66 to 198 nm. The hole mobilities were calculated from the double-logarithmic plots of the I - V characteristics by fitting with a line with a slope of 2.

Scheme 1-1. Synthesis and Structures of Monomers and Polymers



Results and discussion

Synthesis and Thermal properties

The synthetic routes to the monomers and polymers are shown in Scheme 1-1. Four novel TT monomers bearing different phenyl ester groups (TT1–TT4) were easily prepared in one pot from commercially available phenol derivatives and the key precursor compound, 4,6-dibromothieno[3,4-*b*]thiophene-2-carboxylic acid (**1**), which was synthesized by modified literature procedures.^{6b,10} These TT monomers were obtained in good yields (>70%). Initially, the copolymerization of TT1 and bis(trimethylstannyl) BDT comonomer BDTa with 2-ethylhexyloxy substituents, by

Stille cross-coupling, was carried out using $\text{Pd}(\text{PPh}_3)_4$ as a catalyst in a toluene/*N,N*-dimethylformamide (DMF) mixture (4/1, v/v) to yield PTT1BDTa.⁶ However, the resulting PTT1BDTa exhibited very low solubility in common organic solvents such as tetrahydrofuran (THF), chloroform, and chlorobenzene, even at high temperatures. To improve the solubility of the polymer, a novel bis(trimethylstannyl) BDT bearing longer branched alkyl side chains, 2-octyldodecyloxy groups (BDTb), was synthesized and used as the comonomer instead of BDTa.

Table 1-1. Polymerization Results and Thermal, Optical, and Electrochemical Properties of the Polymers

run	polymer	yield (%) ^a	M_n (10^4) ^b	PDI ^b	T_d (°C) ^c	λ_{max} (nm)	λ_{onset} (nm)	E_g (eV) ^d	HOMO (eV) ^e	LUMO (eV) ^f
1	PTT1BDTb	62	5.9	3.0	313	692	761	1.63	-5.60	-3.97
2	PTT2BDTb	60	6.1	3.6	316	686	755	1.64	-5.39	-3.75
3	PTT3BDTb	85	7.1	3.3	315	682	748	1.66	-5.23	-3.57
4	PTT4BDTb	82	6.7	2.3	313	684	751	1.65	-5.12	-3.47
5	PTT5BDTb	77	6.1	2.4	316	671	736	1.68	-5.13	-3.45
6	PTT5BDTa	71	4.7	2.7	326	675	758	1.63	-5.01	-3.38

^a MeOH and hexane insoluble part. ^b Determined by SEC (eluent: THF, PSt standard). ^c The 5% weight-loss temperatures with a heating rate of 10 °C/min in N_2 . ^d Calculated from $E_g = 1240/\lambda_{\text{onset}}$. ^e Measured by photoelectron spectroscopy in air. ^f Calculated from $\text{LUMO} = E_g + \text{HOMO}$.

The results of the copolymerizations of TT1–TT4 with BDTb are summarized in Table 1-1 (runs 1–4). The resulting polymers were purified by successive Soxhlet extractions with methanol (MeOH) and hexane to remove byproducts and oligomers and subsequent filtration through Celite to remove the metal catalyst. The four polymers, PTT1BDTb, PTT2BDTb, PTT3BDTb, and PTT4BDTb, were obtained in relatively good yields (60–85%). The introduction of 2-octyldodecyloxy substituents on the BDT unit enhanced the solubility of the resulting polymers, and the obtained polymers exhibited good solubility in THF, chloroform, and chlorinated benzene. For comparison, the author also prepared the corresponding alkyl ester type polymer PTT5BDTb (run 5 in Table 1-1) and the reported PTB-based polymer PTT5BDTa (run 6 in Table 1-1).^{6b} The molecular weights (M_n) of the obtained polymers were determined by size-exclusion chromatography (SEC) in THF. All the polymers have a similar molecular weight, so the structural modification of the ester groups in the TT units seems to have little effect on the polymerizability of these TT-based monomers. The thermal stability of these polymers was investigated by thermal gravimetric analysis (TGA) under a nitrogen atmosphere (Figure 1-1). All polymers showed good thermal stability with 5% weight loss temperatures (T_d) above 300 °C, which is adequate for application in PSC devices.

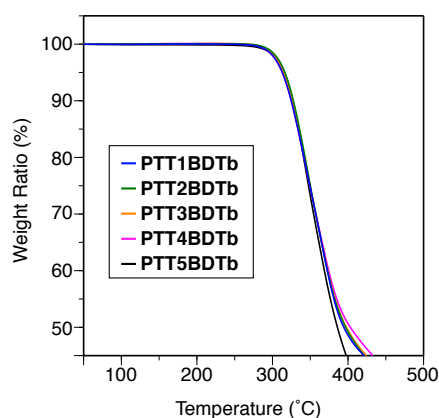


Figure 1-1. Thermogravimetric analysis of the polymers with a heating rate of 10 °C/min in N₂.

Optical properties

Figure 1-2 shows the absorption spectra of the polymers in chlorobenzene and in the film state. The absorption spectra of the polymers in solution are very similar to those in the solid state, suggesting that the polymers possess a similar rigid-rod conformation in both states. The absorption bands of the polymers with phenyl ester groups and those of PTT5BDTb were located at around 500–800 nm; this was consistent with the spectra of previously reported PTB-based polymers with alkyl ester groups, such as PTT5BDTa.^{6b} The optical bandgaps ($E_g^{\text{opt}} = 1240/\lambda_{\text{onset}}$) were estimated based on the absorption onset wavelength (λ_{onset}) of the polymer films and are summarized in Table 1-1. Compared with PTT5BDTb bearing an alkyl ester group, the polymers bearing phenyl ester groups exhibited somewhat narrower E_g^{opt} values, depending on the type of substituent. As the electron-withdrawing ability of the substituent increases, the optical bandgaps tend to be slightly narrower. These results

mean that the phenyl ester groups can contribute to elongation of the π -conjugation length of the polymer main chains.

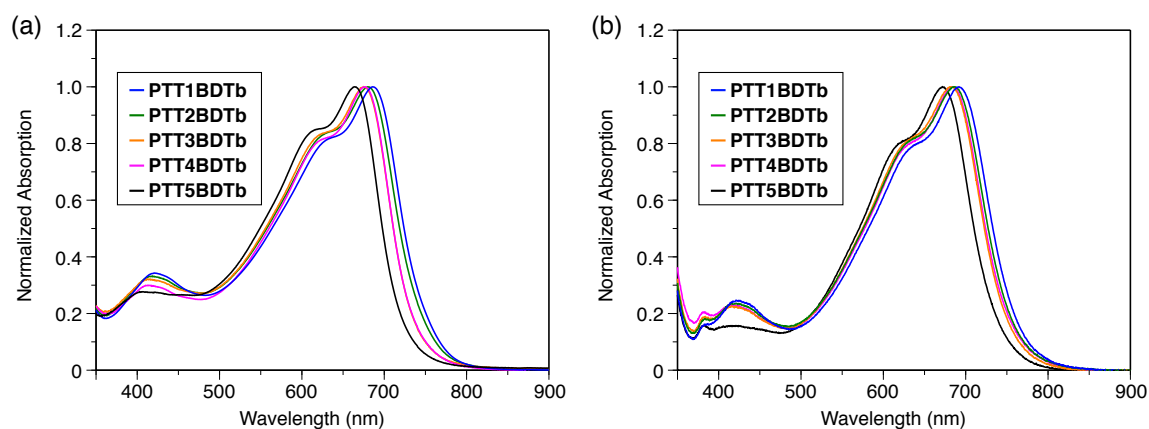


Figure 1-2. Absorption spectra of the polymers in chlorobenzene (a) and in the film state (b).

Energy levels

The HOMO energy levels of the polymers were estimated with a photoelectron spectrometer by measuring the ionic potential of the polymer films in air (Figure 1-3), and the LUMO energy levels were calculated from the values of the HOMO energy level and the E_g^{opt} ($\text{LUMO} = E_g^{\text{opt}} + \text{HOMO}$); the values are listed in Table 1-1. When electron-withdrawing groups such as trifluoromethyl and fluoro groups were introduced on the phenyl groups, the HOMO energy levels became deeper compared with those for the nonsubstituted PTT3BDTb (-5.23 eV). In contrast, electron-donating substituents such as a methoxy group raised the HOMO energy level to -5.12 eV. To visualize the substituent effect, the HOMO energy levels of the polymers are plotted against the

Hammett constants (σ)¹⁶ of the substituents in Figure 1-4. A relatively good linear relationship is observed between the HOMO energy levels and the σ values.

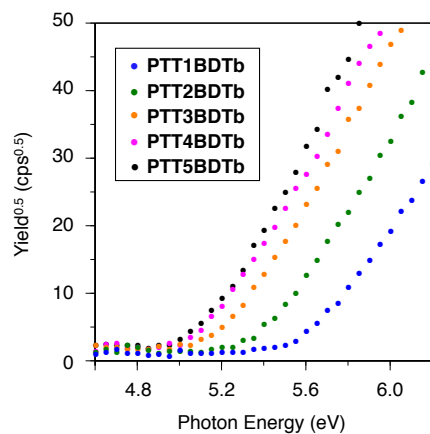


Figure 1-3. Photoelectron spectra of the polymers in air.

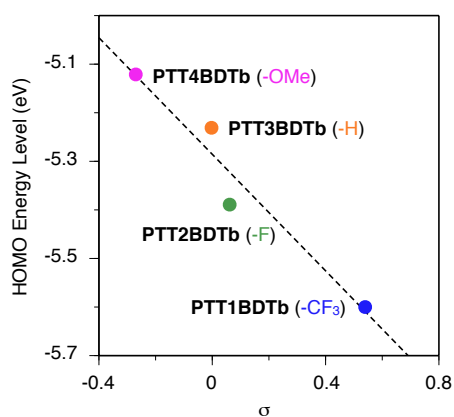


Figure 1-4. Plots of HOMO energy levels of the polymers against the Hammett constants σ of the substituents.

Computational studies using density functional theory (DFT) at the B3LYP/6-31G(d,p) level^{13a} were additionally performed for the corresponding model compounds to evaluate the influence of these substituents on the HOMO energy levels of the polymers (Figure 1-5). The calculated HOMO energy levels for the model compounds also showed a similar tendency to the experimental values for the polymers, although the calculated values were rather higher than the experimental ones (Figure 1-6). These results suggest that the substituents on the phenyl groups can perturb the electron density of the main chain through an ester linkage, and one can finely tune the HOMO energy levels of the polymers by selecting the substituents on the phenyl groups.

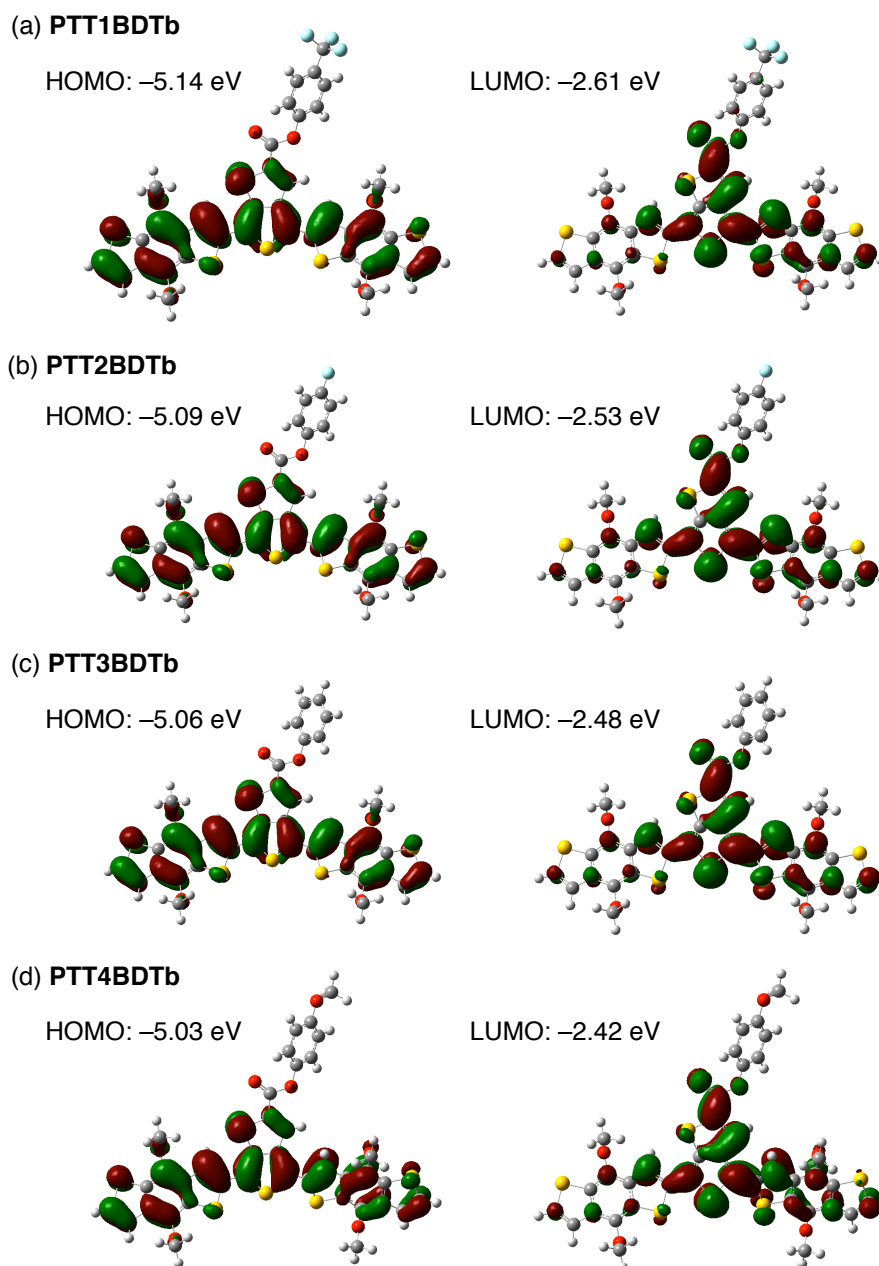


Figure 1-5. HOMO and LUMO energy levels and the frontier molecular orbital obtained from DFT calculations on the model compounds of (a) PTT1BDTb, (b) PTT2BDTb, (c) PTT3BDTb, and (d) PTT4BDTb.

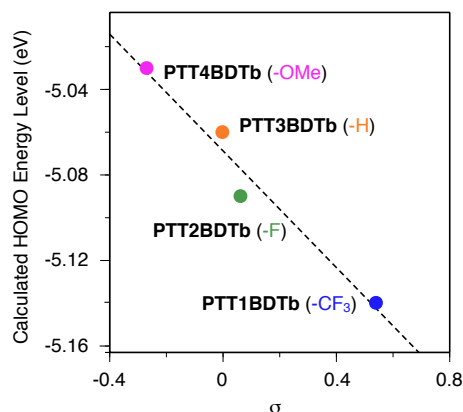


Figure 1-6. Plots of calculated HOMO energy levels of the polymers against the Hammett constants σ of the substituents.

Hole mobilities

The hole mobilities of these polymers were measured by a method based on the space-charge-limited current (SCLC) model using the corresponding hole-only devices.¹⁵ I - V characteristics of the hole-only devices in the dark in air are shown in Figures 1-7. The hole mobilities of PTT1BDTb, PTT2BDTb, PTT3BDTb, and PTT4BDTb bearing phenyl ester groups were estimated to be 1.4×10^{-5} , 2.8×10^{-5} , 2.0×10^{-5} , and $2.7 \times 10^{-5} \text{ cm}^2 \text{ V}^{-1} \text{ s}^{-1}$, respectively, which are comparable to that of PTT5BDTb bearing alkyl ester groups ($3.9 \times 10^{-5} \text{ cm}^2 \text{ V}^{-1} \text{ s}^{-1}$). Replacement of the alkyl esters with phenyl esters therefore seems to bring about only slight changes in the hole mobility for this type of polymer. However, the hole mobilities of these polymers were relatively low compared with that of PTT5BDTa with 2-ethylhexyloxy side chains on the BDT unit ($8.4 \times 10^{-5} \text{ cm}^2 \text{ V}^{-1} \text{ s}^{-1}$) measured with our hole-only device.¹⁷ The bulkier branched side chains, 2-octyldodecyloxy groups, on the BDT unit may increase the

steric hindrance and make it difficult to form efficient intermolecular π - π stacking, which is very important in transporting the holes inside the polymer films. It is therefore necessary to optimize the side-chain structures in consideration of both the solubility and the charge transport properties.

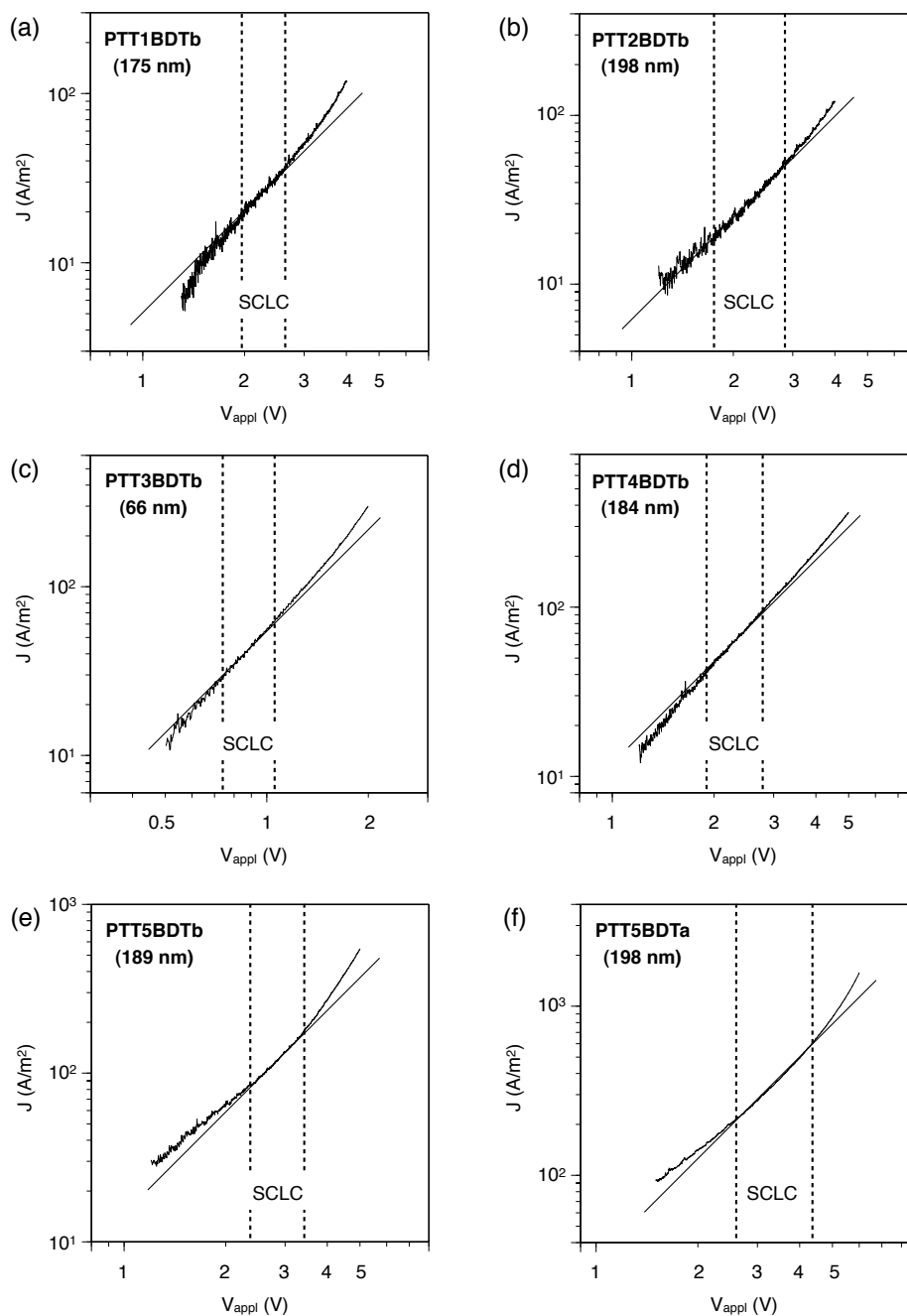


Figure 1-7. Double-logarithmic plots of I - V curves obtained for hole-only devices (ITO/PEDOT:PSS/PTB-based polymer/PEDOT:PSS/Au) in the dark in air: (a) PTT1BDTb, (b) PTT2BDTb, (c) PTT3BDTb, (d) PTT4BDTb, (e) PTT5BDTb, and (f) PTT5BDTa. The thickness (L) of the organic films determined by AFM is shown in the parentheses.

Conclusions

In conclusion, a series of PTB-based polymers consisting of alternating thieno[3,4-*b*]thiophene units bearing 4-substituted phenyl ester pendants and benzo[1,2-*b*:4,5-*b'*]dithiophene units were synthesized, and their thermal and optical properties were investigated. The author found that the HOMO energy levels of the polymers could be finely tuned in the range -5.12 to -5.60 eV by changing the substituents on the phenyl ring, and there was a relatively good linear correlation between the HOMO energy levels and the Hammett substituent constants. Since PTT1BDTb and PTT2BDTb with electron-withdrawing substituents possess deeper HOMO energy levels, at -5.60 and -5.39 eV, respectively, compared with those of previously reported PTB-based polymers,^{6b,8-9,18} the PSCs based on these polymers are expected to show higher V_{oc} values. Further improvements in hole mobility by optimizing the side-chain structures on the benzodithiophene units should therefore yield promising results for realizing high-efficiency PSCs. Detailed investigations of the photovoltaic properties of the PSCs produced using these PTB-based polymers are currently in progress and will be reported in due course.

References

- (1) (a) Günes, S.; Neugebauer, H.; Sariciftci, N. S. *Chem. Rev.* **2007**, *107*, 1324. (b) Thompson, B. C.; Fréchet, J. M. J. *Angew. Chem. Int. Ed.* **2008**, *47*, 58. (c) Cheng, Y.-J.; Yang, S.-H.; Hsu, C.-S. *Chem. Rev.* **2009**, *109*, 5868. (d) Peet, J.; Heeger, A. J.; Bazan, G. C. *Acc. Chem. Res.* **2009**, *42*, 1700. (e) Brabec, C. J.; Gowrisanker, S.; Halls, J. J. M.; Laird, D.; Jia, S.; Williams, S. P. *Adv. Mater.* **2010**, *22*, 3839.
- (2) Yu, G.; Gao, J.; Hummelen, J. C.; Wudl, F.; Heeger, A. J. *Science* **1995**, *270*, 1789.
- (3) (a) Li, G.; Shrotriya, V.; Huang, J.; Yao, Y.; Moriarty, T.; Emery, K.; Yang, Y. *Nat. Mater.* **2005**, *4*, 864. (b) Kim, Y.; Cook, S.; Tuladhar, S. M.; Choulis, S. A.; Nelson, J.; Durrant, J. R.; Bradley, D. D. C.; Giles, M.; McCulloch, I.; Ha, C.-S.; Ree, M. *Nat. Mater.* **2006**, *5*, 197.
- (4) Bundgaard, E.; Krebs, F. C. *Sol. Energy Mater. Sol. Cells* **2007**, *91*, 954.
- (5) (a) Winder, C.; Sariciftci, N. S. *J. Mater. Chem.* **2004**, *14*, 1077. (b) Chen, J.; Cao, Y. *Acc. Chem. Res.* **2009**, *42*, 1709. (c) Zhou, E.; Wei, Q.; Yamakawa, S.; Zhang, Y.; Tajima, K.; Yang, C.; Hashimoto, K. *Macromolecules* **2009**, *43*, 821. (d) Liang, Y.; Yu, L. *Acc. Chem. Res.* **2010**, *43*, 1227. (e) Boudreault, P.-L. T.; Najari, A.; Leclerc, M. *Chem. Mater.* **2011**, *23*, 456.
- (6) (a) Liang, Y.; Wu, Y.; Feng, D.; Tsai, S.-T.; Son, H.-J.; Li, G.; Yu, L. *J. Am. Chem. Soc.* **2009**, *131*, 56. (b) Liang, Y.; Feng, D.; Wu, Y.; Tsai, S.-T.; Li, G.; Ray, C.; Yu, L. *J. Am. Chem. Soc.* **2009**, *131*, 7792.
- (7) (a) Brabec, C. J.; Cravino, A.; Meissner, D.; Sariciftci, N. S.; Fromherz, T.; Rispen, S.

- M. T.; Sanchez, L.; Hummelen, J. C. *Adv. Funct. Mater.* **2001**, *11*, 374. (b) Scharber, M. C.; Mühlbacher, D.; Koppe, M.; Denk, P.; Waldauf, C.; Heeger, A. J.; Brabec, C. J. *Adv. Mater.* **2006**, *18*, 789.
- (8) Hou, J.; Chen, H.-Y.; Zhang, S.; Chen, R. I.; Yang, Y.; Wu, Y.; Li, G. *J. Am. Chem. Soc.* **2009**, *131*, 15586.
- (9) Chen, H.-Y.; Hou, J.; Zhang, S.; Liang, Y.; Yang, G.; Yang, Y.; Yu, L.; Wu, Y.; Li, G. *Nat. Photon.* **2009**, *3*, 649.
- (10) (a) Zwanenburg, D. J.; Haan, H. d.; Wynberg, H. *J. Org. Chem.* **1966**, *31*, 3363. (b) Yao, Y.; Liang, Y.; Shrotriya, V.; Xiao, S.; Yu, L.; Yang, Y. *Adv. Mater.* **2007**, *19*, 3979. (c) Dey, T.; Navarathne, D.; Invernale, M. A.; Berghorn, I. D.; Sotzing, G. A. *Tetrahedron Lett.* **2010**, *51*, 2089.
- (11) Hou, J.; Park, M.-H.; Zhang, S.; Yao, Y.; Chen, L.-M.; Li, J.-H.; Yang, Y. *Macromolecules* **2008**, *41*, 6012.
- (12) Letizia, J. A.; Salata, M. R.; Tribout, C. M.; Facchetti, A.; Ratner, M. A.; Marks, T. *J. J. Am. Chem. Soc.* **2008**, *130*, 9679.
- (13) (a) Lee, C.; Yang, W.; Parr, R. G. *Physical Review B* **1988**, *37*, 785. (b) Becke, A. D. *Physical Review A* **1988**, *38*, 3098. (c) Becke, A. D. *J. Chem. Phys.* **1993**, *98*, 5648.
- (14) Frisch, M. J.; Trucks, G. W.; Schlegel, H. B.; Scuseria, G. E.; Robb, M. A.; Cheeseman, J. R.; Montgomery, J. A. Jr.; Vreven, T.; Kudin, K. N.; Burant, J. C.; Millam, J. M.; Iyengar, S. S.; Tomasi, J.; Barone, V.; Mennucci, B.; Cossi, M.; Scalmani, G.; Rega, N.; Petersson, G. A.; Nakatsuji, H.; Hada, M.; Ehara, M.; Toyota,

K.; Fukuda, R.; Hasegawa, J.; Ishida, M.; Nakajima, T.; Honda, Y.; Kitao, O.; Nakai, H.; Klene, M.; Li, X.; Knox, J. E.; Hratchian, H. P.; Cross, J. B.; Bakken, V.; Adamo, C.; Jaramillo, J.; Gomperts, R.; Stratmann, R. E.; Yazyev, O.; Austin, A. J.; Cammi, R.; Pomelli, C.; Ochterski, J. W.; Ayala, P. Y.; Morokuma, K.; Voth, G. A.; Salvador, P.; Dannenberg, J. J.; Zakrzewski, V. G.; Dapprich, S.; Daniels, A. D.; Strain, M. C.; Farkas, O.; Malick, D. K.; Rabuck, A. D.; Raghavachari, K.; Foresman, J. B.; Ortiz, J. V.; Cui, Q.; Baboul, A. G.; Clifford, S.; Cioslowski, J.; Stefanov, B. B.; Liu, G.; Liashenko, A.; Piskorz, P.; Komaromi, I.; Martin, R. L.; Fox, D. J.; Keith, T.; Al-Laham, M. A.; Peng, C. Y.; Nanayakkara, A.; Challacombe, M.; Gill, P. M. W.; Johnson, B.; Chen, W.; Wong, M. W.; Gonzalez, C.; Pople, J. A. Gaussian 03, Revision B.04; Gaussian, Inc.: Pittsburgh, PA, 2003.

(15) Jung, J. W.; Jo, W. H. *Adv. Funct. Mater.* **2010**, *20*, 2355.

(16) Hansch, C.; Leo, A.; Taft, R. W. *Chem. Rev.* **1991**, *91*, 165.

(17) The hole mobility of PTT5BDTa has been reported to be $4.0 \times 10^{-4} \text{ cm}^2/(\text{V s})$,^{6b} which is rather higher than that estimated in this work. The difference may be ascribed to the different configurations of the hole-only devices.

(18) Son, H. J.; Wang, W.; Xu, T.; Liang, Y.; Wu, Y.; Li, G.; Yu, L. *J. Am. Chem. Soc.* **2011**, *133*, 1885.

Chapter 2

Fine Tuning of Frontier Orbital Energy Levels in Dithieno[3,2-*b*:2',3'-*d*]silole -Based Copolymers Based on the Substituent Effect of Phenyl Pendants

Abstract: A series of dithieno[3,2-*b*:2',3'-*d*]silole-based π -conjugated copolymers containing thieno[3,4-*c*]pyrrole-4,6-dione or thieno[3,4-*b*]thiophene units bearing 4-substituted phenyl pendants were synthesized and their thermal stability, optical properties and frontier orbital energy levels were systematically investigated. The introduction of electron-withdrawing substituents on the phenyl rings lowered their frontier orbital energy levels without deteriorating their thermal and optical properties. By replacing an electron-donating methoxy group with an electron-withdrawing trifluoromethyl group, both the highest occupied molecular orbital (HOMO) and the lowest unoccupied molecular orbital energy levels of the polymers were deepened by more than 0.3 eV. A relatively linear relationship was observed between the HOMO energy levels and the Hammett substituent constants.

Introduction

Much attention has been paid to bulk heterojunction-type polymer solar cells (BHJ-type PSCs) consisting of interpenetrating networks of π -conjugated polymers as electron donors and fullerene derivatives as electron acceptors.¹ This is because BHJ-type PSCs have potential advantages, such as their flexible and lightweight characteristics and the low-cost manufacturing of large-area devices using printing processes.² Regioregular poly(3-hexylthiophene) (P3HT) has been used as a typical electron donor in the active layers of BHJ-type PSCs, because of its solubility, stability and compatibility with the electron acceptor [6,6]-phenyl- C₆₁-butyric acid methyl ester (PC₆₁BM).³ However, P3HT can only harvest ca. 23% of all solar photons because its absorption limit is less than 650 nm.⁴ Therefore, extensive research has been conducted to develop narrow bandgap polymers that can harvest more of the solar photons than P3HT.⁵

The following two approaches have been widely used to narrow the bandgap energies of π -conjugated polymers. The first is to incorporate alternating electron-deficient units (A) and electron-rich units (D) along the polymer main-chains, inducing an intramolecular charge-transfer interaction that effectively narrows the bandgaps.⁶ Among a huge number of D-A-type conjugated polymers developed thus far, thieno[3,4-*c*]pyrrole-4,6-dione (TPD) is one of the most useful A units⁷ and BHJ-type PSCs based on D-A-type conjugated polymers consisting of alternating TPD and benzo[1,2-*b*:4,5-*b'*]dithiophene (BDT) units have exhibited a high power-conversion

efficiency (PCE) of 8.5%.⁷ⁱ The second approach is to use the stabilization of quinoidal resonance structures in the polymer main-chains. Thieno[3,4-*b*]thiophene (TT) is a representative unit used to stabilize the quinoidal resonance structure. TT has been incorporated into polymer backbones as a key component in electron donors.⁸ Particularly, π -conjugated polymers containing TT and BDT units (PTB-based polymers) have exhibited a maximum PCE of over 9%.⁹ The extended absorption properties of these narrow bandgap polymers directly contributed to increasing the short-circuit current density (J_{sc}).

To enhance the PCEs, the open-circuit voltages (V_{oc}) of PSCs should be increased along with improving the J_{sc} . It is well known that the V_{oc} is closely related to the difference between the highest occupied molecular orbital (HOMO) of the electron donors and the lowest unoccupied molecular orbital (LUMO) of the electron acceptors.¹⁰ Therefore, deepening the HOMO energy levels of narrow bandgap polymers is a useful strategy to develop efficient PSCs with high V_{oc} and J_{sc} values. In Chapter 1, the HOMO and LUMO energy levels of PTB-based polymers were effectively deepened by introducing electron-withdrawing substituents on the phenyl rings that were connected to the TT units through an ester linkage.¹¹ An advantage of this method is that the frontier orbital energy levels of the polymers can be precisely controlled by tuning the electron-withdrawing ability of the substituents on the phenyl rings.

In Chapter 2, the author synthesized dithieno[3,2-*b*:2',3'-*d*]silole-based

π -conjugated polymers containing either TPD or TT units as the comonomer units, which possessed 4-substituted phenyl pendants. The influence of the substituents on the phenyl pendants was systematically investigated by measuring the thermal stability, optical properties and frontier orbital energy levels. The DTS unit was used as the common building unit because DTS-based polymers have a higher photostability than the corresponding polymers containing BDT units and are more practical for use as electron donors in PSCs.¹²

Experimental Section

Materials

The anhydrous solvents (toluene, *N,N*-dimethylformamide (DMF) and tetrahydrofuran (THF)), the common organic solvents, aniline and *p*-anisidine were purchased from Kanto (Tokyo, Japan). Acetic anhydride, 2-bromothiophene, 2-(tributylstannyl)thiophene and *n*-octylamine were bought from Tokyo Kasei (TCI, Tokyo, Japan). Thionyl chloride and 4-fluoroaniline were purchased from Wako (Osaka, Japan). Chlorobenzene was obtained from Kishida (Osaka, Japan). Tetrakis(triphenylphosphine)palladium(0) and 4-trifluoromethylaniline were purchased from Nacalai (Kyoto, Japan). The thieno[3,4-*b*]thiophene-based monomers (TT1–TT4)¹¹, 2,5-dibromo-3,4-thiophenedicarboxylic acid (**1**)¹³ and 4,4-bis(2-ethylhexyl)-2,6-bis(trimethyltin)-dithieno[3,2-*b*:2',3'-*d*]silole (DTS)¹⁴ were prepared according to the procedures in the literature.

Instruments

The ^1H and ^{13}C NMR spectra were measured in CDCl_3 at room temperature or $55\text{ }^\circ\text{C}$ with a JEOL ECA-500 spectrometer (JEOL, Tokyo, Japan). The molecular weights and distributions of the polymers were estimated using size-exclusion chromatography (SEC) equipped with a Shodex KF-805L column (Showa Denko, Tokyo, Japan), a JASCO PU-2080 Plus HPLC pump (Jasco, Tokyo, Japan), a JASCO UV-970 UV/VIS detector at 650 nm and a JASCO CO-1560 column oven, where THF was used as the eluent. The molecular weight calibration curve was obtained with polystyrenes (Tosoh). Thermogravimetric analysis (TGA) was conducted using a TG/DTA6200 (SII NanoTechnology Inc., Chiba, Japan) with a heating rate of $10\text{ }^\circ\text{C}/\text{min}$ under a flow of nitrogen. The UV-vis-NIR spectra of the spin-coated films prepared on glass substrates from a chlorobenzene solution (5 mg/mL) were measured using a JASCO V-570 spectrometer. The HOMOs of the polymers were measured using a photoelectron spectrometer AC-2 (Riken Keiki, Tokyo, Japan) by measuring the ionization potential of polymer films in air. The ionization potential of the polymers was estimated using the plots of the photoelectron quantum yield from the polymer solid surface against the incident photon energy. The threshold of the photoelectron quantum yield was correlated with the ionization potential.

Synthesis of TPD-based monomers

1,3-Dibromo-5-(4-trifluoromethylphenyl)thieno[3,4-*c*] pyrrole-4,6-dione

(TPD1). Acetic anhydride (7.6 mL) was added to **1** (0.50 g, 1.52 mmol) under a nitrogen atmosphere. The mixture was heated to 140 °C for 12 h and then cooled to room temperature. The volatile compounds were removed *in vacuo* and the crude product was used in the next step without purification. After the brown solid was dissolved in toluene (1 mL), 4-trifluoromethylaniline (294 mg, 1.83 mmol) was added to the solution and the mixture was heated under reflux for 24 h. After removing the volatile components, thionyl chloride was added to the residue and the reaction mixture was stirred at 90 °C for 12 h. The volatile components were removed *in vacuo* and the residue was extracted with chloroform. The organic phase was dried with anhydrous sodium sulfate and the solvent was removed under a reduced pressure. The crude product was purified by column chromatography with silica gel using chloroform as the eluent. The product was recrystallized from ethanol to afford TPD1 as an off-white solid with a yield of 81%. ¹H NMR (500 MHz, CDCl₃, rt): δ 7.76 (d, *J* = 8.0 Hz, 2H), 7.55 (d, *J* = 8.0 Hz, 2H). ¹³C NMR (125 MHz, CDCl₃, rt): δ 158.73, 134.55, 133.86, 130.14, 126.42, 126.26, 126.23, 114.90. Anal. Calcd for C₁₃H₄Br₂F₃NO₂S: C, 34.31; H, 0.89; N, 3.08. Found: C, 34.11; H, 0.95; N, 3.06.

1,3-Dibromo-5-(4-fluorophenyl)thieno[3,4-*c*]pyrrole-4,6- dione (TPD2). The title compound was prepared from **1** and 4-fluoroaniline in the same way as TPD1 and obtained in 53% yield. ¹H NMR (500 MHz, CDCl₃, rt): δ 7.34 (m, 2H), 7.17 (t, *J* = 10.0

Hz, 2H). ^{13}C NMR (125 MHz, CDCl_3 , rt): δ 161.19, 161.18, 134.11, 128.31, 127.38, 116.20, 114.41. Anal. Calcd for $\text{C}_{12}\text{H}_4\text{Br}_2\text{FNO}_2\text{S}$: C, 35.59; H, 1.00; N, 3.46. Found: C, 35.76; H, 1.22; N, 3.48.

1,3-Dibromo-5-phenylthieno[3,4-*c*]pyrrole-4,6-dione (TPD3). The title compound was prepared from 1 and aniline in the same way as TPD1 and obtained in 85% yield. ^1H NMR (500 MHz, CDCl_3 , rt): δ 7.50 (t, $J = 7.7$ Hz, 2H), 7.42 (t, $J = 7.4$ Hz, 1H), 7.36 (m, 2H). ^{13}C NMR (125 MHz, CDCl_3 , rt): δ 159.27, 134.21, 131.41, 129.11, 128.56, 126.41, 114.15. Anal. Calcd for $\text{C}_{12}\text{H}_5\text{Br}_2\text{NO}_2\text{S}$: C, 37.24; H, 1.30; N, 3.62. Found: C, 37.04; H, 1.39; N, 3.64.

1,3-Dibromo-5-(4-methoxyphenyl)thieno[3,4-*c*]pyrrole-4,6-dione (TPD4). The title compound was prepared from 1 and *p*-anisidine in the same way as TPD1 and obtained in 22% yield. ^1H NMR (500 MHz, CDCl_3 , rt): δ 7.27 (d, $J = 9.0$ Hz, 2H), 6.98 (d, $J = 9.0$ Hz, 2H), 3.83 (s, 3H). ^{13}C NMR (125 MHz, CDCl_3 , rt): δ 159.71, 159.52, 134.59, 127.79, 124.46, 114.55, 113.80, 55.54. Anal. Calcd for $\text{C}_{13}\text{H}_7\text{Br}_2\text{NO}_3\text{S}$: C, 37.44; H, 1.69; N, 3.36. Found: C, 37.31; H, 1.89; N, 3.31.

1,3-Dibromo-5-octylthieno[3,4-*c*]pyrrole-4,6-dione (TPD5). The title compound was prepared from 1 and *n*-octylamine in the same way as TPD1 and obtained in 75% yield. ^1H NMR (500 MHz, CDCl_3 , rt): δ 3.59 (t, $J = 7.3$ Hz, 2H), 1.63 (t, $J = 7.3$ Hz,

2H), 1.4-1.2 (m, 10H), 0.87 ppm (t, $J = 6.8$ Hz, 3H). ^{13}C NMR (125 MHz, CDCl_3 , rt): δ 160.35, 134.76, 112.88, 38.79, 31.73, 29.07, 28.21, 26.75, 22.58, 14.06. Anal. Calcd for $\text{C}_{14}\text{H}_{17}\text{Br}_2\text{NO}_2\text{S}$: C, 39.74; H, 4.05; N, 3.31. Found: C, 39.85; H, 3.95; N, 3.29.

Polymerization

Copolymerization of DTS and TPD-based monomers. Polymerization was carried out in a dry Schlenk flask under a nitrogen atmosphere in a similar manner to that described in Chapter 1.^{7e} Each TPD-based monomer was purified by recrystallization before use. A typical polymerization procedure is described below.

DTS (111 mg, 0.15 mmol), TPD1 (68 mg, 0.15 mmol) and $\text{Pd}(\text{PPh}_3)_4$ (14 mg, 12 μmol) was placed in a Schlenk flask under a nitrogen atmosphere. Anhydrous toluene (2.7 mL) and DMF (0.27 mL) were added with a syringe and the mixture was heated to 110 °C. After 42 h, a solution of 2-(tributylstannyl)thiophene (14 mg, 38 μmol) in 0.27 mL of toluene/DMF (10:1, v/v) was added with a syringe and the reaction mixture was heated to 110 °C for 5 h. A solution of 2-bromothiophene (6 mg, 38 μmol) in 0.27 mL of toluene/DMF (10:1, v/v) was then added and the reaction mixture was further heated at 110 °C for an additional 8 h to complete the end-capping reaction. The reaction mixture was cooled to room temperature and poured into methanol (MeOH). The resulting polymer was collected by centrifugation and washed with hexane for 12 h and then with dichloromethane for 12 h in a Soxhlet apparatus to remove any by-products and oligomers. After the polymer was collected in chloroform, the chloroform solution

was passed through Celite to remove the metal catalyst. The solution was concentrated and poured into hexane. The precipitate was collected by centrifugation and dried *in vacuo* to yield PDTSTPD1, which was a dark purple solid (32 mg, 30%). ^1H NMR (500 MHz, CDCl_3 , 55 °C): δ 8.7–7.4 (br, 6H), 2.0–0.5 (br, 34H). Anal. Calcd for $(\text{C}_{37}\text{H}_{40}\text{F}_3\text{NO}_2\text{S}_3\text{Si})_n$: C, 62.42; H, 5.66; N, 1.97. Found: C, 62.12; H, 5.73; N, 1.93.

In the same way, PDTSTPD2, PDTSTPD3, PDTSTPD4 and PDTSTPD5 were synthesized with their corresponding monomers. The polymerization results are summarized in Table 2-1.

Spectroscopic data for PDTSTPD2. ^1H NMR (500 MHz, CDCl_3 , 55 °C): δ 8.7–8.0 (br, 2H), 7.7–6.9 (br, 4H), 2.0–0.5 (br, 34H). Anal. Calcd for $(\text{C}_{36}\text{H}_{40}\text{FNO}_2\text{S}_3\text{Si})_n$: C, 65.32; H, 6.09; N, 2.12. Found: C, 65.55; H, 6.11; N, 2.10.

Spectroscopic data for PDTSTPD3. ^1H NMR (500 MHz, CDCl_3 , 55 °C): δ 8.7–8.0 (br, 2H), 7.6–7.1 (br, 5H), 1.8–0.7 (br, 34H). Anal. Calcd for $(\text{C}_{36}\text{H}_{41}\text{NO}_2\text{S}_3\text{Si})_n$: C, 67.14; H, 6.42; N, 2.18. Found: C, 66.76; H, 6.78; N, 2.09.

Spectroscopic data for PDTSTPD4. ^1H NMR (500 MHz, CDCl_3 , 55 °C): δ 8.7–8.0 (br, 2H), 7.4–7.0 (br, 4H), 4.1–3.6 (br, 3H), 1.7–0.5 (br, 34H). Anal. Calcd for $(\text{C}_{37}\text{H}_{43}\text{NO}_3\text{S}_3\text{Si})_n$: C, 65.93; H, 6.43; N, 2.08. Found: C, 65.51; H, 6.11; N, 2.05.

Spectroscopic data for PDTSTPD5. ^1H NMR (500 MHz, CDCl_3 , 55 °C): δ 8.2–6.8 (br, 2H), 4.1–3.2 (br, 2H), 2.1–0.5 (br, 49H). Anal. Calcd for $(\text{C}_{38}\text{H}_{53}\text{NO}_2\text{S}_3\text{Si})_n$: C, 67.11; H, 7.86; N, 2.06. Found: C, 67.22; H, 7.69; N, 2.00.

Copolymerization of DTS and TT-based monomers. Polymerization was carried out in a dry Schlenk flask under a nitrogen atmosphere using a similar manner to that described in Chapter 1.¹¹ Each TT-based monomer was purified by recrystallization prior to use. A typical polymerization procedure is described below.

DTS (116 mg, 0.16 mmol), TT1 (76 mg, 0.16 mmol) and Pd(PPh₃)₄ (7.4 mg, 6.4 μmol) were placed in a Schlenk flask under a nitrogen atmosphere. Anhydrous toluene (2.56 mL) and DMF (0.64 mL) were added with a syringe and the mixture was then heated to 120 °C. After 12 h, the reaction mixture was cooled to room temperature and poured into a large amount of MeOH. The resulting polymer was collected by centrifugation and washed with MeOH followed by hexane for 12 h each in a Soxhlet apparatus to remove any by-products and oligomers. After the polymer was collected in chlorobenzene, the chlorobenzene solution was passed through Celite to remove the metal catalyst. The solution was concentrated and poured into hexane. The precipitate was collected by centrifugation and dried *in vacuo* to yield PDTSTT1, which was a dark blue solid (100 mg, 87%). ¹H NMR (500 MHz, CDCl₃, 55 °C): δ 8.0–6.8 (br, 7H), 2.0–0.5 (br, 34H). Anal. Calcd for (C₃₈H₄₁F₃O₂S₄Si·0.5H₂O)_n: C, 60.69; H, 5.63. Found: C, 60.74; H, 5.63.

Using the same method, PDTSTT2, PDTSTT3, PDTSTT4 and PDTSTT5 were synthesized with their corresponding monomers. The polymerization results are summarized in Table 2-1.

Spectroscopic data for PDTSTT2. ¹H NMR (500 MHz, CDCl₃, 55 °C): δ 8.3–6.8

(br, 7H), 2.0–0.4 (br, 34H). Anal. Calcd for $(C_{37}H_{41}FO_2S_4Si \cdot 0.4H_2O)_n$: C, 63.46; H, 6.02. Found: C, 63.42; H, 6.13.

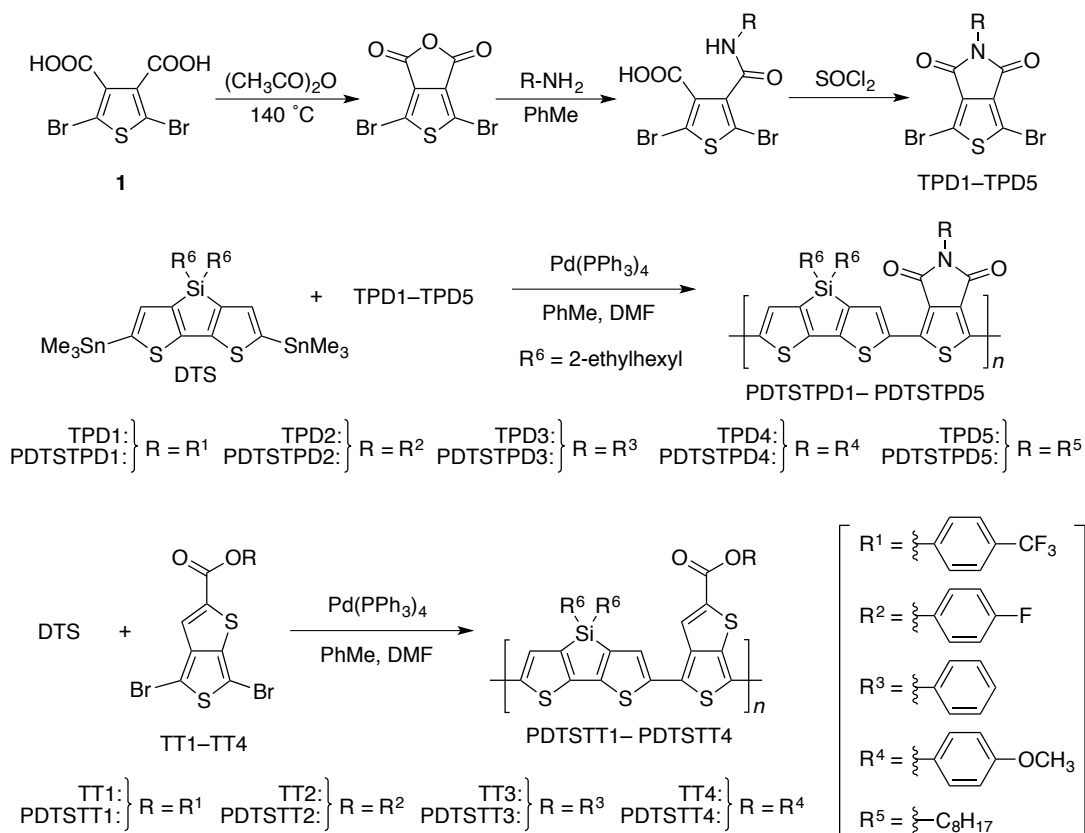
Spectroscopic data for PDTSTT3. 1H NMR (500 MHz, $CDCl_3$, 55 °C): δ 8.2–6.9 (br, 8H), 1.9–0.5 (br, 34H). Anal. Calcd for $(C_{37}H_{42}O_2S_4Si \cdot 0.6H_2O)_n$: C, 64.79; H, 6.35. Found: C, 64.75; H, 6.29.

Spectroscopic data for PDTSTT4. 1H NMR (500 MHz, $CDCl_3$, 55 °C): δ 8.3–6.8 (br, 7H), 4.0–3.7 (br, 3H), 2.0–0.5 (br, 34H). Anal. Calcd for $(C_{38}H_{44}O_3S_4Si \cdot 0.8H_2O)_n$: C, 63.44; H, 6.39. Found: C, 63.42; H, 6.16.

Computational study

The density functional theory (DFT) calculations were performed at the B3LYP/6-31G (d,p) level¹⁵ using the Gaussian 03 package. The model compounds, which consisted of either a TPD or a TT unit and two DTS units bearing methyl groups instead of 2-ethylhexyl groups, were used for the computational study as simplified models.

Scheme 2-1. Synthesis and structures of monomers and polymers.



Results and discussion

Synthesis

The synthetic routes for the monomers and polymers are shown in Scheme 1. Four TPD-based monomers bearing various phenyl groups (TPD1-TPD4) were easily prepared in one pot from commercially available aniline derivatives and the key precursor 1, which was synthesized using modified procedures from the literature.¹³ The copolymerizations of DTS and TPD1-TPD4 by Stille cross-coupling were carried out using $\text{Pd}(\text{PPh}_3)_4$ as the catalyst in a toluene/DMF mixture (10/1, v/v) at 110 °C (Table 2-1). For comparison, the previously reported polymer, PDTSTPD5 (run 5 in Table 2-1)

containing *n*-octyl chains instead of phenyl pendants, was also prepared.^{7c} In addition, PDTSTT-based polymers were also synthesized from DTS and TT1eTT4 comonomers (run 6–9 in Table 2-1) using a similar method as the PDTSTPD-based polymers. Both the PDTSTPD- and PDTSTT-based polymers exhibited good solubility in THF, chloroform and chlorobenzene. The molecular weights (M_n) and distributions (PDI) of the obtained polymers were determined by SEC in THF. All of the polymers had similar molecular weights. Thus, the structural modification of the phenyl groups with TPD and TT units had little effect on the polymerizability of these monomers.

Table 2-1. Polymerization results and thermal and optical properties of the polymers.

run	polymer	yield (%) ^a	M_n (10^4) ^b	PDI ^b	T_{d5} (°C) ^c	λ_{onset} (nm)	E_g^{opt} (eV) ^d	HOMO (eV) ^e	LUMO (eV) ^f
1	PDTSTPD1	30	1.1	1.8	435	742	1.67	-5.88	-4.21
2	PDTSTPD2	34	1.3	1.5	435	733	1.69	-5.56	-3.87
3	PDTSTPD3	40	1.5	1.7	430	729	1.70	-5.42	-3.72
4	PDTSTPD4	25	2.3	1.8	432	729	1.70	-5.38	-3.68
5	PDTSTPD5	41	2.5	1.7	428	719	1.72	-5.38	-3.66
6	PDTSTT1	87	1.6	2.5	348	913	1.36	-5.40	-4.04
7	PDTSTT2	67	1.7	2.7	380	908	1.36	-5.20	-3.84
8	PDTSTT3	69	1.6	2.5	386	900	1.38	-5.09	-3.71
9	PDTSTT4	76	1.4	2.4	367	899	1.38	-5.07	-3.69

^a MeOH and hexane insoluble part. ^b Determined by SEC (eluent: THF, PSt standards). ^c The 5% weight-loss temperatures with a heating rate of 10 °C/min in N₂. ^d Calculated from $E_g = 1240/\lambda_{\text{onset}}$. ^e Measured by photoelectron spectroscopy in air. ^f Calculated from LUMO = E_g + HOMO.

Thermal properties

The thermal stabilities of these polymers were investigated by TGA under a nitrogen atmosphere (Figure 2-1). Both types of polymers demonstrated good thermal stability with 5% weight-loss temperatures (T_{d5}) above 300 °C (Table 2-1), which is adequate for application in PSC devices. Particularly, the T_{d5} values for the PDTSTPD-based polymers were around 430 °C and much higher than those for the corresponding PDTSTT-based polymers. The superior thermal stability of the PDTSTPD-based polymers was likely derived from the imide linkage in the TPD unit, which is more robust than the ester linkage in the TT unit. In addition, the T_{d5} values for the PDTSTPD-based polymers bearing phenyl pendants on the TPD unit were slightly higher than that for PDTSTPD5 bearing alkyl pendants,^{7e} so replacement of alkyl group with phenyl group seems to enhance thermal stability.

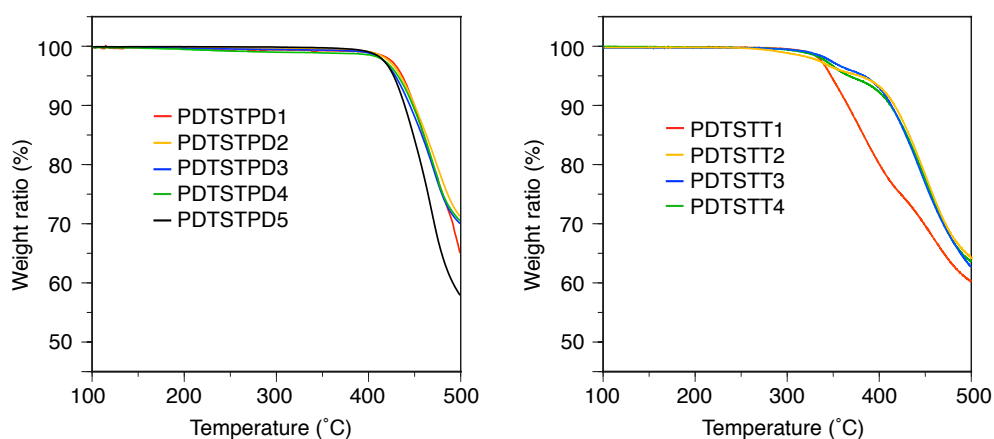


Figure 2-1. Thermogravimetric analysis of the polymers with a heating rate of 10 °C/min in N₂.

Optical properties

Figure 2-2 shows the absorption spectra of the polymers in chlorobenzene and in the film state. The absorption spectrum of each polymer in solution is very similar to that in the solid state, suggesting that both types of polymers possess a rigid-rod conformation in both states. The absorption bands of the PDTSTPD-based polymers with phenyl pendants were located at 500–750 nm. This was consistent with the spectrum of the previously reported PDTSTPD5 polymer with alkyl chains on the TPD unit.^{7e} The optical bandgaps were estimated based on the absorption onset wavelength (λ_{onset}) of the polymer films ($E_{\text{g}}^{\text{opt}} = 1240/\lambda_{\text{onset}}$) and are summarized in Table 2-1. Compared with PDTSTPD5, the PDTSTPD-based polymers bearing phenyl pendants exhibited somewhat narrower $E_{\text{g}}^{\text{opt}}$ values, depending on the type of substituent used. As the electron-withdrawing ability of the substituent increased, the $E_{\text{g}}^{\text{opt}}$ values tended to become narrower. These results were consistent with that described in Chapter 1.¹¹ This showed that the phenyl groups could contribute to elongation of the π -conjugation length in the polymer main-chains. The PDTSTT-based polymers also demonstrated a similar tendency in their absorption spectra, although the replacement of the TPD unit with the TT unit resulted in broadening and large redshifts in the absorption spectra. This is probably due to the stabilization of the quinoidal resonance structure in the main chains.

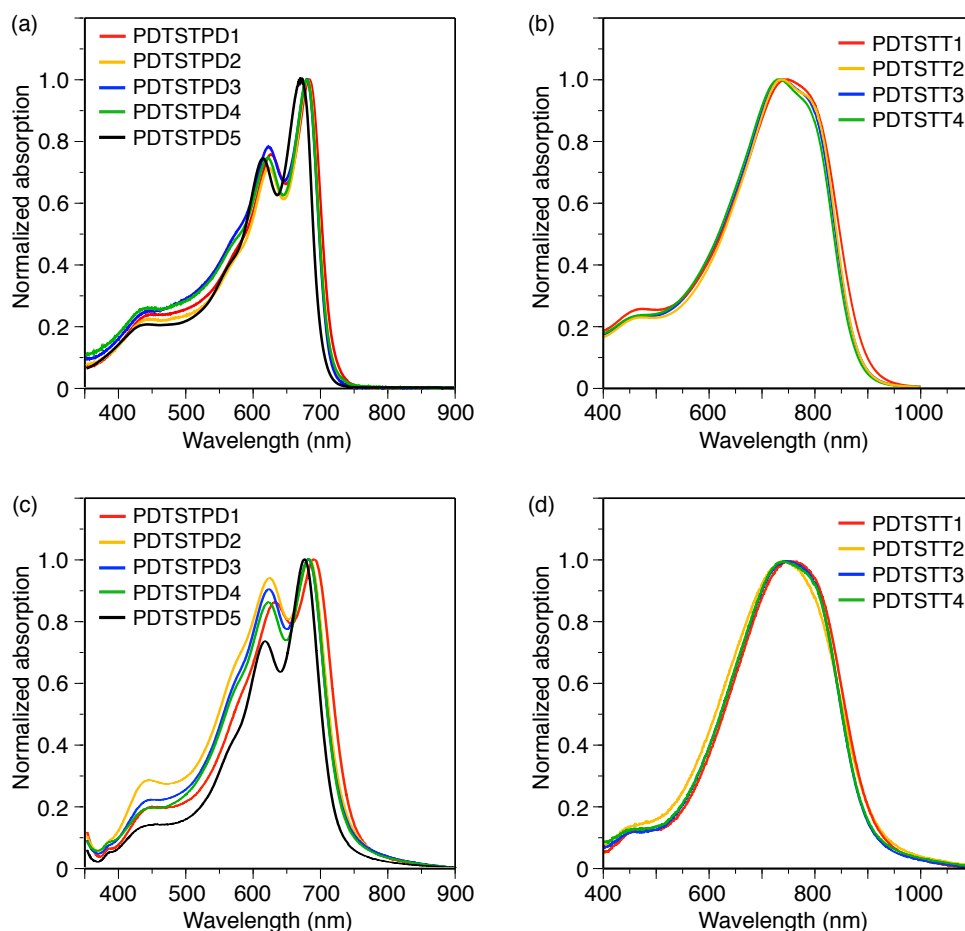


Figure 2-2. Absorption spectra of the polymers in chlorobenzene (a,b) and in the film states (c,d).

Energy levels

The HOMO energy levels of the polymers were estimated with a photoelectron spectrometer by measuring the ionic potential of the polymer films in air (Figure 2-3). The LUMO energy levels were calculated from the values of the HOMO energy levels and the E_g^{opt} ($LUMO = E_g^{opt} + HOMO$). The HOMO and LUMO energy levels for the polymers are listed in Table 2-1. The HOMO energy levels are plotted against the Hammett constant (σ)¹⁶ of the substituents in Figure 2-4 (a, b). When the

electron-withdrawing groups, such as trifluoromethyl and fluoro groups, were introduced on the phenyl groups in both polymers, the HOMO energy levels were deeper than those for the non-substituted PDTSTPD3 (-5.42 eV) and PDTSTT3 (-5.09 eV). In contrast, electron-donating substituents, such as a methoxy group, raised the HOMO energy levels to -5.38 eV for PDTSTPD4 and -5.07 eV for PDTSTT4. A relatively linear relationship was observed between the HOMO energy levels and the σ values.

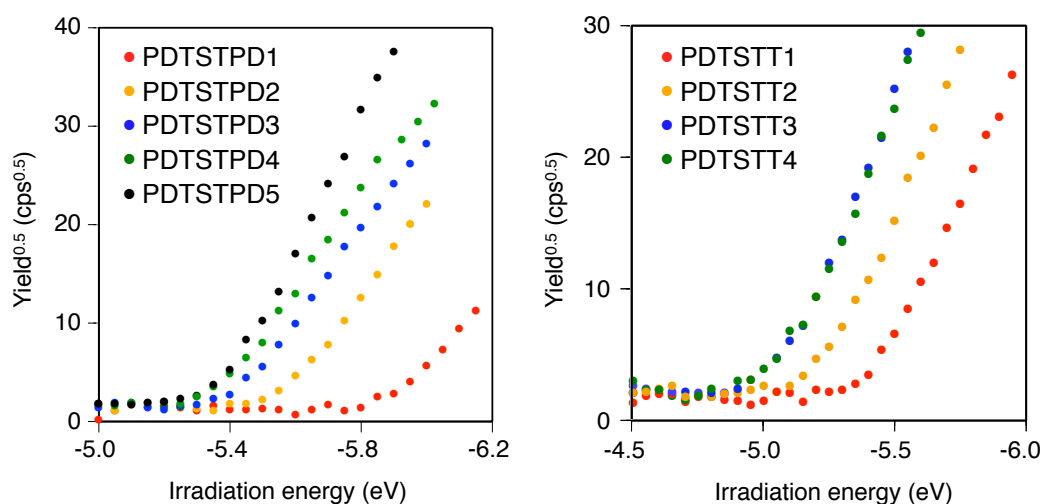


Figure 2-3. Photoelectron spectra of the polymers in air.

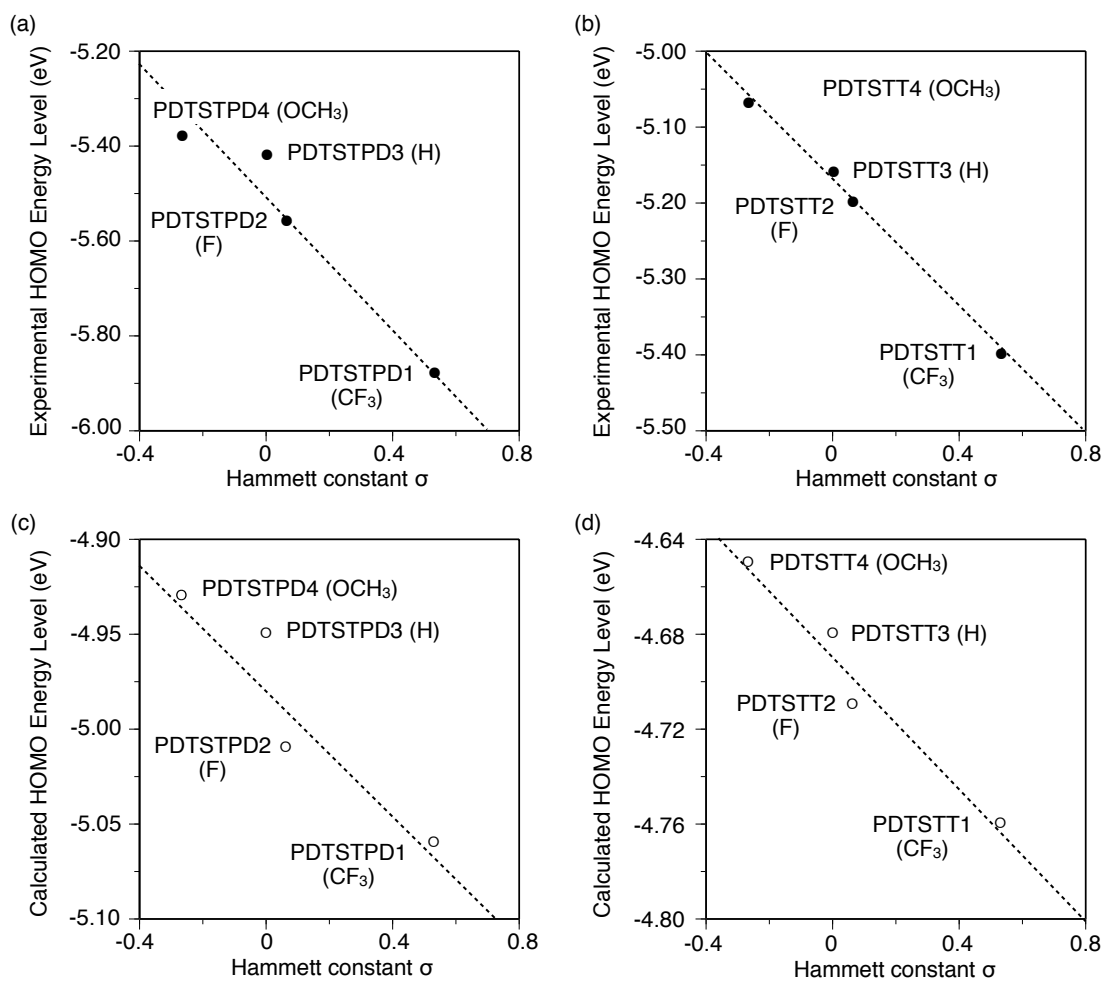


Figure 2-4. Plots of experimental (closed circle) and calculated (open circle) HOMO energy levels of PDTSTPD- (a, c) and PDTSTT- (b, d) based polymers against the Hammett constant σ of the substituents.

Computational studies using DFT at the B3LYP/6-31G (d,p) level¹⁵ were performed using the corresponding model compounds to evaluate the influence of these substituents on the HOMO energy levels of the polymers (Figure 2-5, 2-6). In agreement with the above-mentioned experimental results for the polymers, the introduction of electron-withdrawing substituents onto the phenyl rings of the model compounds lowered their calculated HOMO energy levels and vice versa. Figure 2-4 (c, d) shows that the calculated HOMO energy levels for the model compounds also have an almost linear relationship with the σ values, although the calculated levels are rather higher than the experimental levels. These results suggest that the substituents on the phenyl groups were able to efficiently perturb the electron density of the main chain. Particularly, the tuning range of the PDTSTPD-based polymers was larger than that of the PDTSTT-based polymers. This is probably because the 4-substituted phenyl pendants were directly connected to the TPD units in the PDTSTPD-based polymers, while the phenyl pendants in the PDTSTT-based polymers were connected to the TT units through the ester linkages. The HOMO energy levels of the narrow bandgap polymers could be finely tuned by selecting the substituents on the phenyl groups.

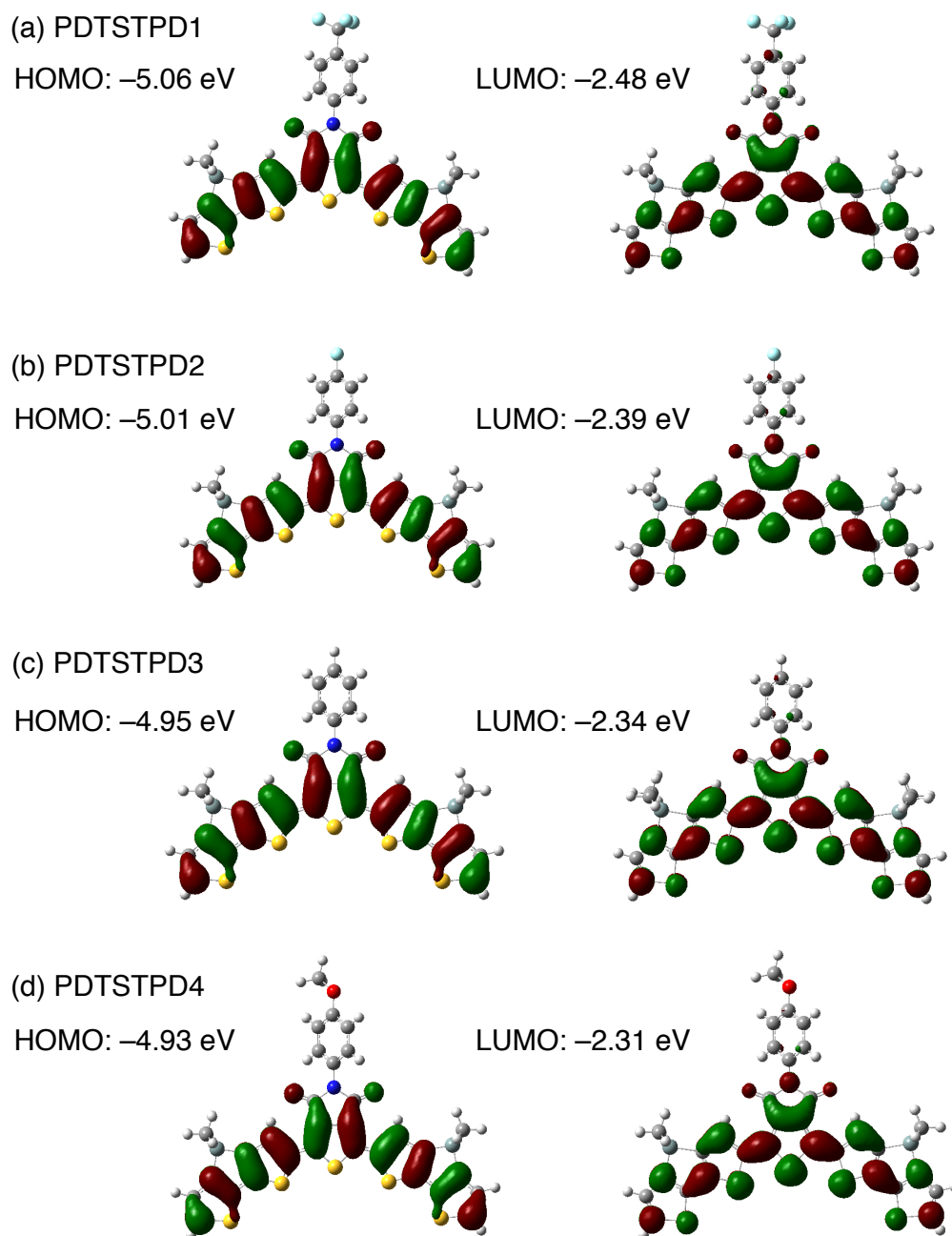


Figure 2-5. HOMO and LUMO energy levels and the frontier molecular orbital obtained from DFT calculations on the model compounds of (a) PDTSTPD1, (b) PDTSTPD2, (c) PDTSTPD3, and (d) PDTSTPD4.

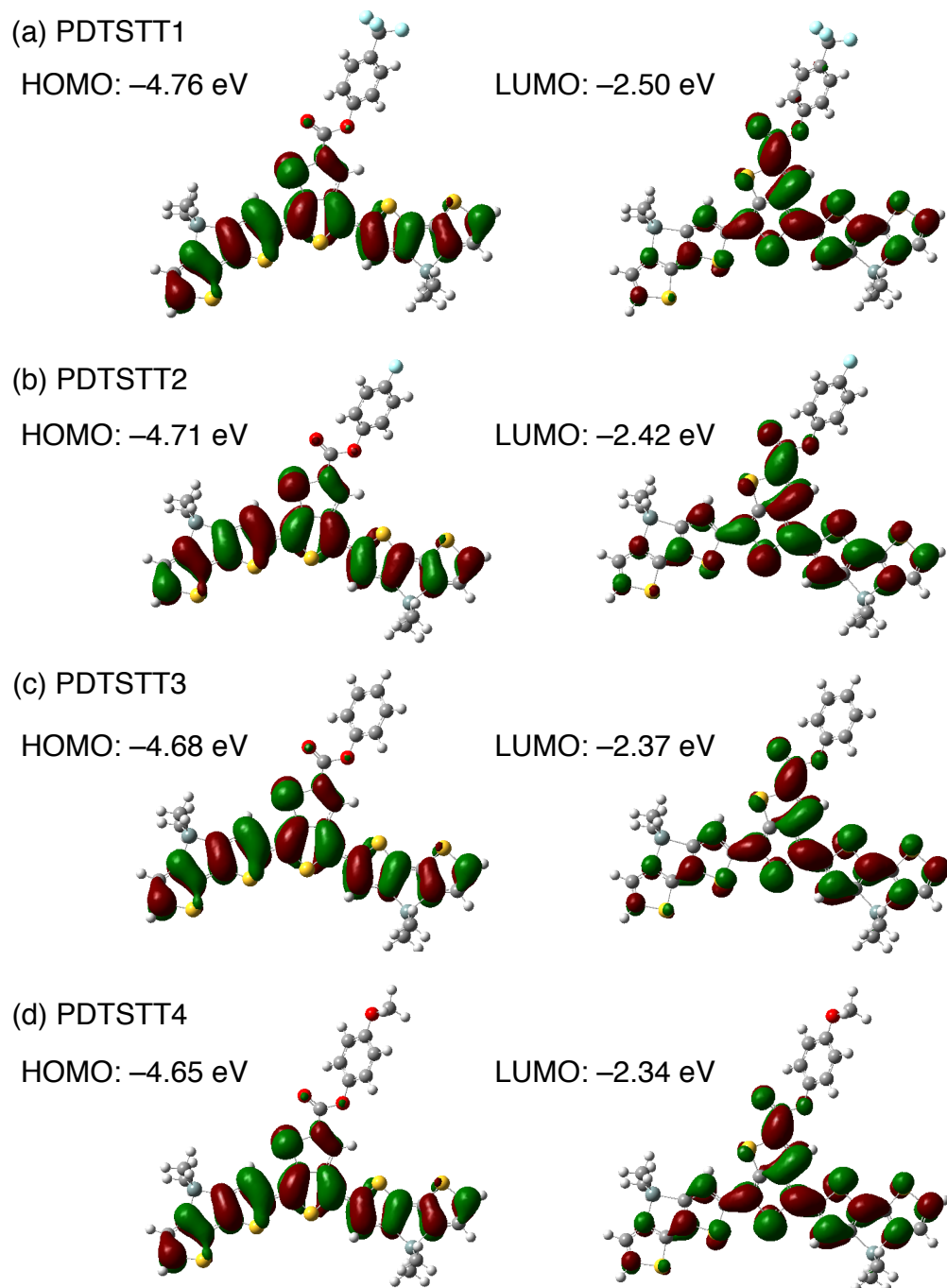


Figure 2-6. HOMO and LUMO energy levels and the frontier molecular orbital obtained from DFT calculations on the model compounds of (a) PDTSTT1, (b) PDTSTT2, (c) PDTSTT3, and (d) PDTSTT4.

Conclusions

A series of dithieno[3,2-*b*:2',3'-*d*]silole-based π -conjugated polymers consisting of thieno[3,4-*c*]pyrrole-4,6-dione or thieno[3,4-*b*]thiophene units bearing 4-substituted phenyl pendants were synthesized and their thermal and optical properties were investigated. The HOMO energy levels of the polymers could be finely tuned in the range -5.88 to -5.38 eV and -5.40 to -5.07 eV for the PDTSTPD- and PDTSTT-based polymers, respectively, by just changing the substituents on the phenyl rings. Because there were relatively linear correlations between the HOMO energy levels and the Hammett substituent constants, an electron donor polymer with optimal energy levels can be purposefully prepared by considering the energy levels of applied electron-acceptors.

References

- (1) (a) Yu, G.; Gao, J.; Hummelen, J. C.; Wudl, F.; Heeger, A. J. *Science* **1995**, *270*, 1789. (b) Günes, S.; Neugebauer, H.; Sariciftci, N. S. *Chem. Rev.* **2007**, *107*, 1324. (c) Cheng, Y.-J.; Yang, S.-H.; Hsu, C.-S. *Chem. Rev.* **2009**, *109*, 5868. (d) Peet, J.; Heeger, A. J.; Bazan, G. C. *Acc. Chem. Res.* **2009**, *42*, 1700. (e) Brabec, C. J.; Gowrisanker, S.; Halls, J. J. M.; Laird, D.; Jia, S.; Williams, S. P. *Adv. Mater.* **2010**, *22*, 3839. (f) Beaujuge, P. M.; Fréchet, J. M. J. *J. Am. Chem. Soc.* **2011**, *133*, 20009. (g) Facchetti, A. *Chem. Mater.* **2011**, *23*, 733. (h) Li, G.; Zhu, R.; Yang, Y. *Nat. Photon.* **2012**, *6*, 153.
- (2) Søndergaard, R.; Hösel, M.; Angmo, D.; Larsen-Olsen, T. T.; Krebs, F. C. *Mater. Today* **2012**, *15*, 36.
- (3) (a) Li, G.; Shrotriya, V.; Huang, J.; Yao, Y.; Moriarty, T.; Emery, K.; Yang, Y. *Nat. Mater.* **2005**, *4*, 864. (b) Kim, Y.; Cook, S.; Tuladhar, S. M.; Choulis, S. A.; Nelson, J.; Durrant, J. R.; Bradley, D. D. C.; Giles, M.; McCulloch, I.; Ha, C.-S.; Ree, M. *Nat. Mater.* **2006**, *5*, 197. (c) Marrocchi, A.; Lanari, D.; Facchetti, A.; Vaccaro, L. *Energy Environ. Sci.* **2012**, *5*, 8457. (d) Dang, M. T.; Hirsch, L.; Wantz, G.; Wuest, J. D. *Chem. Rev.* **2013**, *113*, 3734.
- (4) Bundgaard, E.; Krebs, F. C. *Sol. Energy Mater. Sol. Cells* **2007**, *91*, 954.
- (5) (a) Winder, C.; Sariciftci, N. S. *J. Mater. Chem.* **2004**, *14*, 1077. (b) Chen, J.; Cao, Y. *Acc. Chem. Res.* **2009**, *42*, 1709. (c) Boudreault, P.-L. T.; Najari, A.; Leclerc, M. *Chem. Mater.* **2011**, *23*, 456. (d) Bian, L.; Zhu, E.; Tang, J.; Tang, W.; Zhang, F. *Prog. Polym. Sci.* **2012**, *37*, 1292. (e) Li, Y. *Acc. Chem. Res.* **2012**, *45*, 723. (f) Mayukh, M.;

- Jung, I. H.; He, F.; Yu, L. *J. Polym. Sci., Part B: Polym. Phys.* **2012**, *50*, 1057.
- (6) (a) Beaujuge, P. M.; Amb, C. M.; Reynolds, J. R. *Acc. Chem. Res.* **2010**, *43*, 1396.
(b) Uy, R. L.; Price, S. C.; You, W. *Macromol. Rapid Commun.* **2012**, *33*, 1162.
- (7) (a) Piliago, C.; Holcombe, T. W.; Douglas, J. D.; Woo, C. H.; Beaujuge, P. M.; Fréchet, J. M. J. *J. Am. Chem. Soc.* **2010**, *132*, 7595. (b) Yuan, M.-C.; Chiu, M.-Y.; Liu, S.-P.; Chen, C.-M.; Wei, K.-H. *Macromolecules* **2010**, *43*, 6936. (c) Zou, Y.; Najari, A.; Berrouard, P.; Beaupré, S.; Réda Aïch, B.; Tao, Y.; Leclerc, M. *J. Am. Chem. Soc.* **2010**, *132*, 5330. (d) Amb, C. M.; Chen, S.; Graham, K. R.; Subbiah, J.; Small, C. E.; So, F.; Reynolds, J. R. *J. Am. Chem. Soc.* **2011**, *133*, 10062. (e) Chu, T. Y.; Lu, J.; Beaupré, S.; Zhang, Y.; Pouliot, J. R.; Wakim, S.; Zhou, J.; Leclerc, M.; Li, Z.; Ding, J.; Tao, Y. *J. Am. Chem. Soc.* **2011**, *133*, 4250. (f) Guo, X.; Xin, H.; Kim, F. S.; Liyanage, A. D. T.; Jenekhe, S. A.; Watson, M. D. *Macromolecules* **2011**, *44*, 269. (g) Li, Z.; Tsang, S.-W.; Du, X.; Scoles, L.; Robertson, G.; Zhang, Y.; Toll, F.; Tao, Y.; Lu, J.; Ding, J. *Adv. Funct. Mater.* **2011**, *21*, 3331. (h) Wen, S.; Cheng, W.; Li, P.; Yao, S.; Xu, B.; Li, H.; Gao, Y.; Wang, Z.; Tian, W. *J. Polym. Sci., Part A: Polym. Chem.* **2012**, *50*, 3758. (i) Cabanetos, C.; El Labban, A.; Bartelt, J. A.; Douglas, J. D.; Mateker, W. R.; Frechet, J. M.; McGehee, M. D.; Beaujuge, P. M. *J. Am. Chem. Soc.* **2013**, *135*, 4656. (j) Pron, A.; Berrouard, P.; Leclerc, M. *Macromol. Chem. Phys.* **2013**, *214*, 7.
- (8) (a) Pomerantz, M.; Gu, X.; Zhang, S. X. *Macromolecules* **2001**, *34*, 1817. (b) Yao, Y.; Liang, Y.; Shrotriya, V.; Xiao, S.; Yu, L.; Yang, Y. *Adv. Mater.* **2007**, *19*, 3979. (c) Liang, Y.; Xiao, S.; Feng, D.; Yu, L. *J. Phys. Chem. C* **2008**, *112*, 7866. (d) Liang, Y.;

Feng, D.; Guo, J.; Szarko, J. M.; Ray, C.; Chen, L. X.; Yu, L. *Macromolecules* **2009**, *42*, 1091. (e) Kleinhenz, N.; Yang, L.; Zhou, H.; Price, S. C.; You, W. *Macromolecules* **2011**, *44*, 872.

(9) (a) Chen, H.-Y.; Hou, J.; Zhang, S.; Liang, Y.; Yang, G.; Yang, Y.; Yu, L.; Wu, Y.; Li, G. *Nat. Photon.* **2009**, *3*, 649. (b) Hou, J.; Chen, H.-Y.; Zhang, S.; Chen, R. I.; Yang, Y.; Wu, Y.; Li, G. *J. Am. Chem. Soc.* **2009**, *131*, 15586. (c) Liang, Y.; Feng, D.; Wu, Y.; Tsai, S. T.; Li, G.; Ray, C.; Yu, L. *J. Am. Chem. Soc.* **2009**, *131*, 7792. (d) Liang, Y.; Wu, Y.; Feng, D.; Tsai, S.-T.; Son, H.-J.; Li, G.; Yu, L. *J. Am. Chem. Soc.* **2009**, *131*, 56. (e) Carsten, B.; Szarko, J. M.; Son, H. J.; Wang, W.; Lu, L.; He, F.; Rolczynski, B. S.; Lou, S. J.; Chen, L. X.; Yu, L. *J. Am. Chem. Soc.* **2011**, *133*, 20468. (f) Huo, L.; Zhang, S.; Guo, X.; Xu, F.; Li, Y.; Hou, J. *Angew. Chem. Int. Ed.* **2011**, *50*, 9697. (g) Son, H. J.; Wang, W.; Xu, T.; Liang, Y.; Wu, Y.; Li, G.; Yu, L. *J. Am. Chem. Soc.* **2011**, *133*, 1885. (h) He, Z.; Zhong, C.; Su, S.; Xu, M.; Wu, H.; Cao, Y. *Nat. Photon.* **2012**, *6*, 591.

(10) (a) Brabec, C. J.; Cravino, A.; Meissner, D.; Sariciftci, N. S.; Fromherz, T.; Rispens, M. T.; Sanchez, L.; Hummelen, J. C. *Adv. Funct. Mater.* **2001**, *11*, 374. (b) Scharber, M. C.; Mühlbacher, D.; Koppe, M.; Denk, P.; Waldauf, C.; Heeger, A. J.; Brabec, C. J. *Adv. Mater.* **2006**, *18*, 789.

(11) Yamamoto, T.; Ikai, T.; Kuzuba, M.; Kuwabara, T.; Maeda, K.; Takahashi, K.; Kanoh, S. *Macromolecules* **2011**, *44*, 6659.

(12) Alem, S.; Wakim, S.; Lu, J.; Robertson, G.; Ding, J.; Tao, Y. *ACS Appl Mater*

Interfaces **2012**, *4*, 2993.

(13) Cao, J.; Zhang, W.; Xiao, Z.; Liao, L.; Zhu, W.; Zuo, Q.; Ding, L. *Macromolecules* **2012**, *45*, 1710.

(14) Liao, L.; Dai, L.; Smith, A.; Durstock, M.; Lu, J.; Ding, J.; Tao, Y. *Macromolecules* **2007**, *40*, 9406.

(15) (a) Lee, C.; Yang, W.; Parr, R. G. *Physical Review B* **1988**, *37*, 785. (b) Becke, A. *J. Chem. Phys.* **1993**, *98*, 5648.

(16) Hansch, C.; Leo, A.; Taft, R. W. *Chem. Rev.* **1991**, *91*, 165.

Chapter 3

Influence of 4-Fluorophenyl Pendants in Thieno[3,4-*b*]thiophene– Benzo[1,2-*b*:4,5-*b'*]dithiophene-Based Polymers on the Performance of Photovoltaics

Abstract: Polymers consisting of benzo[1,2-*b*:4,5-*b'*]dithiophene and thieno[3,4-*b*]thiophene units (PTB-based polymers), either fully or partially containing 4-fluorophenyl pendants, are synthesized as electron donor materials for inverted-type polymer solar cells (PSCs). The influence of the 4-fluorophenyl pendant content on the thermal and optical properties, the highest occupied molecular orbital (HOMO) and lowest unoccupied molecular orbital (LUMO), the hole mobilities, and photovoltaic performances are investigated. As the 4-fluorophenyl pendant content increased, the HOMO and LUMO of the polymers were deepened proportionally and the open-circuit voltages of the PSCs improved. Incorporation of 4-fluorophenyl pendants into the polymers also affected the crystallinity, orientation, and compatibility with [6,6]-phenyl-C₆₁-butyric acid methyl ester in the active layers, leading to nonlinearities in the short-circuit current densities and fill factors. The incorporation of an appropriate number of 4-fluorophenyl pendants enhanced the power conversion efficiencies of the PSC devices from 2.25% to 3.96% for identical device configurations.

Introduction

Bulk heterojunction (BHJ) polymer solar cells (PSCs) have attracted much interest because of their potential advantages from a practical application perspective. These include their flexible and lightweight characteristics and the low manufacture cost of large-scale devices using printing processes.¹ Typical BHJ PSCs consist of π -conjugated polymers as the electron donor and fullerene derivatives as the electron acceptor. It has been suggested that ideal electron-donating polymers, for use in PSCs, should possess the following properties: a broad and efficient absorption consistent with the solar spectrum to ensure they efficiently harvest solar light;² a low-lying highest occupied molecular orbital (HOMO), to increase the open-circuit voltage (V_{oc}) and a suitable lowest unoccupied molecular orbital (LUMO) to provide efficient electron transfer to the acceptor materials;³ a high hole mobility for rapid charge transport;⁴ and moderate compatibility with acceptor materials, to form an interpenetrated network on a nanometer scale.⁵ Among the large number of donor materials reported to date, polymers consisting of thieno[3,4-*b*]thiophene (TT) and benzo[1,2-*b*:4,5-*b'*]dithiophene (BDT) repeat units (PTB-based polymers) approximately satisfy these requirements.⁶ Several PTB-based polymers are commercially available and are widely used as powerful donor materials in the research and development of PSC devices. Structurally altering the PTB-based polymers has been performed to improve the power conversion efficiency (PCE) of the PSCs. The direct introduction of fluoro groups into the polymer backbones has been demonstrated to be effective in increasing the photovoltaic

performance.^{6a,7} An excellent PCE over 9% was achieved using a PTB-based polymer containing 3-fluoro-2-[(2-ethylhexyl)carbonyl]thieno[3,4-*b*]thiophene units.⁸ The reasons for the improvement in the PCE are believed to be because of the increase in the V_{oc} , resulting from the deepened HOMO and the appropriate miscibility of the polymer with the fullerene derivatives, forming an ideal bi-continuous BHJ structure. Along with PTB-based polymers, enhancement of the photovoltaic performance by the introduction of fluoro groups into the polymer backbone has also been reported for several donor materials.⁹ In these systems, the dipole moments produced by the appended fluoro groups and fluorine-mediated interactions are thought to be the primary factors for the improved performance.

As described in Chapter 1, the author have developed a series of PTB-based polymers containing various phenyl ester pendants attached to the TT units and found that their HOMOs could be controlled by changing the substituents on the phenyl rings, despite the large distances between the substituents and backbones.¹⁰ The HOMOs of the PTB-based polymers bearing 4-fluorophenyl ester pendants was more than 0.2 eV deeper than those of the corresponding polymers that contain conventional alkyl ester pendants. Because donor polymers with a deeper HOMO tend to have higher V_{oc} values, PTB-based polymers containing 4-fluorophenyl ester pendants have the potential for developing highly efficient PSCs with an increased V_{oc} . Here, the author synthesized a series of PTB-based ternary copolymers consisting of two types of thienothiophene components bearing 4-fluorophenyl and *n*-octyl esters (PTB-F_x) (Scheme 3-1). These

polymers were used as electron donor materials in inverted-type PSCs. The influence of the number of 4-fluorophenyl pendants on the thermal and optical properties, frontier orbitals, morphologies, and crystallinities of the films blended with PC₆₁BM, and the hole mobilities and photovoltaic performances were investigated.

Experimental Section

Materials

Anhydrous solvents (toluene, *N,N*-dimethylformamide (DMF)) and common organic solvents were purchased from Kanto (Tokyo, Japan). Tetrakis(triphenylphosphine)palladium(0) (Pd(PPh₃)₄) was obtained from Nacalai (Kyoto, Japan). PC₆₁BM was purchased from Frontier Carbon (Tokyo, Japan). Poly(3,4-ethylenedioxythiophene):poly(4-styrene sulfonic acid) (PEDOT:PSS) 1.3 wt% dispersion in water was purchased from H. C. Starck (Munich, Germany). Capstone[®] fluorosurfactant FS-31 was kindly supplied by Du Pont (Wilmington, DE, USA). Chlorobenzene was purchased from Aldrich (Milwaukee, WI, USA). Indium tin oxide (ITO) glass substrates (sheet resistance = 10 Ω/sq.) and Au wire were obtained from Furuuchi Chemical (Tokyo, Japan). 4-Fluorophenyl 4,6-dibromothieno[3,4-*b*]thiophene-2-carboxylate (TT-F),¹⁰ octyl 4,6-dibromothieno[3,4-*b*]thiophene-2-carboxylate (TT-C8),¹⁰ and 2,6-bis(trimethyltin)-4,8-bis(2-ethylhexyloxy)benzo[1,2-*b*:4,5-*b'*]dithiophene (BDT-EH)^{6a} were prepared according to literature procedures.

Instruments

The ^1H NMR spectra were measured in 1,1,2,2-tetrachloroethane- d_2 at 140 °C with a JEOL ECA-500 spectrometer (JEOL, Tokyo, Japan). IR spectra were obtained using a JASCO FT/IR-460Plus spectrometer (JASCO, Tokyo, Japan) as a KBr pellet. Molecular weights (M_n) and polydispersity indexes (PDI) of polymers were estimated by size exclusion chromatography (SEC) equipped with a Shodex KF-805L column (Showa Denko, Tokyo, Japan), JASCO PU-2080Plus HPLC pump, JASCO MD-2018Plus photodiode array detector, and JASCO CO-1560 column oven, where tetrahydrofuran (THF) was used as the eluent. The molecular weight calibration curve was obtained with polystyrene standards (Tosoh). Thermal gravimetric analysis (TGA) was conducted with a TG/DTA6200 (SII NanoTechnology Inc., Chiba, Japan) at a heating rate of 10 °C/min under a nitrogen flow. UV-vis-NIR spectra were measured in chlorobenzene with 10 mm quartz cell using a JASCO V-570 spectrometer. Spin-coated films on glass substrates from chlorobenzene solution (5 mg/mL) were used for solid-state UV-vis-NIR spectra measurements. HOMO levels of polymers were measured using a photoelectron spectrometer (AC-2, Riken Keiki, Tokyo, Japan) by measuring the ionization potential of polymer film in air. The ionization potential of the polymers was estimated by the plots of the photoelectron quantum yield from the polymer solid surface against the incident photon energy. That is, the threshold of the photoelectron quantum yield was correlated with the ionization potential. The $I-V$

curves of the PSCs were measured under AM 1.5G simulated sunlight irradiation at an intensity of 100 mW/cm (1 sun). The light source was a solar simulator (XES-502S, SAN-EI Electric, Osaka, Japan) calibrated with a standard silicon photovoltaic detector. The direct current electric and space-charge-limited current (SCLC) measurements were carried out using an HZ-5000 electrochemical analyzer (Hokuto Denko, Tokyo, Japan). The thickness of the PTB-F_x:PC₆₁BM layer was measured by a microfigure measuring instrument (Surfcorder ET200, Kosaka Laboratory, Tokyo, Japan). AFM (atomic force microscopy) was performed using a SII SPI3800N AFM. Grazing incidence X-ray diffraction (GIXD) experiments were conducted at SPring-8 on beamline BL46XU. The sample was irradiated at a fixed incident angle on the order of 0.12° through a Huber diffractometer, and the GIXD patterns were recorded with a 2-D image detector (Pilatus 300K). GIXD patterns were recorded with an X-ray energy of 12.39 keV ($\lambda = 1 \text{ \AA}$). Samples for the X-ray measurements were prepared by spin-casting a solution of PTB-F_x:PC₆₁BM mixture in chlorobenzene onto the ITO/ZnO substrate.

Polymerization

Polymerization was carried out in a dry Schlenk flask under nitrogen atmosphere in a similar way to that described in Chapter 1.¹⁰ Each monomer was purified by recrystallization just before use. A typical polymerization procedure is described below.

Synthesis of PTB-F₇₅. TT-F (327 mg, 0.75 mmol), TT-C8 (114 mg, 0.25 mmol),

BDT-EH (772 mg, 1.00 mmol), and Pd(PPh₃)₄ (50 mg, 0.043 mmol) was placed in a Schlenk flask under nitrogen atmosphere. Anhydrous toluene (16 mL) and DMF (4 mL) were added with a syringe and the mixture was stirred at 120 °C for 12 h. After cooling to room temperature, the reaction mixture was poured into methanol. The resulting polymer was filtered through a Soxhlet thimble and purified via Soxhlet extraction for 12 h with methanol and 12 h with hexane. After the polymer was collected with chlorobenzene, the chlorobenzene solution was passed through Celite to remove the metal catalyst and concentrated. The target polymer PTB-F₇₅ was obtained as dark blue solid (659 mg, 91%) by precipitating in hexane and drying in vacuo. IR (KBr): 1725 cm⁻¹ (ν_{C=O}). ¹H NMR (500 MHz, 1,1,2,2-tetrachloroethane-*d*₂, 140 °C): δ 8.50-6.50 (6H, br), 4.90-3.50 (4.5H, br), 2.60-0.80 (33.75H, br). Anal. Calcd for (C_{39.5}H_{44.25}F_{0.75}O₄S₄)_n: C, 65.39; H, 6.15. Found: C, 65.16; H, 6.19.

In the same way, PTB-F₀, PTB-F₂₅, PTB-F₅₀, and PTB-F₁₀₀ were synthesized with the corresponding monomers. The polymerization results are summarized in Table 1, and the spectroscopic data of the polymers are listed below.

Spectroscopic data of PTB-F₀. IR (KBr): 1712 cm⁻¹ (ν_{C=O}). ¹H NMR (500 MHz, 1,1,2,2-tetrachloroethane-*d*₂, 140 °C): δ 8.30-6.60 (3H, br), 4.90-3.50 (6H, br), 2.40-0.80 (45H, br). Anal. Calcd for (C₄₁H₅₄O₄S₄·0.7H₂O)_n: C, 65.57; H, 7.34. Found: C, 65.61; H, 7.41.

Spectroscopic data of PTB-F₂₅. IR (KBr): 1710 cm⁻¹ (ν_{C=O}). ¹H NMR (500 MHz, 1,1,2,2-tetrachloroethane-*d*₂, 140 °C): δ 8.40-6.70 (4H, br), 4.90-3.50 (5.5H, br), 2.60-

0.80 (41.25H, br). Anal. Calcd for $(C_{40.5}H_{50.75}F_{0.25}O_4S_4 \cdot 0.3H_2O)_n$: C, 65.76; H, 6.96. Found: C, 65.79; H, 6.92.

Spectroscopic data of PTB-F₅₀. IR (KBr): 1719 cm^{-1} ($\nu_{C=O}$). ¹H NMR (500 MHz, 1,1,2,2-tetrachloroethane-*d*₂, 140 °C): δ 8.40–6.60 (5H, br), 4.90–3.50 (5H, br), 2.50–0.80 (37.5H, br). Anal. Calcd for $(C_{40}H_{47.5}F_{0.5}O_4S_4 \cdot 0.6H_2O)_n$: C, 64.85; H, 6.63. Found: C, 64.81; H, 6.59.

Spectroscopic data of PTB-F₁₀₀. IR (KBr): 1727 cm^{-1} ($\nu_{C=O}$). ¹H NMR (500 MHz, 1,1,2,2-tetrachloroethane-*d*₂, 140 °C): δ 8.40–6.40 (7H, br), 4.90–3.50 (4H, br), 2.70–0.80 (30H, br). Anal. Calcd for $(C_{39}H_{41}FO_4S_4 \cdot 0.7H_2O)_n$: C, 63.91; H, 5.73. Found: C, 64.01; H, 5.67.

Fabrication of hole-only devices

The ITO electrode was ultrasonicated in 2-propanol, cleaned in boiling 2-propanol, and then dried in air. Dispersions of PEDOT:PSS (0.65 wt%) in water containing Capstone[®] fluorosurfactant FS-31 (0.5 wt%) were spin-coated onto the clean ITO electrode at 2000 rpm, and then dried at 150 °C for 5 min. Chlorobenzene solutions containing polymer (12.5 mg/mL) and PC₆₁BM (18.75 mg/mL) were spin-coated onto the ITO/PEDOT:PSS substrate at 700 rpm. The above aqueous dispersion of PEDOT:PSS was spin-coated onto the PTB-F_x:PC₆₁BM layer at 2000 rpm. Au electrode was vacuum deposited onto the PEDOT:PSS layer under a pressure of 2×10^{-5} Torr. The structure of the hole-only device is ITO/PEDOT:PSS/PTB-F_x:PC₆₁BM

/PEDOT:PSS/Au, whose effective area is 0.04 cm².

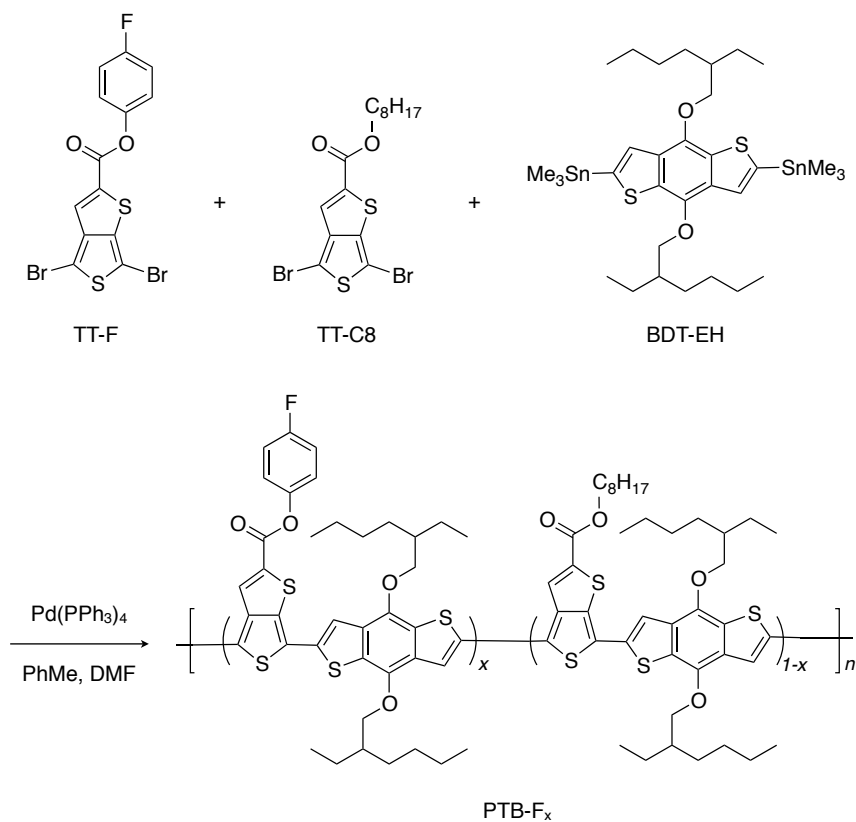
Hole mobility measurements

The hole mobilities of the polymers were measured from the SCLC *I-V* characteristics of the hole-only devices.¹¹ The SCLC behavior in the trap-free region can be characterized using the Mott-Gurney square law ($J = (9/8)\epsilon_0\epsilon_r\mu_h(V^2/L^3)$), where J is the current density (A/cm²), ϵ_0 is the vacuum permittivity (8.85×10^{-12} F/m), ϵ_r is the dielectric constant of the organic material, μ_h is the hole mobility (cm² V⁻¹ s⁻¹), L is the polymer film thickness (m), and V is the applied voltage (V). The ϵ_r is assumed to be 3.0 in our analysis, which is a typical value for conjugated polymers. The L was measured by a microfigure measuring instrument to be from 166 to 192 nm. The μ_h was calculated from the double-logarithmic plots of the *I-V* characteristics by fitting with a line with a slope of 2.0.

Fabrication of inverted polymer solar cells

ITO-glass electrodes were cleaned by sonication in 2-propanol, washed in boiling 2-propanol, and then dried in air. The ZnO film of about 60 nm thickness was prepared on the glass-ITO by a sol-gel method.¹² Chlorobenzene solutions containing polymer (7.5 mg/mL) and PC₆₁BM (11.25 mg/mL) were spin-coated onto the ITO/ZnO substrate at 700 rpm. Dispersions of PEDOT:PSS (0.65 wt%) in water containing Capstone[®]

fluorosurfactant FS-31 (0.5 wt%) were then spin-coated onto the PTB-F_x:PC₆₁BM layer at 2000 rpm. Au back electrode was vacuum deposited onto the PEDOT:PSS layer under a pressure of 2×10^{-5} Torr. The effective area of the solar cell was restricted to 1.0 cm² by depositing the Au electrode through a shadow mask. All spin-coated films were prepared under a relative humidity of less than 30% at room temperature in air.

Scheme 3-1. Synthesis and structures of monomers and polymers.**Table 3-1.** Polymerization Results and Thermal Properties of the Polymers.

run	polymer	feed ratio (mol %)			yield ^a (%)	M_n^b (10^4)	PDI ^b	T_{d5}^c (°C)
		TT-F	TT-C8	BDT-EH				
1	PTB-F ₀	0	100	100	95	4.4	3.0	326
2	PTB-F ₂₅	25	75	100	94	5.2	2.9	321
3	PTB-F ₅₀	50	50	100	88	5.1	2.8	322
4	PTB-F ₇₅	75	25	100	91	6.9	4.4	323
5	PTB-F ₁₀₀	100	0	100	92	9.7	3.4	335

^a Insoluble in MeOH and hexane. ^b Determined by SEC (Eluent: THF, PSt standards). ^c The 5% weight-loss temperatures at a heating rate of 10 °C/min in N₂.

Results and discussion

Synthesis

The synthetic route for PTB-F_x is shown in Scheme 3-1. PTB-F₁₀₀ was synthesized by the Stille cross-coupling between TT-F and BDT-EH in a toluene/DMF mixture (4/1, v/v) at 120 °C. Ternary copolymerizations of TT-F, TT-C8, and BDT-EH were performed using the same procedure, in which the TT-F/TT-C8 molar feed ratios were 75/25, 50/50, and 25/75. The compositional ratios of the TT-F and TT-C8 units in the copolymers were confirmed to be almost consistent with the feed ratios of the two types of TT comonomers, according to their ¹H NMR spectra and elemental analyses. For comparison, the previously reported PTB-based polymer, PTB-F₀, was also prepared.^{6a,7a} The polymerization results are summarized in Table 3-1. The *M_n* and PDI of the polymers obtained were determined by SEC in THF. The photovoltaic performances of PTB-based polymers are affected by their molecular weights.¹³ However, all of the polymers in this study possessed similar molecular weights. Thus, the influence of the molecular weight was negligible.

Thermal properties

The thermal degradation properties of the polymers were investigated by TGA at a heating rate of 10 °C/min under a flow of nitrogen (Figure 3-1). All of the polymers showed similar thermal stabilities with 5% weight loss temperatures (T_{d5}) around 320 °C, indicating that the introduction of 4-fluorophenyl pendants had little effect on the thermal stabilities of the polymers.

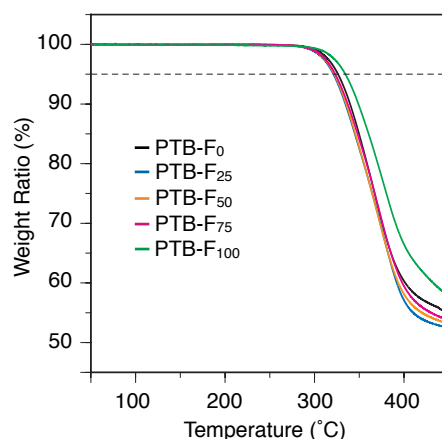


Figure 3-1. Thermogravimetric analysis of the polymers with a heating rate of 10 °C/min in N₂.

Optical properties

The absorption spectra of the polymers measured in chlorobenzene and in the solid state are shown in Figure 3-2a and b, respectively. The optical bandgaps ($E_g^{\text{opt}} = 1240/\lambda_{\text{onset}}$) were estimated from the absorption onset wavelength (λ_{onset}) in the solid state (Table 3-2). As the number of TT-F units in the polymers increased, the absorption regions gradually red-shifted, both in solution and in the solid state and the E_g^{opt} values

decreased. This is consistent with that described in Chapter 1¹⁰ and suggests that the 4-fluorophenyl pendants contributed to the expansion of the absorption range of the PTB-based polymers, which is expected to increase the short-circuit current density (J_{sc}) of the PSC devices.

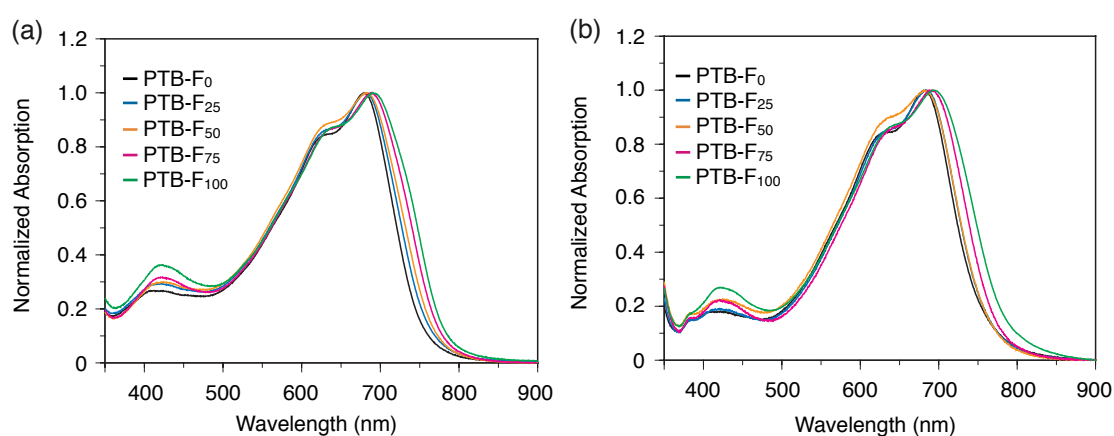


Figure 3-2. Absorption spectra of the polymers in chlorobenzene (a) and in the film state (b).

Table 3-2. Chemical and Physical Properties of the Polymers.

polymer	solution		film		$E_g^{opt\ a}$ (eV)	HOMO ^b (eV)	LUMO ^c (eV)
	λ_{max} (nm)	λ_{max} (nm)	λ_{onset} (nm)	λ_{onset} (nm)			
PTB-F ₀	679	683	754	754	1.64	-5.01	-3.37
PTB-F ₂₅	682	684	759	759	1.63	-5.07	-3.44
PTB-F ₅₀	682	682	761	761	1.63	-5.15	-3.52
PTB-F ₇₅	688	691	771	771	1.61	-5.21	-3.60
PTB-F ₁₀₀	691	694	785	785	1.58	-5.25	-3.67

^a Calculated using $E_g = 1240/\lambda_{onset}$. ^b Measured by photoelectron spectroscopy in air. ^c Calculated using $LUMO = E_g + HOMO$.

Energy levels

The HOMOs of the polymers were estimated from the ionization potentials of the thin films, measured with a photoelectron spectrometer in air (Figure 3-3a). The LUMOs were calculated from the values of the HOMO and E_g^{opt} (LUMO = HOMO + E_g^{opt}). These values are listed in Table 3-2. To visualize the influence of the 4-fluorophenyl pendants on the frontier orbitals, the HOMOs and LUMOs of the polymers are plotted against the TT-F content in Figure 3-3b. Both the HOMO and LUMO were linearly deepened with an increasing TT-F content, indicating that the frontier orbitals of the copolymers could be finely tuned by controlling the 4-fluorophenyl pendant content in the copolymers.

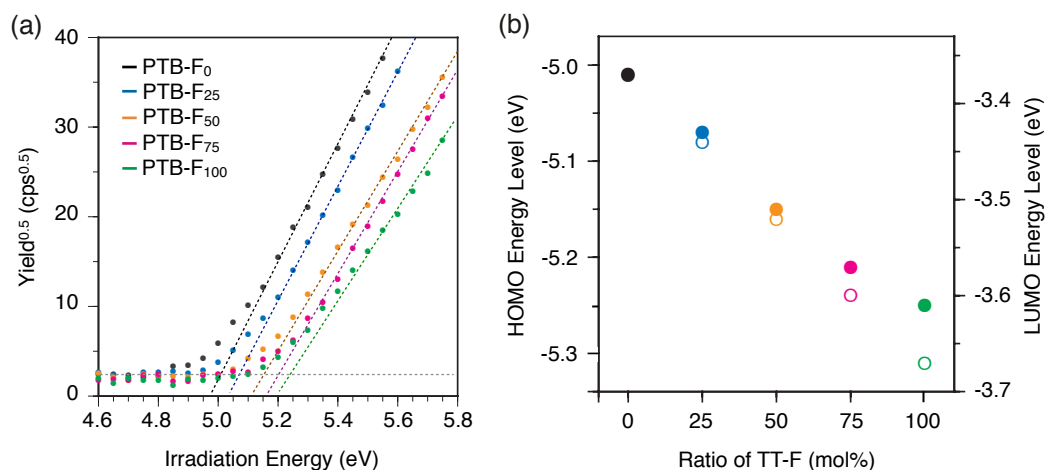


Figure 3-3. (a) Photoelectron spectra of the polymers in air. (b) HOMO (filled circles) and LUMO (open circles) energy levels of the polymers as a function of TT-F content in the polymers.

Photovoltaic properties of PSCs

The photovoltaic properties of the polymers were investigated in inverted-type BHJ PSCs with the configuration: ITO/ZnO/PTB-F_x:PC₆₁BM/PEDOT:PSS/Au. The optimized photovoltaic devices were obtained by spin casting a PTB-F_x:PC₆₁BM mixture (1:1.5, w/w) in chlorobenzene. Figure 3-4 shows the current–voltage (*J*–*V*) characteristics of the devices measured under AM 1.5 G illumination (100 mW cm⁻²) from a solar simulator. The corresponding *V*_{oc}, *J*_{sc}, fill factor (FF), and PCE values are summarized in Table 3-3 and Figure 3-5.

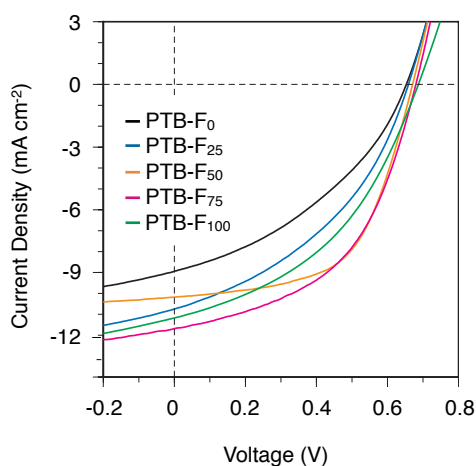


Figure 3-4. *I*–*V* curves for PTB-F_x:PC₆₁BM inverted-type solar cells under AM 1.5 irradiation (100 mW cm⁻²).

Table 3-3. Characteristics of the PTB-F_x:PC₆₁BM Inverted-type Polymer Solar Cells.

polymer	J_{sc} (mA·cm ⁻²)	V_{oc} (V)	FF	PCE (%)
PTB-F ₀	8.95	0.65	0.39	2.25
PTB-F ₂₅	10.75	0.66	0.41	2.88
PTB-F ₅₀	10.18	0.67	0.58	3.96
PTB-F ₇₅	11.69	0.68	0.50	3.94
PTB-F ₁₀₀	11.18	0.69	0.43	3.27

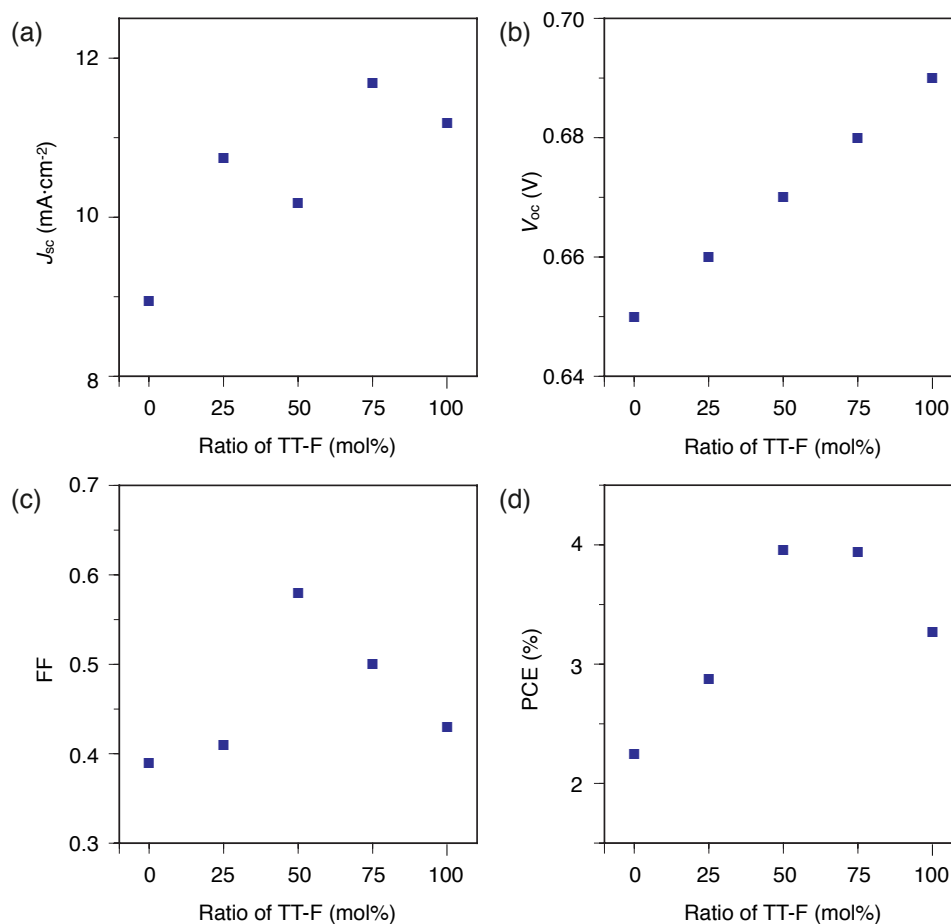


Figure 3-5. J_{sc} (a), V_{oc} (b), FF (c), and PCE (d) for PTB-F_x:PC₆₁BM inverted-type solar cells as a function of the TT-F content in the polymers.

As the 4-fluorophenyl pendant content in the polymers increased, the V_{oc} of the devices increased proportionally from 0.65 V for PTB-F₀ to 0.69 V for PTB-F₁₀₀. The increase in V_{oc} corresponds to the deepening tendency of the HOMOs of the polymers. However, the observed V_{oc} values were lower than those expected from the HOMO energy differences. Improvement in device engineering, which includes the formation of a nanoscale percolated network in the BHJ structures and high interfacial adhesion between the active layers and electrodes, may exploit latent potential for the polymers and lead to a further increase in the V_{oc} . The J_{sc} values of the devices with polymers bearing 4-fluorophenyl pendants were invariably higher than those with PTB-F₀ without 4-fluorophenyl pendants. The J_{sc} tended to increase with increasing 4-fluorophenyl pendant content. The FFs were also influenced by the 4-fluorophenyl pendant content and PTB-F₅₀ had the maximum FF (58%), which was 19% higher than that of PTB-F₀. As a result of the diverse changes in the V_{oc} , J_{sc} , and FF of the PSC devices, PTB-F₅₀ and PTB-F₇₅ exhibited the best performances as donor materials with PCEs of 3.96 and 3.94%, respectively. Taking into account that PTB-F₀ had the lowest value for each device parameter, introducing 4-fluorophenyl pendants into the donor polymers was effective in improving the performance of the PSCs.

Atomic Force Microscopy

The surface morphologies of the PTB-F_x:PC₆₁BM blended films were investigated by AFM, as shown in Figure 3-6. For the PTB-F₀:PC₆₁BM and PTB-F₂₅:PC₆₁BM blended films, there were segregated domains with a size of ca. 200 nm. PC₆₁BM crystals or polymer aggregates were observed all over the surfaces. These domains diminished the interfacial surfaces between the polymers and PC₆₁BM in the active layers and may have caused the charge carrier separation to deteriorate. Therefore, the PTB-F₀ devices had the lowest J_{sc} , which may be attributed to the low miscibility between the donor and acceptor materials. In contrast, the number of segregated domains on the surfaces of the active layers that contained PTB-F₅₀, PTB-F₇₅, and PTB-F₁₀₀ decreased, although some asperities were observed, owing to the inhomogeneity of the films. These results indicate that replacing the *n*-octyl chains with 4-fluorophenyl groups significantly improved the compatibility between the polymers and PC₆₁BM in the active layers. This is most likely because of affinity interactions, derived from the overlapping π orbitals between the 4-fluorophenyl groups and PC₆₁BM.

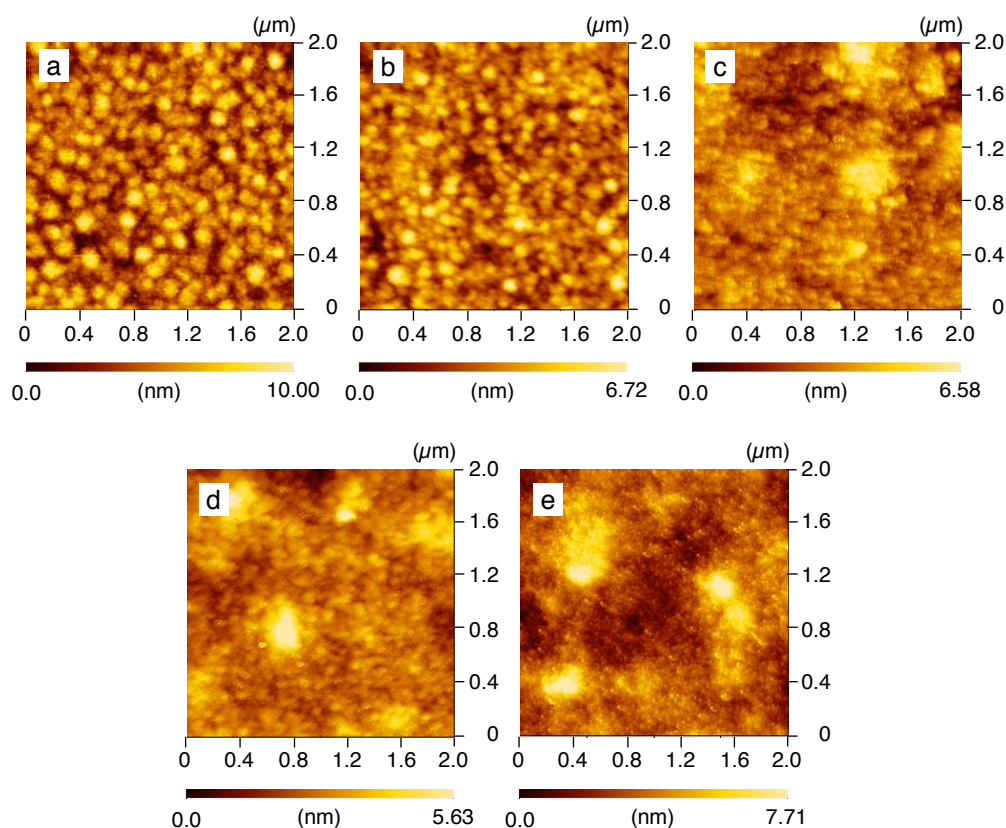


Figure 3-6. Topographic AFM images of PTB-F_x:PC₆₁BM blend films containing (a) PTB-F₀, (b) PTB-F₂₅, (c) PTB-F₅₀, (d) PTB-F₇₅, and (e) PTB-F₁₀₀.

Grazing Incidence X-ray Diffraction

To obtain information on the correlation between the device performance and crystallinity or orientation of the polymers, two-dimensional, grazing incidence X-ray diffraction (2D-GIXD) studies were carried out on the PTB-F_x:PC₆₁BM blended films, which were fabricated on ZnO-coated ITO glass substrates. A 2D-GIXD image of a PTB-F_x:PC₆₁BM blend (Figure 3-7) and line-cut profiles of the in-plane (q_{xy} axis) and out-of-plane (q_z axis) directions for all of the blended films are displayed in Figure 3-8a and 3-8b, respectively. All of the blended films had distinct diffraction signals ($q = ca.$

3.5 nm⁻¹), corresponding to the lamellar structures of the polymers. The lamellar structures in the films seem to be hardly oriented in a specific direction because the diffraction formed ring-like patterns. The peak intensities decreased with an increasing 4-fluorophenyl pendant content in the polymers. The broad diffraction signals corresponding to the 311 Bragg diffraction of PC₆₁BM ($q = \text{ca. } 14 \text{ nm}^{-1}$) also showed a similar tendency, decreasing with the 4-fluorophenyl pendant content. These results indicate that the crystallinity of both the polymers and PC₆₁BM in the blend films became lower with increasing the 4-fluorophenyl pendant content. This is in agreement with the AFM observations of the surface morphologies of the blend films. The 4-fluorophenyl pendants in the polymers appeared to facilitate the compatibilization of the PTB-F_x:PC₆₁BM blends, which resulted in BHJ films with low crystallinities. The distorted diffraction peaks across a range of $q_z = 12\text{--}18 \text{ nm}^{-1}$ in the out-of-plane direction were presumed to consist of two intrinsic peaks, which were resolved by two Gaussian functions centered at $q_z = 13.8 \text{ nm}^{-1}$ and $q_z = 16.0 \text{ nm}^{-1}$, corresponding to the 311 Bragg diffraction of PC₆₁BM and $\pi\text{--}\pi$ stacking between the polymers, respectively (Figure 3-9). The intensities of the peaks derived from $\pi\text{--}\pi$ stacking were also affected by the 4-fluorophenyl pendant content. The blended film containing PTB-F₀ exhibited the most intense $\pi\text{--}\pi$ stacking peaks, followed by PTB-F₂₅ and PTB-F₅₀. The absence of the corresponding $\pi\text{--}\pi$ stacking peak in the in-plane direction suggests that PTB-F₀, PTB-F₂₅, and PTB-F₅₀ in the BHJ films were more or less arranged with a face-on orientation rather than edge-on. Conversely, PTB-F₇₅ and PTB-F₁₀₀, with high

4-fluorophenyl pendant contents contained almost no π - π stacking peak in the out-of-plane direction, indicating that there was no face-on orientation in these blended films.

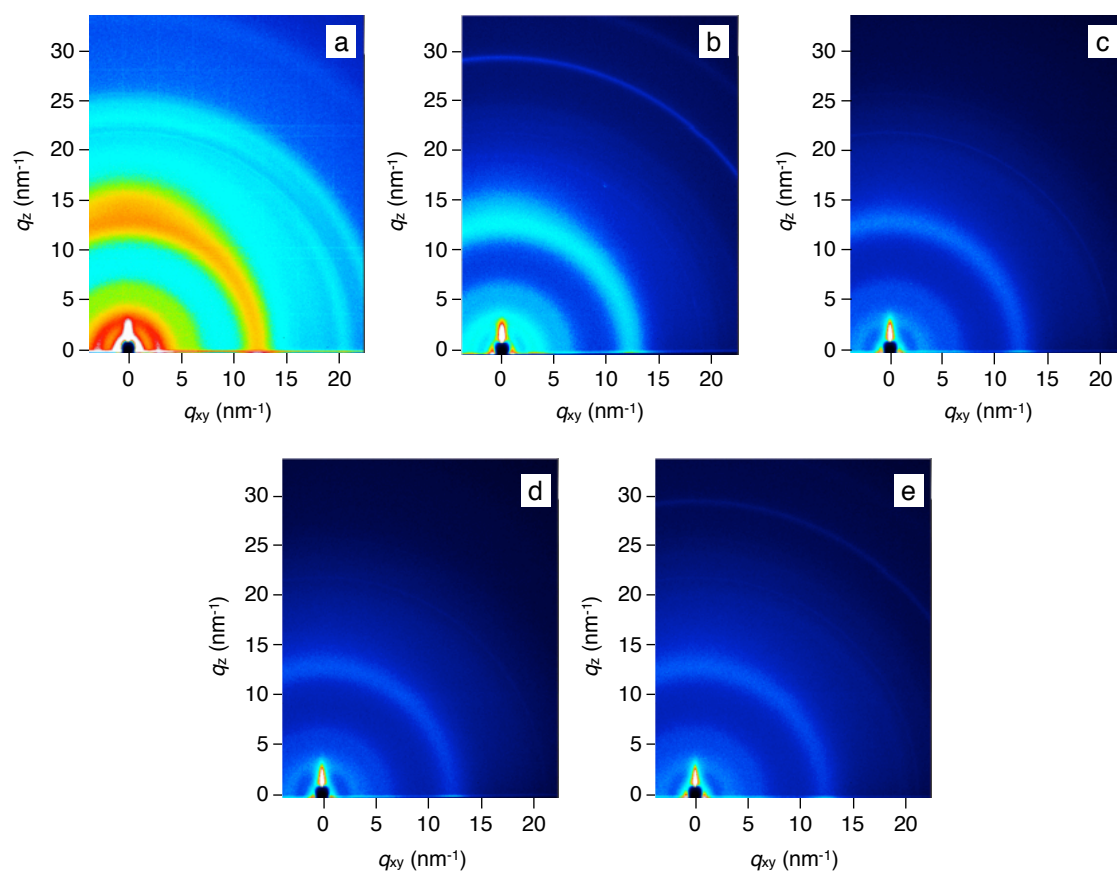


Figure 3-7. 2D-GIXD images for the PTB-F_x:PC₆₁BM blended films of PTB-F₀ (a), PTB-F₂₅ (b), PTB-F₅₀ (c), PTB-F₇₅ (d), and PTB-F₁₀₀ (e).

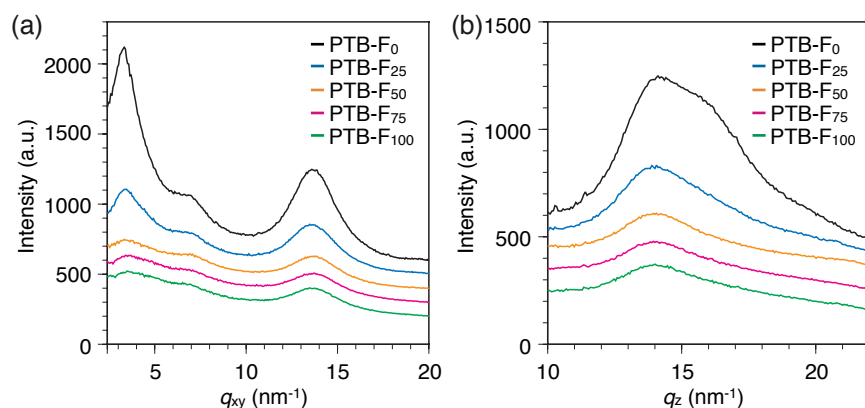


Figure 3-8. In-plane (a) and out-of-plane (b) line-cut profiles of the 2D-GIXD images for the PTB-F_x:PC₆₁BM blended films.

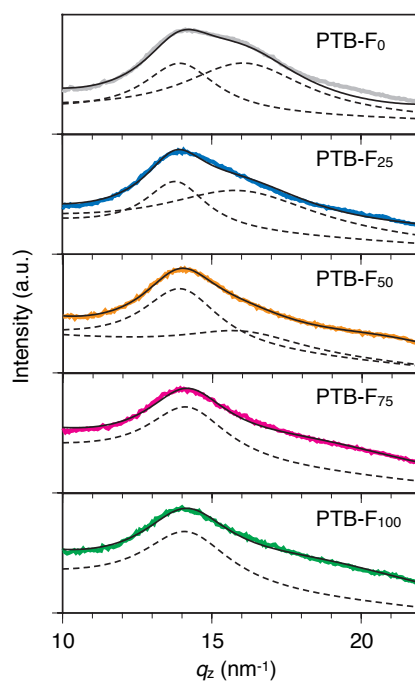


Figure 3-9. Out-of-plane line-cut profiles of 2D-GIXD images for the PTB-F_x:PC₆₁BM blended films. Gaussian fits were used to determine peak positions and FWHMs, as represented using black solid lines for the overall profiles and black dash lines for the individual peaks.

Hole Mobilities

The hole mobilities of the PTB-F_x:PC₆₁BM (1:1.5, w/w) blended films were measured in accordance with the SCLC model using hole-only devices with the configuration: ITO/PEDOT:PSS/PTB-F_x:PC₆₁BM/PEDOT:PSS/Au. *I-V* characteristics of the hole-only devices in the dark in air are shown in Figure 3-10. The blended films containing PTB-F₂₅ and PTB-F₅₀ had μ_h values of 3.3×10^{-4} and $3.7 \times 10^{-4} \text{ cm}^2 \text{ V}^{-1} \text{ s}^{-1}$, respectively, which are comparable to that of the PTB-F₀:PC₆₁BM blended film ($3.6 \times 10^{-4} \text{ cm}^2 \text{ V}^{-1} \text{ s}^{-1}$, Figure 3-11). Conversely, the μ_h values in the blended films containing PTB-F₇₅ and PTB-F₁₀₀ were estimated to be 1.3×10^{-4} and $1.5 \times 10^{-4} \text{ cm}^2 \text{ V}^{-1} \text{ s}^{-1}$, respectively, which are less than half of those of the other polymers. In conjunction with the above 2D-GIXD results, it was speculated that the differences in the hole mobilities resulted from the differences in the crystallinity and orientation of the polymers in the PTB-F_x:PC₆₁BM blended films. The enhancement of the J_{sc} with an increase in the 4-fluorophenyl content was ascribed to the broad absorption properties and the number of the donor/acceptor interfaces in the active layers, which sufficiently compensated for the decrease in the hole mobility.

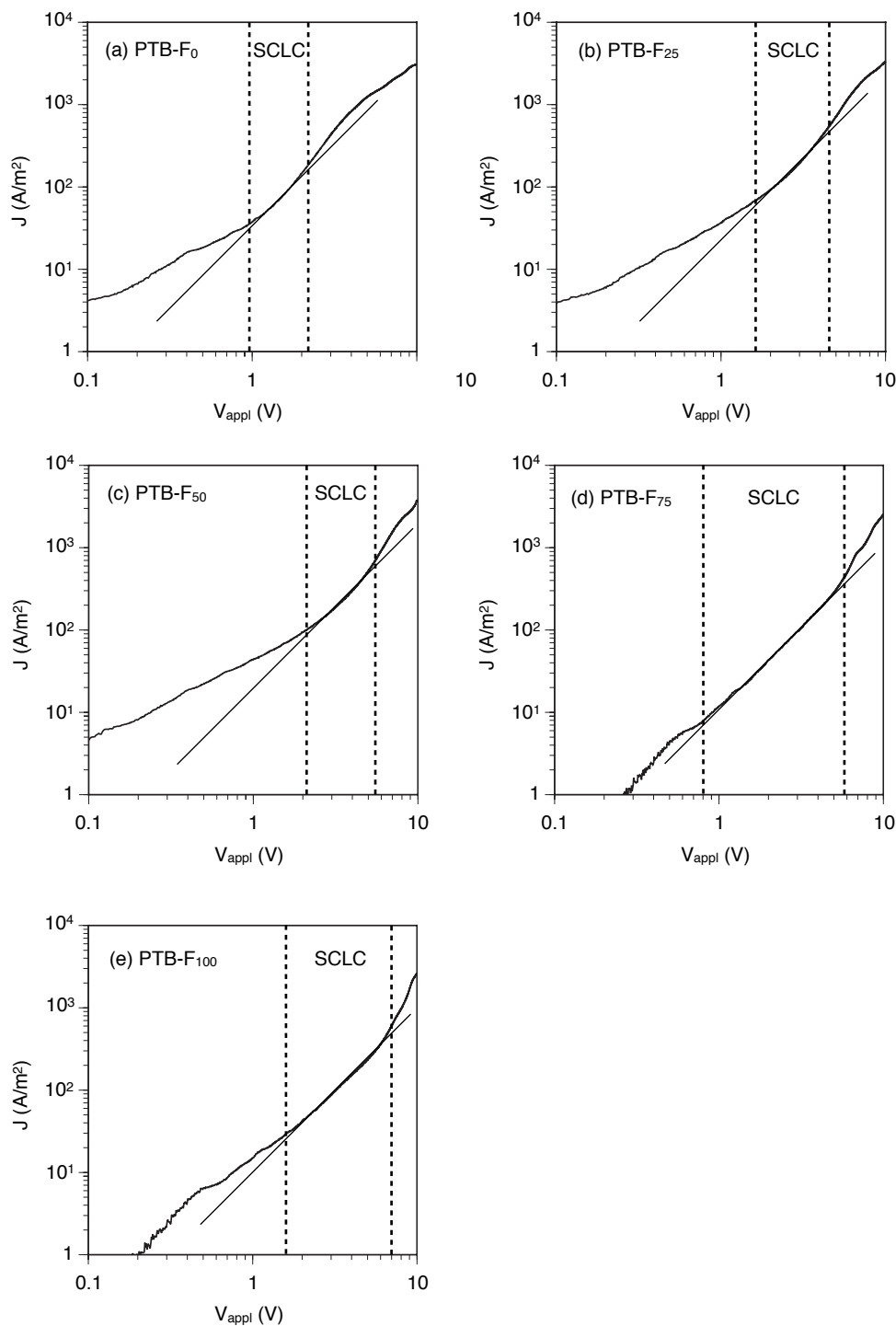


Figure 3-10. Double-logarithmic plots of I - V curves obtained for hole-only devices (ITO/PEDOT:PSS/PTB-F_x:PC₆₁BM/PEDOT:PSS/Au) in the dark in air: (a) PTB-F₀, (b) PTB-F₂₅, (c) PTB-F₅₀, (d) PTB-F₇₅, and (e) PTB-F₁₀₀.

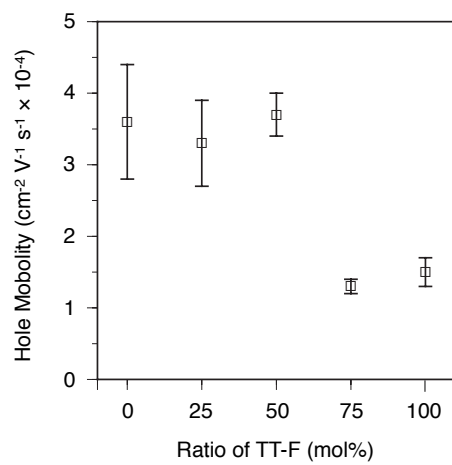


Figure 3-11. Hole mobilities of the PTB-F_x:PC₆₁BM blended films.

Conclusions

The PTB-based polymers containing TT-F units were synthesized to investigate the effect of the 4-fluorophenyl pendants in TT-F on the thermal stability, absorption properties, HOMO and LUMO energy levels, hole mobilities, and photovoltaic performances. The author found that the HOMO energy levels of the polymers could be finely tuned by changing the compositional ratio in copolymers and the V_{oc} of the inverted-type PSCs are clearly improved with increasing the content of TT-F in the copolymers. 4-Fluorophenyl pendants also influenced the morphology of the PTB-F_x:PC₆₁BM blends, the crystallinity and orientation in the active layers, and hole mobility, which appear to be closely related to the up-and-down J_{sc} and FF values of the corresponding devices. As a result of the diverse alterations in the V_{oc} , J_{sc} , and FF of the devices, PTB-F₅₀ and PTB-F₇₅ bearing a moderate content of 4-fluorophenyl pendants provided superior PSC performances with the PCE of nearly 4% compared with PTB-F₀, PTB-F₂₅, and PTB-F₁₀₀ bearing too small or too large contents of the 4-fluorophenyl pendants. These findings suggest that the incorporation of an appropriate amount of the 4-fluorophenyl groups instead of the alkyl chains can contribute to enhance the PSC performance. The author believes that this methodology is applicable to other types of donor polymers.

References

- (1) (a) Yu, G.; Gao, J.; Hummelen, J. C.; Wudl, F.; Heeger, A. J. *Science* **1995**, *270*, 1789. (b) Günes, S.; Neugebauer, H.; Sariciftci, N. S. *Chem. Rev.* **2007**, *107*, 1324. (c) Cheng, Y.-J.; Yang, S.-H.; Hsu, C.-S. *Chem. Rev.* **2009**, *109*, 5868. (d) Brabec, C. J.; Gowrisanker, S.; Halls, J. J. M.; Laird, D.; Jia, S.; Williams, S. P. *Adv. Mater.* **2010**, *22*, 3839. (e) Beaujuge, P. M.; Fréchet, J. M. J. *J. Am. Chem. Soc.* **2011**, *133*, 20009. (f) Facchetti, A. *Chem. Mater.* **2011**, *23*, 733. (g) Li, G.; Zhu, R.; Yang, Y. *Nat. Photon.* **2012**, *6*, 153. (h) Søndergaard, R.; Hösel, M.; Angmo, D.; Larsen-Olsen, T. T.; Krebs, F. C. *Mater. Today* **2012**, *15*, 36. (i) Heeger, A. J. *Adv. Mater.* **2014**, *26*, 10.
- (2) (a) Bundgaard, E.; Krebs, F. C. *Sol. Energy Mater. Sol. Cells* **2007**, *91*, 954. (b) Chen, J.; Cao, Y. *Acc. Chem. Res.* **2009**, *42*, 1709. (c) Boudreault, P.-L. T.; Najari, A.; Leclerc, M. *Chem. Mater.* **2011**, *23*, 456. (d) Zhou, H.; Yang, L.; You, W. *Macromolecules* **2012**, *45*, 607. (e) Ohshita, J.; Nakashima, M.; Tanaka, D.; Morihara, Y.; Fueno, H.; Tanaka, K. *Polym. Chem.* **2014**, *5*, 346.
- (3) (a) Brabec, C. J.; Cravino, A.; Meissner, D.; Sariciftci, N. S.; Fromherz, T.; Rispen, M. T.; Sanchez, L.; Hummelen, J. C. *Adv. Funct. Mater.* **2001**, *11*, 374. (b) Scharber, M. C.; Mühlbacher, D.; Koppe, M.; Denk, P.; Waldauf, C.; Heeger, A. J.; Brabec, C. J. *Adv. Mater.* **2006**, *18*, 789. (c) Li, Y. *Acc. Chem. Res.* **2012**, *45*, 723.
- (4) (a) McCulloch, I.; Heeney, M.; Chabinyc, M. L.; DeLongchamp, D.; Kline, R. J.; Cölle, M.; Duffy, W.; Fischer, D.; Gundlach, D.; Hamadani, B.; Hamilton, R.; Richter, L.; Salleo, A.; Shkunov, M.; Sparrowe, D.; Tierney, S.; Zhang, W. *Adv. Mater.* **2009**, *21*,

1091. (b) Osaka, I.; Kakara, T.; Takemura, N.; Koganezawa, T.; Takimiya, K. *J. Am. Chem. Soc.* **2013**, *135*, 8834. (c) Kuwabara, J.; Yasuda, T.; Choi, S. J.; Lu, W.; Yamazaki, K.; Kagaya, S.; Han, L.; Kanbara, T. *Adv. Funct. Mater.* **2014**, *24*, 3226.
- (5) (a) Chen, L.-M.; Hong, Z.; Li, G.; Yang, Y. *Adv. Mater.* **2009**, *21*, 1434. (b) Brabec, C. J.; Heeney, M.; McCulloch, I.; Nelson, J. *Chem. Soc. Rev.* **2011**, *40*, 1185. (c) Dang, M. T.; Hirsch, L.; Wantz, G.; Wuest, J. D. *Chem. Rev.* **2013**, *113*, 3734.
- (6) (a) Liang, Y.; Feng, D.; Wu, Y.; Tsai, S. T.; Li, G.; Ray, C.; Yu, L. *J. Am. Chem. Soc.* **2009**, *131*, 7792. (b) Liang, Y.; Wu, Y.; Feng, D.; Tsai, S.-T.; Son, H.-J.; Li, G.; Yu, L. *J. Am. Chem. Soc.* **2009**, *131*, 56.
- (7) (a) Chen, H.-Y.; Hou, J.; Zhang, S.; Liang, Y.; Yang, G.; Yang, Y.; Yu, L.; Wu, Y.; Li, G. *Nat. Photon.* **2009**, *3*, 649. (b) Liang, Y.; Xu, Z.; Xia, J.; Tsai, S.-T.; Wu, Y.; Li, G.; Ray, C.; Yu, L. *Adv. Mater.* **2010**, *22*, E135. (c) Wang, H.; Yu, X.; Yi, C.; Ren, H.; Liu, C.; Yang, Y.; Xiao, S.; Zheng, J.; Karim, A.; Cheng, S. Z. D.; Gong, X. *J. Phys. Chem. C* **2013**, *117*, 4358. (d) Liu, P.; Zhang, K.; Liu, F.; Jin, Y.; Liu, S.; Russell, T. P.; Yip, H.-L.; Huang, F.; Cao, Y. *Chem. Mater.* **2014**, *26*, 3009.
- (8) He, Z.; Zhong, C.; Su, S.; Xu, M.; Wu, H.; Cao, Y. *Nat. Photon.* **2012**, *6*, 591.
- (9) (a) Son, H. J.; Wang, W.; Xu, T.; Liang, Y.; Wu, Y.; Li, G.; Yu, L. *J. Am. Chem. Soc.* **2011**, *133*, 1885. (b) Zhang, Y.; Zou, J.; Cheuh, C.-C.; Yip, H.-L.; Jen, A. K. Y. *Macromolecules* **2012**, *45*, 5427. (c) Albrecht, S.; Janietz, S.; Schindler, W.; Frisch, J.; Kurpiers, J.; Kniepert, J.; Inal, S.; Pingel, P.; Fostiropoulos, K.; Koch, N.; Neher, D. *J. Am. Chem. Soc.* **2012**, *134*, 14932. (d) Tumbleston, J. R.; Collins, B. A.; Yang, L.;

Stuart, A. C.; Gann, E.; Ma, W.; You, W.; Ade, H. *Nat. Photon.* **2014**, *8*, 385.

(10) Yamamoto, T.; Ikai, T.; Kuzuba, M.; Kuwabara, T.; Maeda, K.; Takahashi, K.; Kanoh, S. *Macromolecules* **2011**, *44*, 6659.

(11) Jung, J. W.; Jo, W. H. *Adv. Funct. Mater.* **2010**, *20*, 2355.

(12) Kuwabara, T.; Omura, Y.; Yamaguchi, T.; Taima, T.; Kohshin, T.; Higashimine, K.; Vohra, V.; Murata, H. *J. Phys. Chem. C* **2014**, *118*, 4050.

(13) He, X.; Mukherjee, S.; Watkins, S.; Chen, M.; Qin, T.; Thomsen, L.; Ade, H.; McNeill, C. R. *J. Phys. Chem. C* **2014**, *118*, 9918.

Chapter 4

Thieno[3,4-*b*]thiophene–benzo[1,2-*b*:4,5-*b'*]dithiophene-based polymers bearing optically pure 2-ethylhexyl pendants: Synthesis and application in polymer solar cells

Abstract: Optically active narrow-bandgap polymers ((*R,R*)- and (*S,S*)-PTB5) consisting of alternating *n*-octyl thieno[3,4-*b*]thiophene-2-carboxylate and benzo[1,2-*b*:4,5-*b'*]dithiophene units bearing optically pure (*R*)- and (*S*)-2-ethylhexyl pendants, respectively, were synthesized for the first time. (*R,R*)- and (*S,S*)-PTB5 films showed apparent circular dichroism in their absorption regions of the polymer backbone due to the formation of a chirally ordered superstructure induced by the chirality of the branched alkyl pendants. Inverted-type bulk heterojunction polymer solar cells (PSCs) were fabricated using (*R,R*)- or (*S,S*)-PTB5 as electron donors and [6,6]-phenyl-C₆₁-butyric acid methyl ester as an electron acceptor. The photovoltaic properties of the PSCs were compared with those of the corresponding PSC containing optically inactive PTB5 bearing racemic 2-ethylhexyl pendants.

Introduction

Organic photovoltaics (OPVs) show great potential for cost-effective solar energy conversion and have been recognized as prospective alternatives to silicon-based photovoltaics. In particular, polymer solar cells (PSCs) containing electron-donating π -conjugated polymers and electron-accepting fullerene derivatives in their active layers have attracted substantial attention because of their unique advantages including flexibility, lightness, colorfulness, transparency and large-area device production by roll-to-roll printing.¹ To improve the photovoltaic performance of PSCs, extensive research effort has been devoted to developing π -conjugated polymers using rational synthetic strategies, e.g., narrowing bandgap,² expanding absorption range,³ tuning highest occupied molecular orbital (HOMO) and lowest unoccupied molecular orbital (LUMO) energy levels⁴ and increasing hole mobility.⁵ Since π -conjugated polymers consisting of thieno[3,4-*b*]thiophene (TT) and benzo[1,2-*b*:4,5-*b'*]dithiophene (BDT) units (PTB-based polymers) have been reported as a promising donor for PSCs in 2009,⁶ various structural modifications of the PTB-based polymers have been investigated to improve the power conversion efficiency (PCE) of their PSCs. For example, replacements of the alkyl esters with alkylketones⁷ or phenyl esters^{4b} and direct introduction of fluoro groups⁸ or thienyl units⁹ onto the polymer backbone increase the PCE of the resulting PSCs.

The solubility of donor polymers is an important concern in the fabrication of PSC devices. The introduction of long or branched alkyl chains as pendants is the simplest

way to increase the solubility of donor polymers. However, alkyl pendants that are too long or bulky inhibit the π - π stacking interactions between donor polymers, which are essential for efficient hole transport, impairing the performance of donor materials.¹⁰ Therefore, the alkyl chains introduced onto polymer backbones need to be appropriate. Considering the trade-off between polymer solubility and hole-transporting ability, branched alkyl chains, particularly 2-ethylhexyl chains, have been introduced onto π -conjugated polymers as solubilizing pendants. Because a 2-ethylhexyl chain possesses an asymmetric center, there are two enantiomeric structures with different absolute configurations. Almost no attention has been paid to the chirality of alkyl pendants, and racemic alkyl chains have been introduced onto donor polymers to increase their solubility. Recently, it was reported that the hole mobility of small molecule-based donor materials was enhanced by controlling the chirality of their branched alkyl chains,¹¹ although use of the corresponding materials in OPVs was not demonstrated. PSCs containing donor polymers bearing enantiopure 2-ethylhexyl pendants have not been reported previously. Because the chirality control of 2-ethylhexyl pendants in donor polymers enhances a structural regularity of the polymers, intermolecular interactions between optically active polymers is expected to be more effective compared with conventional donor polymers randomly bearing (*R*)- and (*S*)-2-ethylhexyl pendants. In addition, the introduction of enantiopure 2-ethylhexyl pendants has a potential to provide characteristic chiral aggregate formations in the film states.¹² Therefore, it is important to clarify the effect of the chirality of the branched

alkyl chains in donor polymers on the photovoltaic properties of their PSCs.

In the present study, the author synthesized optically active PTB-based polymers ((*R,R*)- and (*S,S*)-PTB5) containing BDT units bearing optically pure (*R*)- and (*S*)-2-ethylhexyl pendants, respectively. The influence of the pendant chirality on the thermal stability, absorption and chiroptical properties, frontier orbital energy levels and photovoltaic performance of (*R,R*)- and (*S,S*)-PTB5 was investigated by direct comparison with the properties of optically inactive PTB5 bearing racemic 2-ethylhexyl pendants. To the best of my knowledge, this is the first report on the synthesis and application of donor polymers bearing the enantiopure 2-ethylhexyl pendants to the PSC devices. PTB5 was used to investigate the effect of pendant chirality on PSC properties because it is the simplest structure bearing alkyl esters on TT and alkoxy groups on BDT of PTB-based polymers reported to date.

Experimental Section

Materials

The anhydrous solvents (toluene, *N,N*-dimethylformamide (DMF), pyridine and tetrahydrofuran (THF)) and the common organic solvents were purchased from Kanto (Tokyo, Japan). Capstone[®] fluorosurfactant FS-31 was kindly supplied by Du Pont (Wilmington, DE, USA). Trimethyltin chloride and *N*-(*p*-toluenesulfonyl)-*L*-phenylalanyl chloride ((*S*)-**6**) were bought from Tokyo Kasei (TCI, Tokyo, Japan). Zinc, 4-(dimethylamino)pyridine and *n*-butyllithium (1.6 M in *n*-hexane) were purchased from Wako (Osaka, Japan). *p*-Toluenesulfonyl chloride was obtained from Kishida (Osaka, Japan). Tetrakis(triphenylphosphine)palladium(0) (Pd(PPh₃)₄) and sodium hydroxide (NaOH) were purchased from Nacalai (Kyoto, Japan). Tetrabutylammonium bromide and *rac*-2-ethylhexanol (*rac*-**2**-OH) were from Aldrich (Milwaukee, WI, USA). Poly(3,4-ethylenedioxylenethiophene):poly(4-styrene sulfonic acid) (PEDOT:PSS) 1.3 wt% dispersion in water was from H. C. Starck (Munich, Germany). Chiralcel OJ (25 x 2.0 cm ID) and Chiralcel OJ-H (25 x 0.46 cm ID) were purchased from Daicel Chemical Industries (Tokyo, Japan). 4,8-Dihydrobenzo[1,2-*b*:4,5-*b'*]dithiophen-4,8-dione (**1**)¹³ and *n*-octyl 4,6-dibromothieno[3,4-*b*]thiophene-2-carboxylate (**5**)^{4b} were prepared according to the procedures in the literature.

Instruments

The ^1H and ^{13}C NMR spectra were measured in CDCl_3 at room temperature and $50\text{ }^\circ\text{C}$ with a JEOL ECA-500 spectrometer (JEOL, Tokyo, Japan). IR spectra were obtained using a JASCO FT/IR-460Plus spectrometer (JASCO, Tokyo, Japan) as a KBr pellet. The molecular weights and distributions of the polymers were estimated using size-exclusion chromatography (SEC) equipped with a Shodex KF-805L column (Showa Denko, Tokyo, Japan), a JASCO CO-1560 column oven, a JASCO PU-2080 Plus HPLC pump and a JASCO UV-970 UV/VIS detector at 650 nm , where THF was used as the eluent. The molecular weight calibration curve was obtained with polystyrene standards (Tosoh). The optical rotation was measured at $25\text{ }^\circ\text{C}$ with a JASCO P-1030 polarimeter. Thermogravimetric analysis (TGA) was conducted using a TG/DTA6200 (SII NanoTechnology Inc., Chiba, Japan) with a heating rate of $10\text{ }^\circ\text{C}/\text{min}$ under a flow of nitrogen. The UV-vis-NIR absorption and circular dichroism (CD) spectra were measured in chlorobenzene with 1.0 mm quartz cell and in spin-coated films prepared on glass substrates from chlorobenzene solution (5 mg/mL) using JASCO V-570 and JASCO J-720 spectrometers. The concentrations of the chlorobenzene solutions were adjusted in a way that is approximately consistent with the absorbance in the corresponding polymer films. Thin-film X-ray diffraction (XRD) was recorded on an X-ray diffractometer RINT 2500 (Rigaku, Tokyo, Japan) with $\text{Cu K}\alpha$ radiation ($\lambda = 1.540\text{ \AA}$) operated at 40 keV and 200 mA . The thickness of the polymer:PC₆₁BM blend film was measured by a microfigure measuring instrument

Surfcoorder ET200 (Kosaka Laboratory, Tokyo, Japan). The HOMO of the polymer was measured using a photoelectron spectrometer AC-2 (Riken Keiki, Tokyo, Japan) by measuring the ionization potential of polymer films in air. The ionization potential of the polymers was estimated using the plots of the photoelectron quantum yield from the polymer solid surface against the incident photon energy. The threshold of the photoelectron quantum yield was correlated with the ionization potential.

Synthesis of optically active BDT-based monomers

N-(*p*-Toluenesulfonyl)-L-phenylalanine 2-ethylhexyl ester ((*S,R*)-7 and (*S,S*)-7).

To a solution of *rac*-2-OH (9.64 g, 74.0 mmol) in anhydrous toluene (74 mL) was added (*S*)-6 (32.0 g, 94.7 mmol) and the mixture was stirred at 80 °C. After 12 h, the reaction system was diluted with ethyl acetate, and the organic layer was washed with saturated NaHCO₃ aqueous solution and water, and then dried over Na₂SO₄. After evaporating the solvent, the crude product was purified by silica gel chromatography using *n*-hexane—ethyl acetate (2/1, v/v) as the eluent to give a diastereomeric mixture of (*S,R*)-7 and (*S,S*)-7. The diastereomers were separated by chiral high-performance liquid chromatography (HPLC) on Chiralcel OJ (column dimensions 25 x 2.0 cm ID; eluent methanol (MeOH); flow rate 8.0 mL/min; temperature 20 °C) to give (*S,R*)-7 (13.5 g, 31.3 mmol, 42% yield) and (*S,S*)-7 (13.7 g, 31.7 mmol, 43% yield) as a white solid. The diastereomeric excess (de) of the isolated products was determined by HPLC analysis on Daicel Chiralcel OJ-H (column dimensions 25 x 0.46 cm ID; eluent MeOH;

flow rate 0.5 mL/min; temperature 20 °C; λ 254 nm; $t_{(S,R)-7} = 17.9$ min, $t_{(S,S)-7} = 24.9$ min) and the author confirmed that each isomer possesses a high diastereomeric purity (>99% de). (*S,R*)-**7**: $^1\text{H NMR}$ (500 MHz, CDCl_3 , rt): δ 7.64 (d, $J = 8.0$ Hz, 2H), 7.25-7.21 (m, 5H), 7.10-7.06 (m, 2H), 5.03 (d, $J = 9.2$ Hz, 1H), 4.23-4.17 (m, 1H), 3.78-3.66 (m, 2H), 3.08-2.97 (m, 2H), 2.40 (s, 3H), 1.39-1.03 (m, 9H), 0.88 (t, $J = 7.2$ Hz, 3H), 0.78 (t, $J = 7.5$ Hz, 3H). (*S,S*)-**7**: $^1\text{H NMR}$ (500 MHz, CDCl_3 , rt): δ 7.64 (d, $J = 8.0$ Hz, 2H), 7.25-7.21 (m, 5H), 7.11-7.06 (m, 2H), 5.03 (d, $J = 9.2$ Hz, 1H), 4.23-4.17 (m, 1H), 3.79-3.67 (m, 2H), 3.07-2.99 (m, 2H), 2.40 (s, 3H), 1.37-1.04 (m, 9H), 0.88 (t, $J = 7.2$ Hz, 3H), 0.78 (t, $J = 7.5$ Hz, 3H).

(*R*)-2-Ethylhexanol ((*R*)-2-OH). (*S,R*)-**7** (6.9 g, 16 mmol) was dissolved in THF (29 mL) and then an aqueous solution of NaOH (5 N, 29 mL) was added to the solution. The mixture was stirred at 60 °C for 24 h. After cooling to room temperature, the solvent was removed under reduced pressure. The residue was diluted with hexane, and the solution was washed with saturated NaHCO_3 aqueous solution and water, and dried over Na_2SO_4 . After filtration, the solvent was removed by evaporation to give the desired product as a colorless oil (2.0 g, 96% yield). $[\alpha]_{\text{D}}^{25} = -3.5$ (neat); lit. $[\alpha]_{\text{D}}^{25} = -3.4$ (c 5.3, CHCl_3).¹⁴ $^1\text{H NMR}$ (500 MHz, CDCl_3 , rt): δ 3.55 (t, $J = 5.4$ Hz, 2H), 1.45-1.20 (m, 8H), 1.16 (t, $J = 5.5$ Hz, 1H), 0.90 (t, $J = 7.2$ Hz, 6H).

(S)-2-Ethylhexanol ((S)-2-OH). The title compound was prepared from (*S,S*)-**7** in the same way as (*R*)-**2-OH** and obtained in 90% yield. $[\alpha]_{\text{D}}^{25} = +3.9$ (neat); lit. $[\alpha]_{\text{D}}^{25} = +3.4$ (*c* 5.3, CHCl_3). $^1\text{H NMR}$ (500 MHz, CDCl_3 , rt): δ 3.56 (t, $J = 5.4$ Hz, 2H), 1.45-1.20 (m, 8H), 1.15 (t, $J = 5.7$ Hz, 1H), 0.90 (t, $J = 6.9$ Hz, 6H).

(R)-2-Ethylhexyl *p*-toluenesulfonate ((R)-2-OTs). To a solution of (*R*)-**2-OH** (1.0 g, 7.7 mmol) in anhydrous pyridine (3.5 mL) was added *p*-toluenesulfonyl chloride (2.2 g, 11.5 mmol) and 4-(dimethylamino)pyridine (5.6 mg, 0.05 mmol). The mixture was stirred at 0 °C. After 12 h, the reaction system was diluted with hexane, and the organic layer was washed with 1 N HCl aqueous solution, saturated NaHCO_3 aqueous solution and water, and then dried over Na_2SO_4 . After evaporating the solvent, the crude product was purified by silica gel chromatography using hexane–ethyl acetate (20/1, v/v) to yield (*R*)-**2-OTs** as a colorless oil (1.7 g, 80%). $^1\text{H NMR}$ (500 MHz, CDCl_3 , rt): δ 7.79 (d, $J = 8.6$ Hz, 2H), 7.35 (d, $J = 8.0$ Hz, 2H), 3.95-3.89 (m, 2H), 2.45 (s, 3H), 1.61-1.49 (m, 1H), 1.37-1.09 (m, 8H), 0.84 (t, $J = 7.2$ Hz, 3H), 0.79 (t, $J = 7.5$ Hz, 3H).

(S)-2-Ethylhexyl *p*-toluenesulfonate ((S)-2-OTs). The title compound was prepared from (*S*)-**2-OH** in the same way as (*R*)-**2-OTs** and obtained in 72% yield. $^1\text{H NMR}$ (500 MHz, CDCl_3 , rt): δ 7.79 (d, $J = 8.3$ Hz, 2H), 7.35 (d, $J = 8.3$ Hz, 2H), 3.95-3.89 (m, 2H), 2.45 (s, 3H), 1.59-1.48 (m, 1H), 1.37-1.08 (m, 8H), 0.84 (t, $J = 7.1$ Hz, 3H), 0.79 (t, $J = 7.4$ Hz, 3H).

4,8-Bis((*R*)-2-ethylhexyloxy)benzo[1,2-*b*:4,5-*b'*]dithiophene ((*R,R*)-3). To an aqueous solution of NaOH (5 N, 9.0 mL) was added **1** (0.45 g, 2.0 mmol) and metallic zinc (sandy, 0.29 g, 4.5 mmol) and the mixture was stirred under reflux for 1 h. After tetrabutylammonium bromide (0.13 g, 0.41 mmol) and (*R*)-2-OTs (1.73 g, 6.08 mmol) were added to the mixture, the reaction mixture was further refluxed for 12 h. The reaction mixture was then extracted with dichloromethane, and the organic layer was washed with brine and dried over anhydrous Na₂SO₄. After evaporating the solvent, the crude product was purified by silica gel chromatography using hexane–dichloromethane (10/1, v/v) to yield (*R,R*)-**3** as a pale yellow oil (0.648 g, 1.46 mmol, 73%). ¹H NMR (500 MHz, CDCl₃, rt): δ 7.47 (d, *J* = 5.2 Hz, 2H), 7.36 (d, *J* = 5.7 Hz, 2H), 4.20-4.15 (m, 4H), 1.85-1.76 (m, 2H), 1.74-1.30 (m, 16H), 1.01 (t, *J* = 7.5 Hz, 6H), 0.94 (t, *J* = 7.2 Hz, 6H).

4,8-Bis((*S*)-2-ethylhexyloxy)benzo[1,2-*b*:4,5-*b'*]dithiophene ((*S,S*)-3). The title compound was prepared from (*S*)-2-OTs in the same way as (*R,R*)-**3** and obtained in 87% yield. ¹H NMR (500 MHz, CDCl₃, rt): δ 7.47 (d, *J* = 5.8 Hz, 2H), 7.37 (d, *J* = 5.2 Hz, 2H), 4.20-4.15 (m, 4H), 1.85-1.76 (m, 2H), 1.74-1.30 (m, 16H), 1.01 (t, *J* = 7.5 Hz, 6H), 0.94 (t, *J* = 7.2 Hz, 6H).

2,6-Bis(trimethyltin)-4,8-bis((*R*)-2-ethylhexyloxy)benzo[1,2-*b*:4,5-*b'*]dithiophene

((*R,R*)-4). To a solution of (*R,R*)-**3** (0.64 g, 1.4 mmol) in anhydrous THF (2.5 mL) was added dropwise *n*-butyllithium (1.6 M in hexane, 2.3 mL, 3.7 mmol) via syringe at -78 °C under nitrogen atmosphere. The mixture was stirred at -78 °C for 30 min and then at room temperature for 30 min. After the mixture was cooled to -78 °C again, trimethyltin chloride (0.87 g, 4.4 mmol) in anhydrous THF (0.9 mL) was added. The mixture was warmed to room temperature and stirred for 12 h. After adding a small amount of water to quench the reaction, the solvent was removed under reduced pressure. The residue was diluted with hexane, and the organic layer was washed with water, dried over anhydrous Na₂SO₄ and concentrated. The crude product was purified by recrystallization from ethanol to yield (*R,R*)-**4** as colorless crystals (0.68 g, 0.88 mmol, 63%). Mp 74.7–75.2 °C. [α]_D²⁵ = +1.0 (*c* 1.0, CHCl₃). ¹H NMR (500 MHz, CDCl₃, rt): δ 7.51 (s, 2H), 4.18 (d, *J* = 5.2 Hz, 4H), 1.86–1.76 (m, 2H), 1.75–1.33 (m, 16H), 1.02 (t, *J* = 7.4 Hz, 6H), 0.94 (t, *J* = 6.6 Hz, 6H), 0.44 (s, 18H). ¹³C NMR (125 MHz, CDCl₃, rt): δ 143.59, 140.73, 134.21, 133.24, 128.31, 75.97, 41.00, 30.86, 29.58, 24.23, 23.54, 14.55, 11.70, -8.01. Anal. Calcd for C₃₂H₅₄O₂S₂Sn₂: C, 49.77; H, 7.05. Found: C, 49.53; H, 6.93.

2,6-Bis(trimethyltin)-4,8-bis((*S*)-2-ethylhexyloxy)benzo[1,2-*b*:4,5-*b'*]dithiophene

((*S,S*)-4). The title compound was prepared from (*S,S*)-**3** in the same way as (*R,R*)-**4** and obtained in 68% yield. Mp 75.1–75.3 °C. [α]_D²⁵ = -0.93 (*c* 1.0, CHCl₃). ¹H NMR (500

MHz, CDCl₃, rt): δ 7.51 (s, 2H), 4.19 (d, $J = 5.2$ Hz, 4H), 1.86-1.76 (m, 2H), 1.75-1.33 (m, 16H), 1.02 (t, $J = 7.4$ Hz, 6H), 0.94 (t, $J = 6.6$ Hz, 6H), 0.44 (s, 18H). ¹³C NMR (125 MHz, CDCl₃, rt): δ 143.59, 140.73, 134.21, 133.24, 128.31, 75.98, 41.00, 30.86, 29.58, 24.23, 23.54, 14.56, 11.71, -8.00. Anal. Calcd for C₃₂H₅₄O₂S₂Sn₂: C, 49.77; H, 7.05. Found: C, 49.60; H, 6.93.

Polymerization

Polymerization was carried out in a dry Schlenk flask under a nitrogen atmosphere in a similar manner to that previously reported.^{7a} Each monomer was purified by recrystallization just before use. A typical polymerization procedure is described below.

(*R,R*)-**4** (400 mg, 0.52 mmol), **5** (235 mg, 0.52 mmol) and Pd(PPh₃)₄ (24 mg, 21 μ mol) were placed in a Schlenk flask under a nitrogen atmosphere. Anhydrous toluene (8.3 mL) and DMF (2.1 mL) were added with a syringe and the mixture was heated to 120 °C. After 12 h, the reaction mixture was cooled to room temperature and poured into MeOH. The resulting polymer was collected by centrifugation and washed with MeOH for 12 h and then with hexane for 12 h in a Soxhlet apparatus to remove any by-products and oligomers. After the polymer was collected with chlorobenzene, the chlorobenzene solution was passed through Celite to remove the metal catalyst. The solution was concentrated and poured into hexane. The precipitate was collected by centrifugation and dried *in vacuo* to yield (*R,R*)-PTB5 as a dark purple solid (351 mg, 92%). IR (KBr): 1712 cm⁻¹ ($\nu_{\text{C=O}}$). ¹H NMR (500 MHz, CDCl₃, 50 °C): δ 8.3-6.3 (3H,

br), 4.8-3.5 (6H, br), 2.6-0.7 (45H, br). Anal. Calcd for $(C_{41}H_{54}O_4S_4)_n$: C, 66.63; H, 7.36. Found: C, 66.34; H, 7.48.

In the same way, (*S,S*)-PTB5 and PTB5 were prepared from the corresponding monomers. The polymerization results are summarized in Table 4-1.

Spectroscopic data for (*S,S*)-PTB5. IR (KBr): 1712 cm^{-1} ($\nu_{C=O}$). 1H NMR (500 MHz, $CDCl_3$, 50 °C): δ 8.3-6.3 (3H, br), 4.8-3.5 (6H, br), 2.6-0.7 (45H, br). Anal. Calcd for $(C_{41}H_{54}O_4S_4)_n$: C, 66.63; H, 7.36. Found: C, 66.37; H, 7.57.

Spectroscopic data for PTB5. IR (KBr): 1712 cm^{-1} ($\nu_{C=O}$). 1H NMR (500 MHz, $CDCl_3$, 50 °C): δ 8.3-6.3 (3H, br), 4.8-3.5 (6H, br), 2.6-0.7 (45H, br). Anal. Calcd for $(C_{41}H_{54}O_4S_4 \cdot 0.7H_2O)_n$: C, 65.51; H, 7.43. Found: C, 65.61; H, 7.41.

Fabrication of hole-only devices

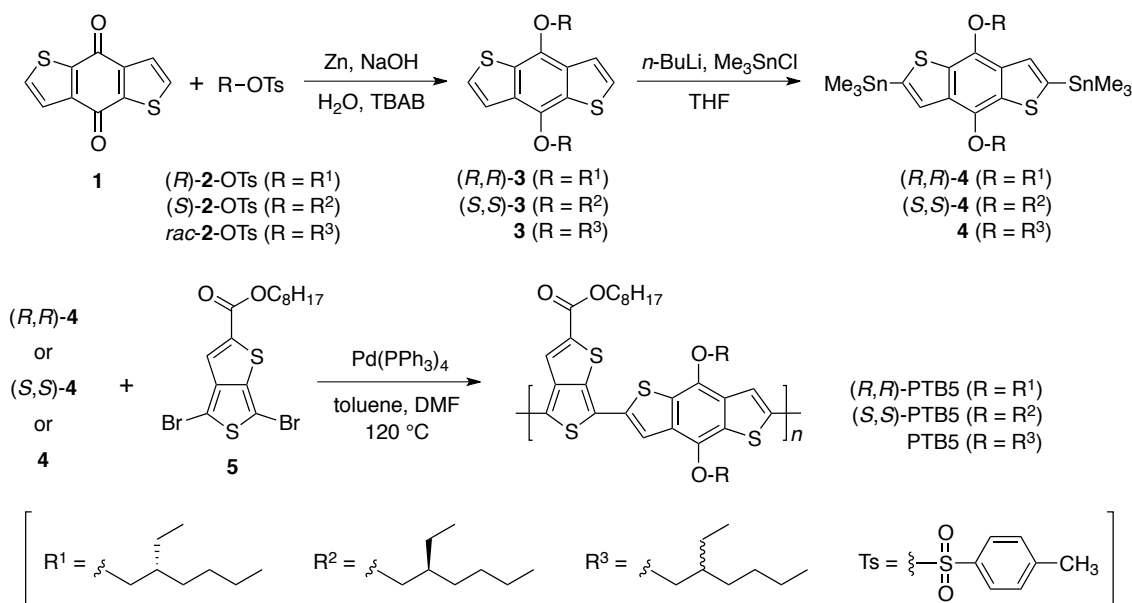
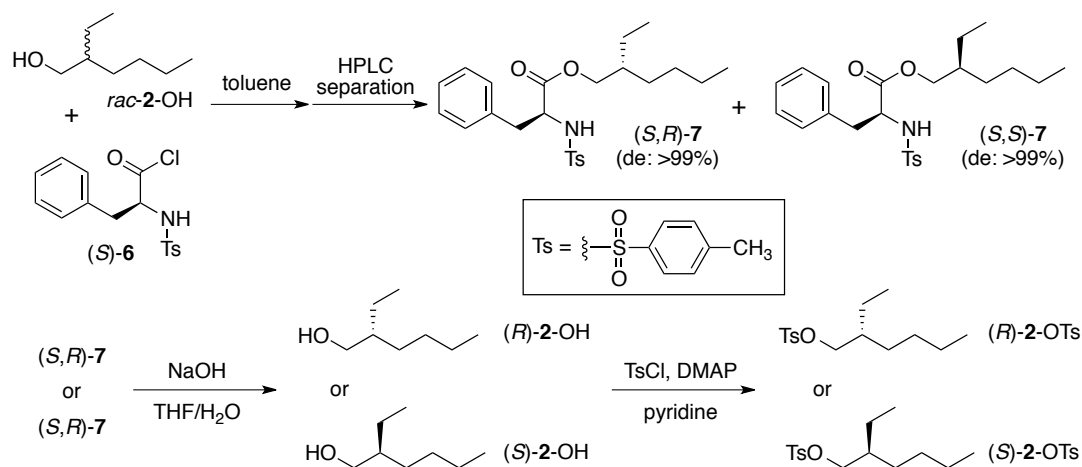
ITO electrode was ultrasonicated in 2-propanol, cleaned in boiling 2-propanol, and then dried in air. A dispersion of PEDOT:PSS (0.65 wt%) in water containing Capstone[®] fluorosurfactant FS-31 (0.5 wt%) was spin-coated onto the clean ITO electrode at 2000 rpm, and then dried at 150 °C for 5 min. A solution of the polymers in chlorobenzene (25 mg/mL) was spin-coated onto the ITO/PEDOT:PSS substrate at 700 rpm. The above aqueous dispersion of PEDOT:PSS was spin-coated onto the polymer:PC₆₁BM layer at 2000 rpm. The Au electrode was vacuum deposited onto the PEDOT:PSS layer under a pressure of 2×10^{-5} Torr. The structure of the hole-only device is ITO/PEDOT:PSS/polymer:PC₆₁BM/PEDOT:PSS/Au, whose effective area is

0.04 cm².

Fabrication of polymer solar cells

ITO-glass electrodes were washed by sonication in 2-propanol, rinsed with boiling 2-propanol, and then dried in air. Zinc oxide film (ZnO) of about 60 nm thickness was prepared on the clean ITO substrate using a sol-gel method¹⁵. Solutions of *o*-dichlorobenzene containing polymer (12.5 mg/mL) and PC₆₁BM (18.75 mg/mL) were spin-coated onto the ITO/ZnO substrate at 700 rpm. Dispersions of PEDOT:PSS (0.65 wt%) in water containing Capstone[®] fluorosurfactant FS-31 (0.5 wt%) were spin-coated onto the polymer:PC₆₁BM layer at 2000 rpm. An Au back electrode was vacuum deposited onto the PEDOT:PSS layer under a pressure of 2×10^{-5} Torr. The effective area of the solar cell was restricted to 1.0 cm² by depositing the Au electrode through a shadow mask. All spin-coated films were prepared under a relative humidity of less than 35% at room temperature in air.

Scheme 4-1. Synthesis of monomers and polymers.

Scheme 4-2. Synthesis of (*R*)- and (*S*)-2-OTs.

Results and discussion

Synthesis

The synthetic routes to the optically active BDT-based monomers ((*R,R*)- and (*S,S*)-4) and polymers ((*R,R*)- and (*S,S*)-5) are summarized in Scheme 4-1. Reaction of 1

with alkyl tosylates, which can be easily derivatized from the corresponding alkyl alcohols, has been used to prepare BDT-based monomers bearing alkoxy pendants.^{8a} According to this strategy, enantiopure (*R*)- and (*S*)-2-OH were needed to prepare (*R,R*)- and (*S,S*)-4, respectively. Several methods to prepare (*R*)- and (*S*)-2-OH, such as catalytic asymmetric synthesis,¹⁶ asymmetric induction^{12c,17} and enzymatic reactions,^{14,18} have been reported. However, none of these methods satisfy all of the requirements of high enantiomeric purity, high scalability and simplicity. Therefore, the author used the following approach to synthesize (*R*)- and (*S*)-2-OH that included a reliable, scalable and simple diastereomer separation as an important step (Scheme 4-2). Optically inactive *rac*-2-OH was first converted to a diastereomeric mixture of (*S,R*)- and (*S,S*)-7 using chiral derivatizing agent (*S*)-6. The author then successfully isolated (*S,R*)- and (*S,S*)-7 (de > 99%) by preparative HPLC separation on Daicel Chiralcel OJ using MeOH as an eluent. Alkaline hydrolysis of the isolated (*S,R*)- and (*S,S*)-7 gave optically pure (*R*)- and (*S*)-2-OH, respectively. The absolute configurations of (*R*)- and (*S*)-2-OH were determined by comparison of the signs of optical rotation with literature data.¹⁴ Finally, the BDT-based monomers (*R,R*)- and (*S,S*)-4 were synthesized via reaction of 1 with (*R*)- and (*S*)-2-OTs derived from (*R*)- and (*S*)-2-OH, respectively, followed by stannylation at the 2- and 6-positions of (*R,R*)- and (*S,S*)-3. Copolymerization of (*R,R*)- or (*S,S*)-4 and 5 by Stille cross-coupling was performed using Pd(PPh₃)₄ as the catalyst in a mixture of toluene/ DMF (4/1, v/v) at 120 °C (Table 4-1). For comparison, the author also prepared the previously reported optically inactive

PTB5 (run 3 in Table 4-1).^{8a} The molecular weight (M_n) and polydispersity index (PDI) of the polymers were determined by SEC analysis in THF. The obtained polymers possessed similar M_n within experimental variation. The thermal stabilities of (*R,R*)- and (*S,S*)-PTB5 were investigated by thermogravimetric analysis under a nitrogen atmosphere (Figure 4-1). The 5% weight-loss temperatures (T_{d5}) of (*R,R*)- and (*S,S*)-PTB5 are 326 and 323 °C, respectively, which are comparable to that of conventional PTB5 (326 °C). The slightly smaller T_{d5} of (*S,S*)-PTB5 may be attributed to low-molecular-weight components present in (*S,S*)-PTB5. These results indicate that controlling the chirality of the branched alkyl pendants has little effect on the polymerizability and thermal stability of these polymers.

Table 4-1. Polymerization results and thermal and optical properties of the polymers.

run	polymer	yield (%) ^a	M_n (10^4) ^b	PDI ^b	T_{d5} (°C) ^c	λ_{onset} (nm)	E_g^{opt} (eV) ^d	HOMO (eV) ^e	LUMO (eV) ^f
1	(<i>R,R</i>)-PTB5	92	5.3	2.0	326	755	1.64	-5.01	-3.37
2	(<i>S,S</i>)-PTB5	88	4.1	1.9	323	755	1.64	-4.99	-3.35
3	PTB5	95	5.9	2.1	326	754	1.64	-5.00	-3.36

^a MeOH and hexane insoluble part. ^b Determined by SEC (eluent: THF, polystyrene standards). ^c The 5% weight-loss temperatures with a heating rate of 10 °C/min in N₂. ^d Calculated from $E_g = 1240/\lambda_{\text{onset}}$. ^e Measured by photoelectron spectroscopy in the atmosphere. ^f Calculated from LUMO = HOMO + E_g^{opt} .

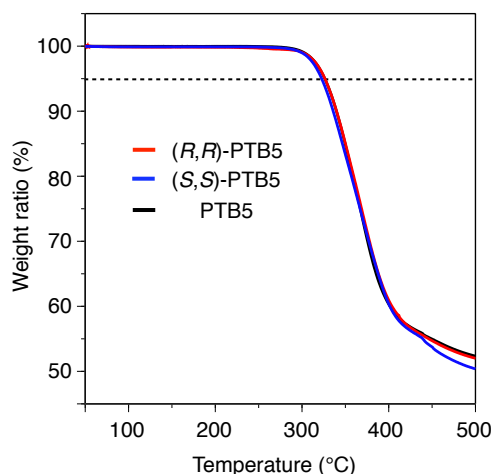


Figure 4-1. Thermogravimetric analysis of the polymers with a heating rate of 10 °C/min in N₂.

Absorption and chiroptical properties

Absorption and CD spectra of the polymers in chlorobenzene and films are shown in Figure 4-2. The optical bandgaps (E_g^{opt}) of the polymers were calculated from the absorption onset wavelength (λ_{onset}) in the film state (Table 4-1). As expected because (*R,R*)-PTB5 and (*S,S*)-PTB5 are enantiomers, the absorption spectrum and E_g^{opt} of (*R,R*)-PTB5 were coincident with those of (*S,S*)-PTB5. In addition, the absorption spectrum of PTB5 was also similar to those of the optically active polymers both in solution and film states. These results suggest that controlling the chirality of the 2-ethylhexyl pendants hardly affects the absorption properties of the PTB-based polymers, which is consistent with a previous report using small molecule-based donor materials.¹¹ The (*R,R*)- and (*S,S*)-PTB5 films exhibited apparent Cotton effects in the polymer backbone region located around 500–800 nm and their CD spectral patterns were almost mirror images of each other. The optically inactive PTB5 film did not show

a CD signal, which suggests that the observed CD signals for (*R,R*)- and (*S,S*)-PTB5 in the film state are not artificial peaks. In contrast, (*R,R*)- and (*S,S*)-PTB5 hardly exhibited apparent Cotton effects in chlorobenzene. This indicates that (*R,R*)- and (*S,S*)-PTB5 form chirally ordered superstructures induced by the chirality of the optically pure pendants in the film state. Similar chiral aggregate formation has been observed for various π -conjugated polymers bearing optically active pendants in the film state as well as in poor solvents.¹²

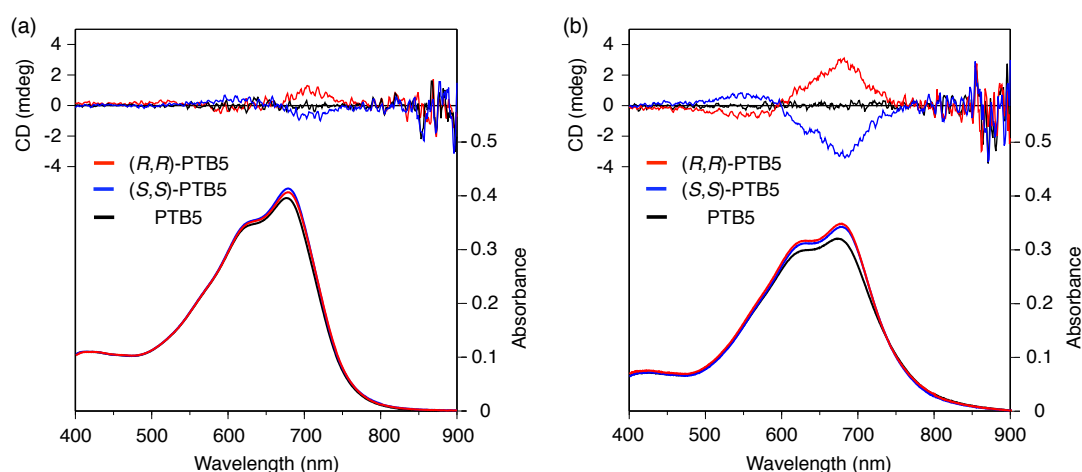


Figure 4-2. CD and absorption spectra of the polymers in chlorobenzene (a) and in the film states (b).

Energy levels

The HOMO energy levels of the polymers were estimated by photoelectron spectroscopy by measuring the ionic potential of the polymer films in the atmosphere (Figure 4-3). LUMO energy levels were estimated as the sum of the HOMO energy

levels and E_g^{opt} values. The HOMO and LUMO energy levels of the polymers are summarized in Table 4-1. The three polymers exhibit almost identical HOMO and LUMO energy levels and the frontier orbital energy levels of the PTB-based polymers are almost independent on the chirality of the 2-ethylhexyl pendants.

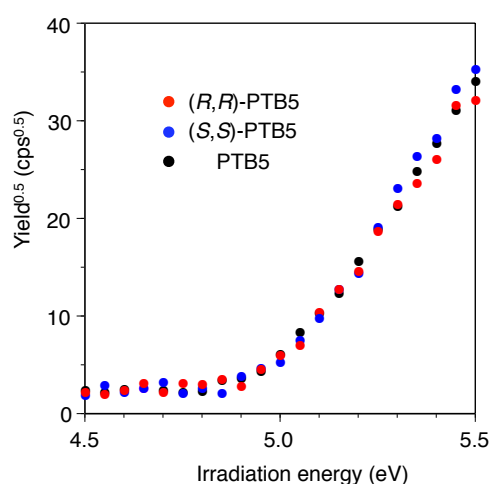


Figure 4-3. Photoelectron spectra of the polymers in air.

Photovoltaic properties of PSCs

The photovoltaic properties of the polymers were evaluated in inverted-type bulk heterojunction (BHJ) PSCs with a configuration of ITO/ZnO/Polymer:PC₆₁BM/PEDOT:PSS/Au.¹⁵ Optimized photovoltaic devices were obtained by spin-coating a solution of polymer:PC₆₁BM (1:1.5, w/w) in *o*-dichlorobenzene. The thickness of the active layers was around 100 nm. The current–voltage (J – V) characteristics of the devices measured under AM 1.5 G irradiation (100 mW/cm²) from a solar simulator are depicted in Figure 4-4. The corresponding device

parameters including short-circuit current density (J_{sc}), open-circuit voltage (V_{oc}), fill factor (FF) and PCE are summarized in Table 4-2. The three kinds of polymers with different chiral information showed approximately similar device behavior, although slight deviation was found in each device.

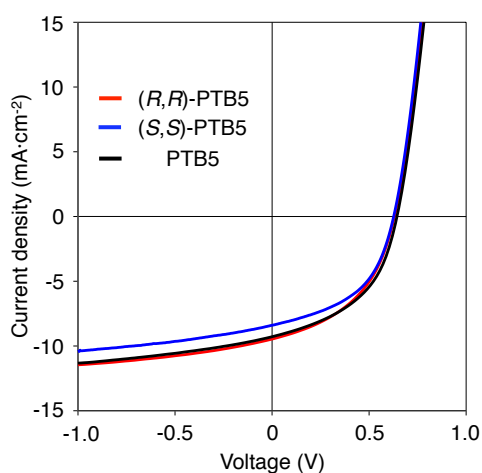


Figure 4-4. J - V curves of the polymer:PC₆₁BM bulk heterojunction photovoltaic devices under AM 1.5 irradiation.

Table 4-2. Photovoltaic performance of the polymer:PC₆₁BM bulk heterojunction

run	polymer	J_{sc} (mA·cm ⁻²)	V_{oc} (V)	FF	PCE (%)
1	(<i>R,R</i>)-PTB5	9.28	0.64	0.47	2.80
2	(<i>S,S</i>)-PTB5	8.40	0.63	0.48	2.53
3	PTB5	9.46	0.63	0.45	2.71

In addition, no clear differences were observed in the hole mobilities of the polymer films ($\mu_h = \text{ca. } 3.0 \times 10^{-4} \text{ cm}^2 \text{ V}^{-1} \text{ s}^{-1}$, Figure 4-5), which were measured in accordance with the space-charge-limited current model, and the π - π stacking distances between the polymers ($d = 3.91 \text{ \AA}$) determined by XRD (Figure 4-6). In light of the overall results for the optically active and inactive polymers, the differences in the parameters of the PSCs seem to be caused by the batch-to-batch variability in the devices or the difference in molecular weight of the polymers. These results mean that controlling the chirality of the 2-ethylhexyl pendants does not lead to obvious improvement in the performance of our inverted-type PSC devices using BDT-based polymers as a donor material. Recently, Castellano and coworkers reported OPV devices containing small molecule-based donor materials bearing optically active 2-ethylhexyl groups.¹⁹ They also did not achieve meaningful differences in device performance through chirality control of the branched alkyls. The performance of PSCs is determined not only by the inherent nature of donor polymers but also by complicating factors such as the morphology of polymer/PC₆₁BM blend films and interfacial adhesion between the active layers and electrodes.²⁰ Further device engineering may be required to elicit the effect of the chirality of alkyl pendants on the performance of photovoltaic devices.

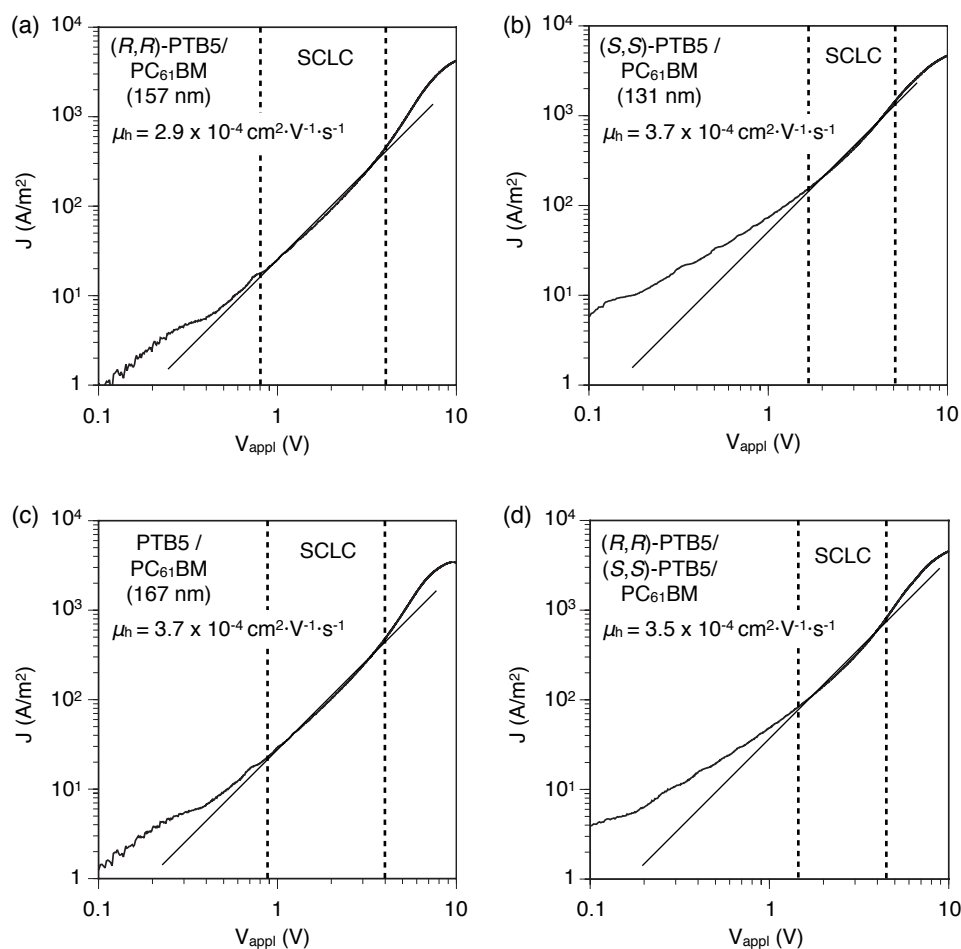


Figure 4-5. Double-logarithmic plots of I - V curves obtained for hole-only devices (ITO/PEDOT:PSS/Polymer:PC₆₁BM/PEDOT:PSS/Au) in the dark in air: (a) (*R,R*)-PTB5/PC₆₁BM (1:1.5, w/w), (b) (*S,S*)-PTB5/PC₆₁BM (1:1.5, w/w), (c) PTB5/PC₆₁BM (1:1.5, w/w) and (d) (*R,R*)-PTB5/(*S,S*)-PTB5/PC₆₁BM (0.5:0.5:1.5, w/w/w) blend films. The thickness (L) of the organic films determined by microfigure measuring instrument is shown in the parentheses.

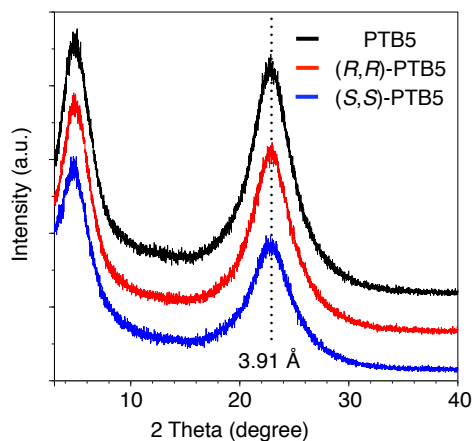


Figure 4-6. Thin-film X-ray diffraction patterns of the polymers.

Conclusions

The author have successfully synthesized the novel optically active narrow-bandgap polymers (*R,R*)- and (*S,S*)-PTB5 containing the BDT units bearing (*R*)- and (*S*)-2-ethylhexyl pendants, respectively, as electron donors for PSCs. The effect of the pendant chirality on the thermal, optical and photovoltaic properties of the polymers was investigated by direct comparison with the properties of optically inactive PTB5 bearing racemic 2-ethylhexyl pendants. In terms of thermal stability, absorption behavior and frontier orbital energy levels, optically active (*R,R*)- and (*S,S*)-PTB5 showed almost identical characteristics to the conventional optically inactive PTB5. The formation of a chirally ordered superstructure in the (*R,R*)- and (*S,S*)-PTB5 films was confirmed using CD spectroscopy. The photovoltaic properties of the donor polymers were evaluated using preliminary inverted-type BHJ solar cells consisting of PC₆₁BM as an acceptor. The (*R,R*)- and (*S,S*)-PTB5-based PSCs showed comparable performance to that of the PTB5-based PSC. However, it might be premature to conclude that the

author can ignore the chirality of the branched alkyl chain in PSCs because the performance of PSCs cannot be determined solely by the inherent nature of donor polymers. The latent potential of polymers bearing optically active branched alkyls may be realized through innovation in device engineering, which includes a formation of a nanoscale percolating network in the BHJ structures and a high interfacial adhesion between active layers and electrodes, and lead to unexpected improvement in PSC performance including efficiency and stability.

References

- (1) (a) Yu, G.; Gao, J.; Hummelen, J. C.; Wudl, F.; Heeger, A. J. *Science* **1995**, *270*, 1789. (b) Günes, S.; Neugebauer, H.; Sariciftci, N. S. *Chem. Rev.* **2007**, *107*, 1324. (c) Cheng, Y.-J.; Yang, S.-H.; Hsu, C.-S. *Chem. Rev.* **2009**, *109*, 5868. (d) Peet, J.; Heeger, A. J.; Bazan, G. C. *Acc. Chem. Res.* **2009**, *42*, 1700. (e) Brabec, C. J.; Gowrisanker, S.; Halls, J. J. M.; Laird, D.; Jia, S.; Williams, S. P. *Adv. Mater.* **2010**, *22*, 3839. (f) Beaujuge, P. M.; Fréchet, J. M. J. *J. Am. Chem. Soc.* **2011**, *133*, 20009. (g) Facchetti, A. *Chem. Mater.* **2011**, *23*, 733. (h) Li, G.; Zhu, R.; Yang, Y. *Nat. Photon.* **2012**, *6*, 153. (i) Søndergaard, R.; Hösel, M.; Angmo, D.; Larsen-Olsen, T. T.; Krebs, F. C. *Mater. Today* **2012**, *15*, 36. (j) Cao, W.; Xue, J. *Energy Environ. Sci* **2014**, *7*, 2123.
- (2) (a) Winder, C.; Sariciftci, N. S. *J. Mater. Chem.* **2004**, *14*, 1077. (b) Boudreault, P.-L. T.; Najari, A.; Leclerc, M. *Chem. Mater.* **2011**, *23*, 456. (c) Bian, L.; Zhu, E.; Tang, J.; Tang, W.; Zhang, F. *Prog. Polym. Sci.* **2012**, *37*, 1292. (d) Zhou, E.; Hashimoto, K.; Tajima, K. *Polymer* **2013**, *54*, 6501.
- (3) (a) Lim, Y.; Ihn, S.-G.; Bulliard, X.; Yun, S.; Chung, Y.; Kim, Y.; Chang, H.; Choi, Y. S. *Polymer* **2012**, *53*, 5275. (b) Tamilavan, V.; Song, M.; Kim, S.; Agneeswari, R.; Kang, J.-W.; Hyun, M. H. *Polymer* **2013**, *54*, 3198. (c) Chen, J.; Xiao, M.; Su, W.; Duan, X.; Duan, L.; Peng, W.; Tan, H.; Yang, R.; Zhu, W. *Polymer* **2014**, *55*, 4857. (d) Wang, H.-J.; Chen, C.-P.; Jeng, R.-J. *Materials* **2014**, *7*, 2411. (e) Ye, L.; Zhang, S.; Huo, L.; Zhang, M.; Hou, J. *Acc. Chem. Res.* **2014**, *47*, 1595.
- (4) (a) Huo, L.; Hou, J. *Polym. Chem.* **2011**, *2*, 2453. (b) Yamamoto, T.; Ikai, T.;

- Kuzuba, M.; Kuwabara, T.; Maeda, K.; Takahashi, K.; Kanoh, S. *Macromolecules* **2011**, *44*, 6659. (c) Li, Y. *Acc. Chem. Res.* **2012**, *45*, 723. (d) Ikai, T.; Kudo, T.; Nagaki, M.; Yamamoto, T.; Maeda, K.; Kanoh, S. *Polymer* **2014**, *55*, 2139.
- (5) (a) Takimiya, K.; Shinamura, S.; Osaka, I.; Miyazaki, E. *Adv. Mater.* **2011**, *23*, 4347. (b) Jiang, W.; Li, Y.; Wang, Z. *Chem. Soc. Rev.* **2013**, *42*, 6113.
- (6) Liang, Y.; Wu, Y.; Feng, D.; Tsai, S.-T.; Son, H.-J.; Li, G.; Yu, L. *J. Am. Chem. Soc.* **2009**, *131*, 56.
- (7) (a) Chen, H.-Y.; Hou, J.; Zhang, S.; Liang, Y.; Yang, G.; Yang, Y.; Yu, L.; Wu, Y.; Li, G. *Nat. Photon.* **2009**, *3*, 649. (b) Hou, J.; Chen, H.-Y.; Zhang, S.; Chen, R. I.; Yang, Y.; Wu, Y.; Li, G. *J. Am. Chem. Soc.* **2009**, *131*, 15586.
- (8) (a) Liang, Y.; Feng, D.; Wu, Y.; Tsai, S. T.; Li, G.; Ray, C.; Yu, L. *J. Am. Chem. Soc.* **2009**, *131*, 7792. (b) Son, H. J.; Wang, W.; Xu, T.; Liang, Y.; Wu, Y.; Li, G.; Yu, L. *J. Am. Chem. Soc.* **2011**, *133*, 1885.
- (9) Huo, L.; Zhang, S.; Guo, X.; Xu, F.; Li, Y.; Hou, J. *Angew. Chem. Int. Ed.* **2011**, *50*, 9697.
- (10) Mei, J.; Bao, Z. *Chem. Mater.* **2014**, *26*, 604.
- (11) Liu, J.; Zhang, Y.; Phan, H.; Sharenko, A.; Moonsin, P.; Walker, B.; Promarak, V.; Nguyen, T. Q. *Adv. Mater.* **2013**, *25*, 3645.
- (12) (a) LangeveldVoss, B. M. W.; Janssen, R. A. J.; Christiaans, M. P. T.; Meskers, S. C. J.; Dekkers, H.; Meijer, E. W. *J. Am. Chem. Soc.* **1996**, *118*, 4908. (b) Oda, M.; Nothofer, H. G.; Scherf, U.; Šunjić, V.; Richter, D.; Regenstein, W.; Neher, D.

- Macromolecules* **2002**, *35*, 6792. (c) Grenier, C. R. G.; George, S. J.; Joncheray, T. J.; Meijer, E. W.; Reynolds, J. R. *J. Am. Chem. Soc.* **2007**, *129*, 10694.
- (13) Hou, J.; Park, M.-H.; Zhang, S.; Yao, Y.; Chen, L.-M.; Li, J.-H.; Yang, Y. *Macromolecules* **2008**, *41*, 6012.
- (14) Baczko, K.; Larpent, C. *J. Chem. Soc., Perkin Trans. 2* **2000**, 521.
- (15) Kuwabara, T.; Omura, Y.; Yamaguchi, T.; Taima, T.; Kohshin, T.; Higashimine, K.; Vohra, V.; Murata, H. *J. Phys. Chem. C* **2014**, *118*, 4050.
- (16) (a) Kondakov, D. Y.; Negishi, E.-i. *J. Am. Chem. Soc.* **1996**, *118*, 1577. (b) Vilaplana, M. a. J.; Molina, P.; Arques, A.; Andrés, C.; Pedrosa, R. *Tetrahedron: Asymmetry* **2002**, *13*, 5. (c) Gemma, S.; Gabellieri, E.; Sanna Coccone, S.; Marti, F.; Tagliatalata-Scafati, O.; Novellino, E.; Campiani, G.; Butini, S. *J. Org. Chem.* **2010**, *75*, 2333. (d) Parfenova, L. V.; Berestova, T. V.; Tyumkina, T. V.; Kovyazin, P. V.; Khalilov, L. M.; Whitby, R. J.; Dzhemilev, U. M. *Tetrahedron: Asymmetry* **2010**, *21*, 299.
- (17) (a) Hodgson, D. M.; Kaka, N. S. *Angew. Chem. Int. Ed.* **2008**, *47*, 9958. (b) Cisko-Anic, B.; Hamersak, Z. *Chirality* **2009**, *21*, 894. (c) Grost, C.; Graber, M.; Hell, M.; Berg, T. *Biorg. Med. Chem.* **2013**, *21*, 7357.
- (18) (a) Bianchi, D.; Cesti, P.; Battistel, E. *J. Org. Chem.* **1988**, *53*, 5531. (b) Barth, S.; Effenberger, F. *Tetrahedron: Asymmetry* **1993**, *4*, 823. (c) Majerić, M.; Šunjić, V. *Tetrahedron: Asymmetry* **1996**, *7*, 815. (d) Huang, Y.; Zhang, F.; Gong, Y. *Tetrahedron Lett.* **2005**, *46*, 7217. (e) Xu, S.; Lee, C. T.; Wang, G.; Negishi, E. *Chemistry – An*

Asian Journal **2013**, 8, 1829.

(19) Zerdan, R. B.; Shewmon, N. T.; Zhu, Y.; Mudrick, J. P.; Chesney, K. J.; Xue, J.; Castellano, R. K. *Adv. Funct. Mater.* **2014**, 24, 5993.

(20) Huang, Y.; Kramer, E. J.; Heeger, A. J.; Bazan, G. C. *Chem. Rev.* **2014**, 114, 7006.

List of Publications

Chapter 1

“Synthesis and Characterization of Thieno[3,4-*b*]thiophene-Based Copolymers Bearing 4-Substituted Phenyl Ester Pendants: Facile Fine-Tuning of HOMO Energy Levels”

Tomoyuki Yamamoto, Tomoyuki Ikai, Mitsuhiro Kuzuba, Takayuki Kuwabara, Katsuhiko Maeda, Kohshin Takahashi, and Shigeyoshi Kanoh

Macromolecules **2011**, *44*, 6659–6662.

Chapter 2

“Fine Tuning of Frontier Orbital Energy Levels in Dithieno[3,2-*b*:2',3'-*d*]silole-Based Copolymers Based on the Substituent Effect of Phenyl Pendants”

Tomoyuki Ikai, Tomoya Kudo, Masahiro Nagaki, Tomoyuki Yamamoto, Katsuhiko Maeda, and Shigeyoshi Kanoh

Polymer **2014**, *55*, 2139–2145.

Chapter 3

“Influence of 4-Fluorophenyl Pendants in Thieno[3,4-*b*]thiophene–Benzo[1,2-*b*:4,5-*b'*]dithiophene-Based Polymers on the Performance of Photovoltaics”

Tomoyuki Yamamoto, Tomoyuki Ikai, Shinji Katori, Takayuki Kuwabara, Katsuhiko Maeda, Tomoyuki Koganezawa, Kohshin Takahashi, and Shigeyoshi Kanoh

Journal of Polymer Science Part A: Polymer Chemistry, accepted on January 31, 2015.

Chapter 4

“Thieno[3,4-*b*]thiophene–Benzo[1,2-*b*:4,5-*b'*]dithiophene-Based Polymers Bearing Optically Pure 2-Ethylhexyl Pendants: Synthesis and Application in Polymer Solar Cells”

Tomoyuki Ikai, Ryotaro Kojima, Sinji Katori, Tomoyuki Yamamoto, Takayuki Kuwabara, Katsuhiko Maeda, Kohshin Takahashi, and Shigeyoshi Kanoh

Polymer **2015**, *56*, 171–177.

Acknowledgement

The present studies were carried out at the Graduate School of Natural Science and Technology, Kanazawa University, during 2009–2015.

The author would like to express his gratitude to Associate Professor Katsuhiko Maeda for his insightful guidance and suggestions. Professor Shigeyoshi Kanoh gave the author pertinent comments and humorous encouragement. Special thanks go to Associate Professor Tomoyuki Ikai for his constant guidance and constructive advice. The author is also grateful to Professor Kohshin Takahashi and Associate Professor Takayuki Kuwabara for their generous support and fruitful discussions. It is pleasure to express his appreciation to all members of the research groups of Professor Kanoh Laboratory and the first department of Research Center for Sustainable Energy and Technology for their useful discussions and kind friendship.

March, 2015

Tomoyuki Yamamoto